AN EXPERIMENTAL STUDY OF FRETTING CORROSION AT A BEARING/CARTRIDGE INTERFACE

by

Robert Dean Frantz

Thesis submitted to the Graduate Faculty of the

Virginia Polytechnic Institute and State University

in partial fulfillment of the requirements for the degree of

MASTER OF SCIENCE

in

Mechanical Engineering

APPROVED:

M. J. Futey, Chairman

H. H. Mabie | D. W. Dwight

February 1983

Blacksburg, Virginia

ACKNOWLEDGEMENTS

I would like to express my sincere appreciation to the following people for their help in this research:

Dr. M. J. Furey, for his guidance, advice, and, most of all, his sincere encouragement that made this research project a truly rewarding experience.

Dr. H. H. Mabie, for his warmth and assistance over the past year.

Dr. D. W. Dwight, for serving on my committee and for his sincere help during troubled times.

Mr. Richard Stover whose friendship made my studies at Virginia Tech much more enjoyable.

The Naval Research Laboratories who sponsored this research project.

To my mother and father, Mr. and Mrs. Robert E. Frantz, who provided the love, patience, support, and belief in me that made my entire college education possible, I remain eternally grateful.

Finally, I want to thank my wife Lynda, who not only typed this thesis but gave me continual strength and encouragement during the entire course of this research project. To her, I dedicate this thesis.

TABLE OF CONTENTS

TABLE OF CONTENTS (Continued)

TABLE OF CONTENTS (Continued)

LIST OF FIGURES

LIST OF FIGURES (Continued)

LIST OF FIGURES (Continued)

LIST OF TABLES

INTRODUCTION

Practically speaking, fretting is a complex tribological phenomenon which is very far from being understood. The damage done to mechanical systems as a result of fretting action is not minor. Splines, couplings, taper fits, shrink fits, and bearing/housing assemblies are just a few of many mechanical systems that are subject to fretting corrosion. Fretting not only disrupts the surfaces of two mating parts but it destroys tolerances; this can eventually render many mechanical systems useless. The problem of fretting corrosion is even more complex in that it includes both oxidation and wear. Furthermore, very little has been published on fretting of actual machine components. Most fretting corrosion investigations begin in the laboratory with simple, well-defined geometries; various factors which are thought to influence the fretting corrosion process are examined and a hypothesis is set forth which describes the fretting corrosion phenomena. Whether or not the results of such investigations can be applied to physically real problems with any degree of confidence is debatable.

The following study is concerned with a smaller portion of a problem that exists in certain shipboard service motor-generator sets. Inspection of these units revealed a substantial amount of "reddish-brown" debris that formed at the interface of two bearing/cartridge assemblies which simply support the unit's electrical rotor. Analysis of the debris showed it to be a product of fretting corrosion that occurred at the interface of the assembly(1)*. Fretting in such systems can lead to excessive surface damage, misalignment, noise, and even bearing failures through primary and secondary effects.

The purpose, then, of this study is not to begin in the laboratory with simple, well-defined geometries but instead, to confront the problem of fretting corrosion occurring at a bearing/cartridge interface directly, i.e., to learn as much as possible about the actual field problem and include this knowledge along with key field parameters in a laboratory test device possessing the same geometry.

The specific goals of the present study are as follows:

1. To design and construct a laboratory test apparatus that will be capable of examining pertinent variables such as load, frequency, amplitude, and presence of a grease for a bearing/cartridge geometry.
2. To carry out a designed experiment using the device mentioned above to determine the significance of load, frequency, amplitude, and presence of a grease on the extent of fretting corrosion damage at a bearing/cartridge interface.
3. To compare the results found above with the Archard wear theory to determine whether or not it can be used to predict fretting wear of the bearing/cartridge interface.

---

*Numbers in parenthesis refer to references cited by the author of the thesis. Numbers in brackets refer to references cited in other publications. All references may be found in the reference section.

REVIEW OF LITERATURE

Introduction

In general, our knowledge concerning the phenomenon of fretting corrosion has progressed over the years through a better understanding of how surfaces interact on a microscopic scale. With the advent of sophisticated surface analytical tools such as the scanning electron microscope (SEM) and the x-ray photoelectron spectrometer (XPS), we are now able to gather much more information about fretting corrosion and related tribological phenomena than ever before. But even with the aid of such tools, the mechanism of fretting corrosion is not yet clearly understood. Beginning in 1927 with the first published work on fretting corrosion by Tomlinson(2), many papers have appeared which present theories as to how the mechanism proceeds. A survey of the literature will quickly reveal, though, that many of these ideas are conflicting. Part of this controversy lies in the fact that the geometries being studied and the parameters influencing fretting corrosion differ greatly. Before continuing this discussion though, a definition of fretting corrosion is appropriate.

In a research proposal submitted to the Naval Research Laboratories, Furey(3) gives an excellent description of fretting corrosion:

> "According to the OECD (Organization for Economic Co-operation and Development) glossary of tribological terms [4]:
>
> > Fretting is defined as 'wear phenomena occurring between two surfaces having oscillatory relative motion of small amplitude';

> <u>Fretting Corrosion</u> is defined as 'a form of fretting in which chemical reaction predominates'.

Two notes are added to the OECD definition, namely that (a) fretting corrosion is often characterized by the removal of particles and subsequent formation of oxides, which are often abrasive and so increase the wear, and (b) fretting corrosion can involve other chemical reaction products, which may not be abrasive."

Following now is a brief discussion of the more significant fretting wear theories that have evolved and of the various parameters which have been found to influence fretting corrosion.

Fretting Wear Theories

In his work using sphere-on-plane and cylinder contacting cylinder geometries, Tomlinson[2,5] proposed a fretting wear mechanism that operates by molecular cohesion:

> "The nature of the bonds between the molecules appears to be such that the cohesive force of a visiting molecule is quite insufficient to pluck the molecule out normally, but is sufficient to detach it from the solid when applied tangentially . . . To use a crude analogy, a tooth is more easily uprooted by a side pull than a normal pull. The molecules so detached combine very quickly with oxygen molecules from the atmosphere[forming the reddish-brown oxide typical of fretting corrosion]."

Tomlinson rejected the idea of mechanical abrasion as being a factor in the fretting corrosion process and showed quite conclusively that relative motion is a necessary condition for the occurrence of fretting corrosion.

In the early part of 1950, Godfrey[6,7] presented simple experiments which added to an understanding of the mechansim of fretting corrosion. By vibrating a sphere in contact with a plane glass surface under pressure and observing the contact point through a microscope, Godfrey concluded that fretting is caused by the removal of, "finely divided and apparently virgin material due to inherent adhesive forces, and that its primary action is independent of vibratory motion or high sliding speeds." By fretting fully oxidized materials such as quartz and mica, Godfrey also demonstrated that oxidation is a secondary factor in the fretting corrosion process.

In 1953 Feng and Rightmire[8] described fretting wear as beginning entirely by mechanical wear and shifting to complete abrasive wear by oxidation of wear particles. Mechanical wear begins by an interlocking that occurs at contacting high spots between two surfaces. The interlocking results from a roughening of the high spots by plastic deformation which occurs during loading. The immediate points of contact are work-hardened so that when an applied tangential force reaches a sufficiently high magnitude, shearing will occur below the interlocked surfaces and a wear particle will be produced. Wear particles created in this manner then oxidize and accumulate in valleys on the surface, the valleys being part of a large-scale waviness that exists on the surface. As the process continues, the load supported by the high spots is more evenly distributed by accumulation of debris. The wear mechanism then shifts from shearing to abrasive action.

In 1953, one of the most comprehensive studies regarding fretting corrosion appeared. Uhlig et al.[(9)] developed an equation to describe the fretting corrosion process in terms of a mechanical component and a chemical component using a device which produced fretting corrosion between cylindrical components contacting at their end faces.

> "A review of the facts suggests that the mechanism of fretting corrosion includes a chemical factor and a mechanical factor, with observed damage, in general, resulting from both. An asperity rubbing on a metal surface is considered to produce a track of clean metal which immediately oxidizes, or upon which gas rapidly adsorbs. The next asperity wipes off the oxide or initiates reaction of metal with adsorbed gas to form oxide. This is the so-called chemical factor. In addition, asperities dig below the surface to cause a certain amount of wear by welding or shearing action in which metal particles are dislodged. This is the mechanical factor of fretting. Metallic debris produced by fretting is thought not to oxidize spontaneously . . . but instead converts partially to iron oxide by secondary fretting action of particles rubbing against themselves or adjacent surfaces."

In their work on fretting corrosion, Halliday, and Hirst[(10)] describe the fretting wear mechanism as a sequence of processes which is independent of amplitude. The device on which the experiments were performed consists basically of a cylinder that is oscillated about its longitudinal axis in contact with a v-block, the cylinder making two parallel line contacts with the block. In the initial stage of the process, plastic flow of contacting asperities leads to cold welding of the junctions. After welding, the junctions rupture leading to the production of loose metallic fragments and to scoring and tearing of the opposing metal surfaces. Metallic debris created in this manner subsequently oxidizes, forming a coarse black oxide particle and eventually a fine red-brown powder--both of which are α-Fe_2O_3. Wear then continues as an abrasive process with large amplitude oscillation ($\approx$400 μm, 0.0157 in.) resembling unidirectional wear and small amplitude oscillation ($\approx$2 μm, 0.00008 in.) producing much reduced wear rates. The unexpected finding by Halliday and Hirst is that in all cases the coefficient of friction dropped to a value of approximately 0.05. They attribute this discovery to the small amplitude oscillatory motion produced between the cylinder and block in that trapped debris acts like tiny ball bearings and thus reduces the friction coefficient to its final value.

Rabinowicz and Stowers[11] suggest that fretting wear resembles unidirectional adhesive wear much more closely than it does other types of wear and that the amount of wear produced by the adhesive mechanism can be computed by the use of Archard's wear equation. The authors use a device in which two cylinders are loaded end to end with the top cylinder being vibrated by an audio amplifier. The friction force is monitored with time and the amount of wear is determined by weight loss.

In a paper published in 1978, Waterhouse(12) proposes that fretting wear proceeds by a delamination process. Adhesive wear is thought to initiate fatigue cracks which propagate into the interior of the material and enhance delamination; abrasive wear is not thought to contribute significantly to the fretting wear process.

In a study done on fretting wear of titanium and nickle-chromium-aluminum alloys, R.C. Bill(13) believes that four distinct types of fretting behavior can be identified with respect to the role played by oxidation.

1. The first type of fretting behavior results from fretting of metals in an inert atmosphere. When the presence of oxygen is minimized, metal-to-metal adhesive contact predominates. In this environment, fretting corrosion is either minimized or eliminated when oxygen is kept from two contacting surfaces.
2. The second type of fretting behavior involves the cyclic removal of an oxide layer from the metallic surface with each half cycle of relative motion.
3. The third type of fretting wear behavior takes into account surface fatigue. This idea asserts that fretting wear takes place through a surface fatigue process in which micropitting and spalling result. Oxidation enters into the fretting wear mechanism in that the behavior described in number 2 may occur on the load bearing portions of contact while at the same time oxygen diffuses into fatigue cracks formed at the base of an asperity.

4. According to the fourth type of behavior, oxide remains intact and adherent to the metal substrate during fretting conditions. All wear taking place occurs directly in the oxide film and metal-to-metal contact never occurs.

Factors Influencing Fretting

Our understanding of the fretting corrosion process has grown with time but a tremendous amount of conflicting data still appears. Possible reasons for the apparent discrepancies include questionable measurements, variations in geometry, inadequate description of test conditions, and differences in corrosion/wear mechanisms. A complete review of fretting corrosion is beyond the scope of this thesis. Instead, some of the more important factors which are thought to influence fretting corrosion will be highlighted. These factors are separated into three categories: material properties, environmental conditions, and contact conditions.

Material Properties

Generally speaking, it is the combination of materials in contact which determines the vulnerability of either material to fretting corrosion attack. For steel, non-ferrous, and non-metals, the softer materials are more susceptible to fretting damage(3,5,14); softer materials have a greater tendency toward seizure which results from the formation of large intermetallic welds.

Environmental Conditions

Atmosphere: Investigations conducted in inert environments have shown that oxidation plays a very significant role in the fretting corrosion process. Many investigators(9,15,16) have found that little or no fretting occurs in tests conducted in inert atmospheres such as nitrogen, hydrogen, and helium. Measurements of the friction coefficient during such tests suggest that the actual area of contact approaches the apparent area of contact due to the formation of large intermetallic welds.[10]

Humidity: Relative humidity affects fretting corrosion in an inverse manner, i.e., an increase in humidity results in a decrease in fretting and vice versa.[9,16] The moisture present at higher relative humidities acts as a lubricant which reduces fretting.[17,21] It has also been suggested that at higher relative humidities, a softer oxide is produced which would tend to reduce abrasive wear.[9,17]

Temperature: Temperature has also been shown to affect fretting corrosion in an inverse manner.[9,13,17] Two reasons have been suggested to explain this effect: first, an increase in temperature of a metal will make it more ductile.[9] Contacting asperities that are more ductile allow a greater degree of relative motion without the formation of wear debris. Secondly, it has been shown that an increase in temperature leads to a greater rate of oxidation between two rubbing surfaces which results in thicker oxide films to retard metallic contact.[9,13,18,19]

Contact Conditions

Load: The majority of the studies done concerning the effect of load show that fretting increases with load.[9,15,17] Conflicting views on the effect of load are probably due to the combination of parameters used in the test. Where smaller amplitudes are used, for example, a significant increase in the load may cause all motion to be taken up by elastic deflection of the test apparatus.[9,15,17,20,21] With all other variables remaining constant, though, fretting increases with load.[15]

Frequency: Many discrepancies exist regarding the effect of frequency on fretting corrosion. Some have found fretting damage to increase with frequency, some have found fretting damage to decrease with frequency, and others have found that frequency has no effect. In tests carried out on cylindrical end contacts, Uhlig et al.[9] found that damage decreased with frequency. This effect supported his theory regarding the importance of chemical action in fretting.[3] At higher rates of relative motion, a worn surface does not have time to reoxidize and the resulting wear is a consequence of a mechanical factor--the chemical factor being suppressed.[21] Uhlig's theory also predicts a disappearance of the frequency effect in an inert atmosphere and that only the mechanical factor will exist.

Cycle Duration: The results of a majority of investigations show the wear rate produced by fretting to be rapid initially and then to eventually settle down to steady-state wear that is linear with respect to time.[3] The initially high wear rate has been attributed to a wear-in period. The transition period between wear-in and steady-state wear depends on motion, material, and environment.[3]

Lubrication: The presence of an oily or greasy substance between two surfaces reduces but does not prevent fretting corrosion.[20] For maximum effectiveness, the lubricant should have easy and continuous access to all parts of the surfaces.[15] The action of a lubricant has generally been attributed to its ability to prevent access of oxygen to the surface. The reciprocating motion characteristic of fretting prohibits the maintenance of a hydrodynamic film which would separate the rubbing surfaces and thus eliminate fretting.

Amplitude of Slip: Relative motion between two contacting surfaces is a necessary condition for fretting corrosion to occur.[5] Practically speaking, fretting has no lower limiting amplitude; Tomlinson obtained fretting for amplitudes as low as 1.6×10^{-3} μm (6.5×10^{-8} in.). The damage which results from fretting is thought to be caused by relative motion beyond the elastic range of the contacting asperities.[2,3,5] As the amplitude of relative motion is increased, the metallic-wear-particle content of the debris also increases. If the amplitude is increased still further, a point is reached where fretting wear closely resembles wear produced by unidirectional motion.[10,11]

EXPERIMENTAL WORK

Introduction

The main objective of this study is to determine the important parameters influencing fretting corrosion at the interface of a bearing and its housing (cartridge). The objective was accomplished in two segments:

1. A device was designed and built which is capable of producing fretting corrosion at a bearing/cartridge interface with independent control of axial vibration, frequency, amplitude, and load.
2. Using this device, a statistically designed experiment was carried out to determine the significance of various factors on the extent of fretting corrosion.

The device is capable of producing axial relative motion between five sets of bearings and cartridges; parameters such as load, frequency, and amplitude can be varied independently. Other factors which can be examined include cartridge surface finish, clearance, bearing/cartridge materials, presence and composition of a lubricant at the interface, surface films, coatings, treatments (e.g., ion-implantation), and environment. In the present study, four fundamental factors were investigated, namely load, frequency, amplitude, and presence of a grease at the interface.

Once the apparatus was built, preliminary experiments were run using the device. The purpose of the experiments was two-fold:

1. To learn the machine's operation characteristics and make any necessary modifications.
2. To serve as a guide in choosing parameter magnitudes for use in the statistically designed experiment.

As a further benefit, the preliminary experiments were an aid in examining the fretting wear process which took place between a bearing and cartridge. A detailed discussion of the apparatus and the experiments performed on it now follows.

Description of Apparatus

Introduction

Basically, the apparatus (Mark III) is an extension of a vibration fatigue testing machine. An addition to the vibration machine converts vertical motion to horizontal motion. Photographs of Mark III are shown in Figures 1 through 4. The conversion from vertical motion to horizontal motion is necessary for two reasons:

1. To reduce the magnitude of motion produced by the shaker table to values more suitable for a fretting corrosion study.
2. For convenience of load application to the test specimens.

Motion produced by the shaker table is transmitted through a drive linkage to bearings which are locked on to drive shafts. The cartridges, which house the bearings, are clamped to a stationary angle-iron bar. Movement of the shaker table produces relative motion between the bearings and cartridges. Load is applied to each bearing by suspending containers holding lead shot from the drive shafts. The machine capacities are given below for reference and will be discussed in more detail later.

TABLE 1

MARK III CHARACTERISTICS

Geometry	Bearing in Cartridge (cylinder in cylinder)
Load	0 → 200 N (0 → 45 lbf)
Amplitude	0 → 500 μm (0 → 0.0197 in.)
Frequency	2.5 → 100 Hz
Temperature	Ambient
Humidity	Ambient
Atmosphere	Normal

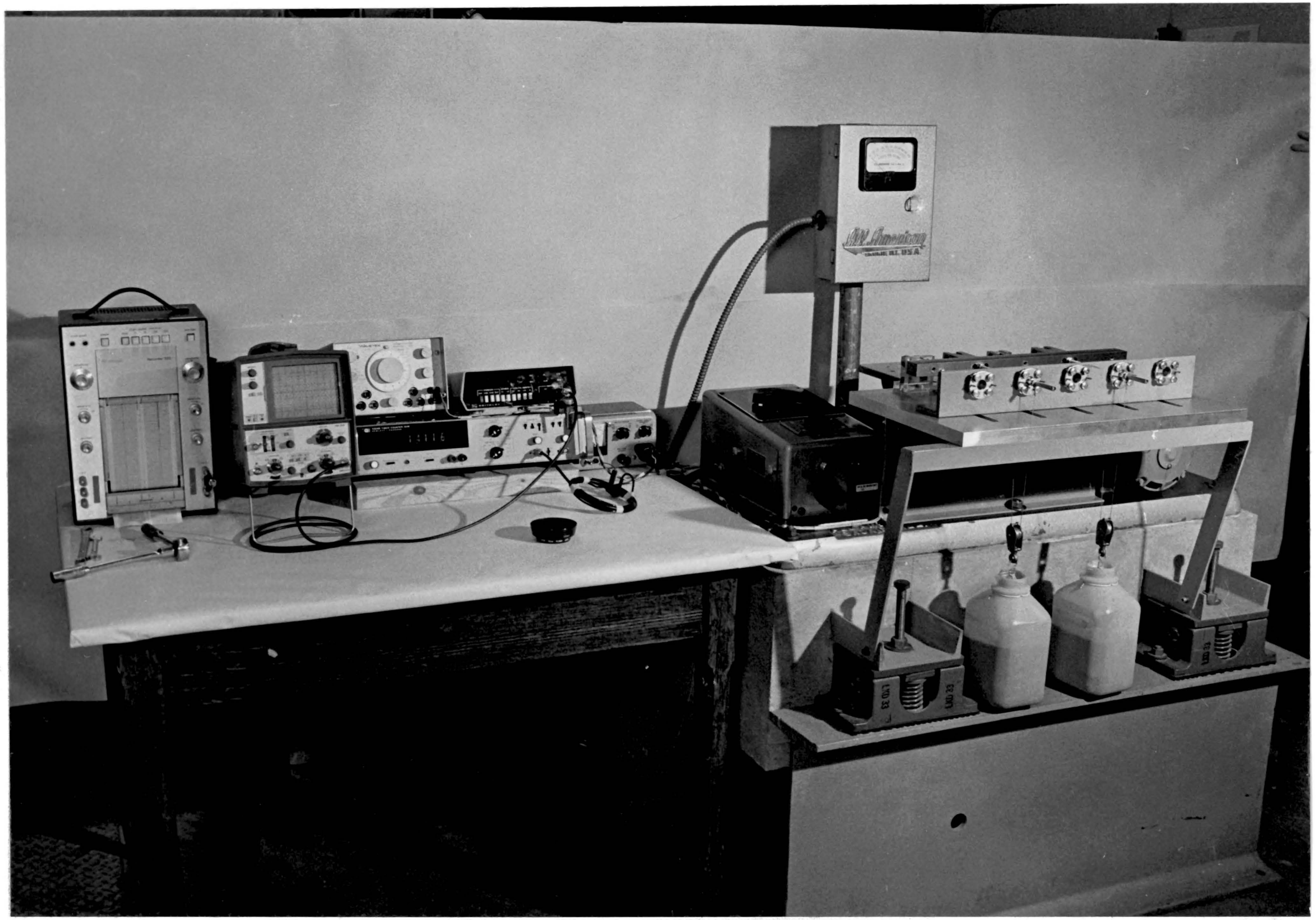

Figure 1. Overall View of Mark III

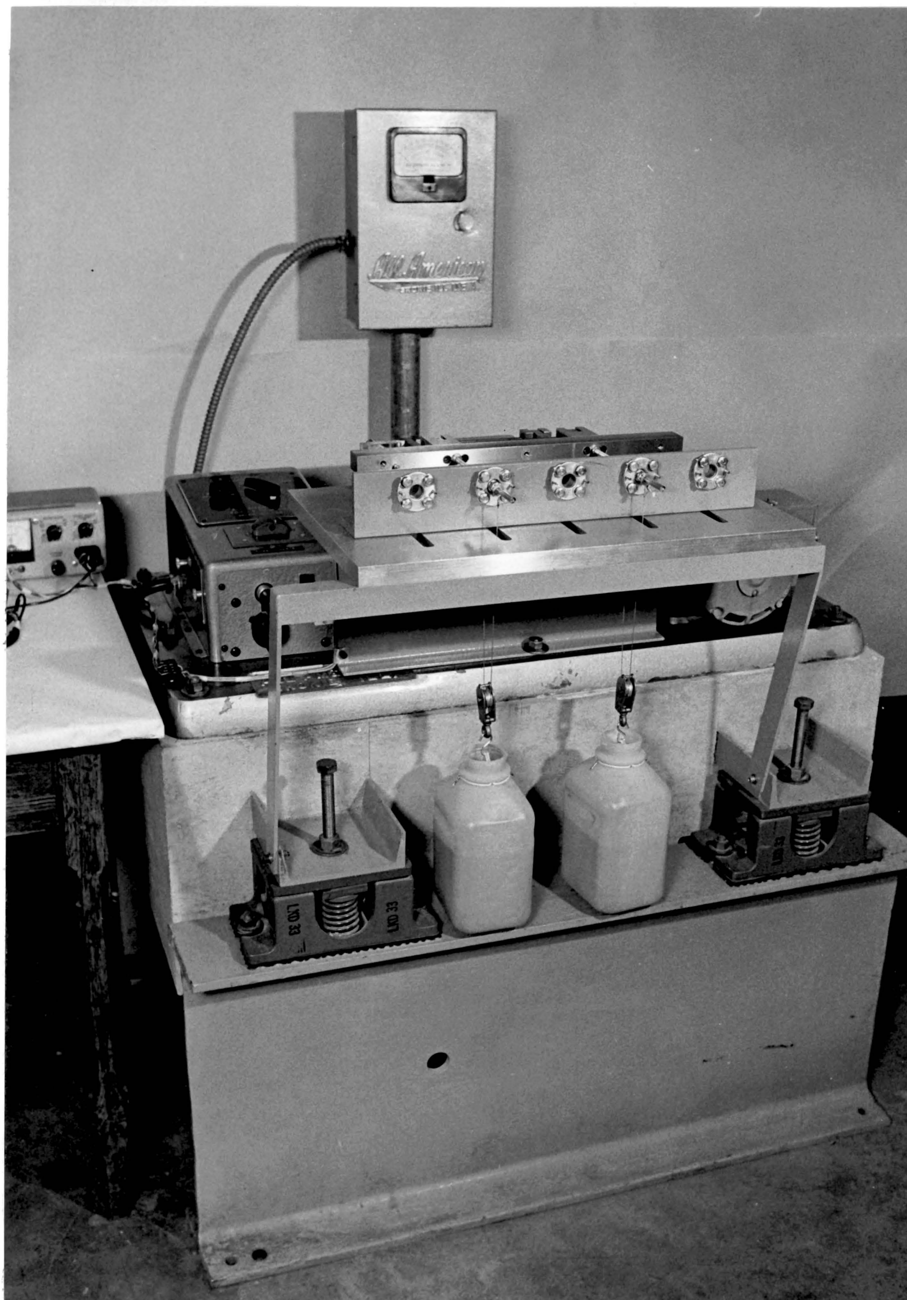

Figure 2. Overall View of Mark III

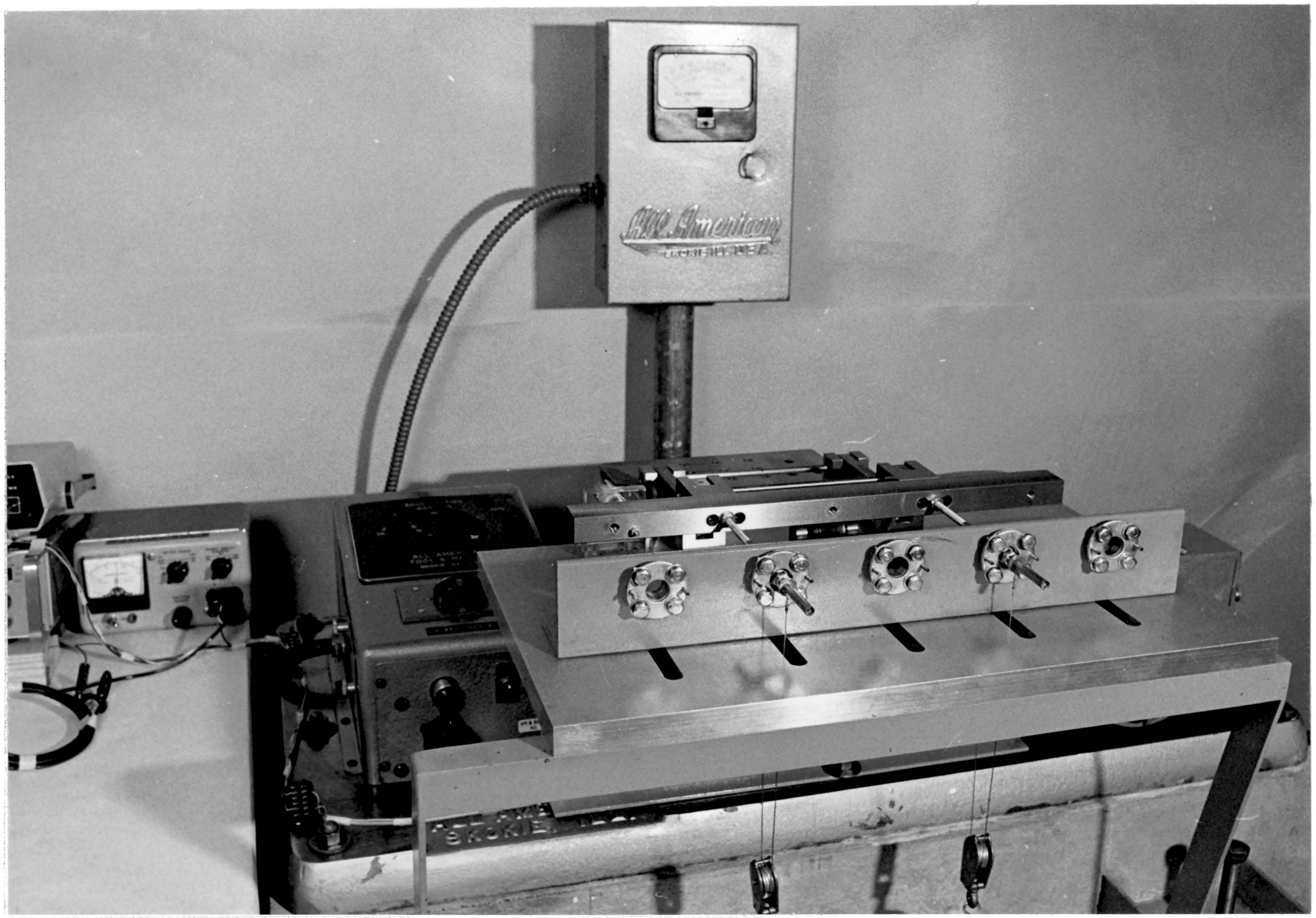

Figure 3. Overall View of Bearing/Cartridge Mounting Assembly

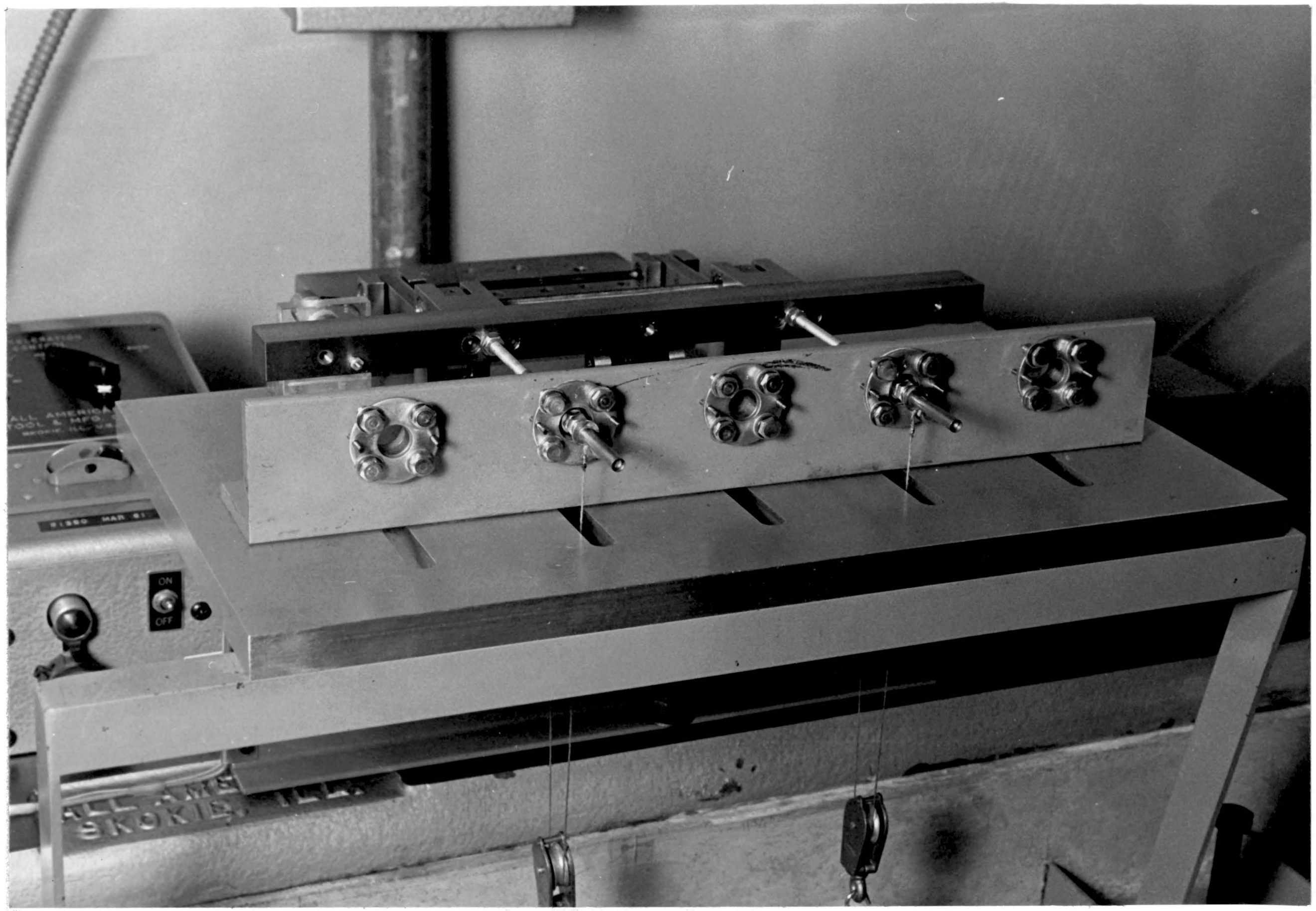

Figure 4. Overall View of Bearing/Cartridge Mounting Assembly

Test Specimens

Test samples used in this analysis consist of two parts: a bearing and a cartridge. When put together, an assembly of this type essentially represents a method of simply supporting a rotating shaft; a bearing supports the rotating shaft and it is in turn supported by the cartridge in which it is housed. Two such bearing/cartridge assemblies exist in each SSMG unit. Before going into a detailed description of the test samples and of the larger bearing/cartridge assemblies from which the samples were modeled, a brief description of the SSMG unit will be given.

The purpose of a ship service motor-generator set is to supply the ship with either AC or DC electrical power. The unit is manufactured by the General Electric Company of Erie, Pennsylvania. Design of the unit consists basically of a shaft-electrical rotor assembly which is supported at either end by radial ball bearings. When the unit is driven by a separate AC source, it supplies power to the ship's DC auxiliaries; when driven by batteries, the motor-generator set produces power for the ship's AC auxiliaries. The total weight of the unit is 110640 N (24878 lbf); the total rotor weight without its cooling fans is 32367 N (7278 lbf). The unit operates at a single speed of 1200 RPM. A photograph of the SSMG unit is shown in Fig. 5. To accommodate thermal expansion of the shaft, the motor-generator set is designed as a fixed-free system. The bearing on the DC end of the unit is locked axially by a cap pressing against the face of its outer race. The bearing on the AC end is allowed to float axially under a 8546 N (1920 lbf) preload applied to the face of its outer race by a spring pack assembly.[22] Sectional views of

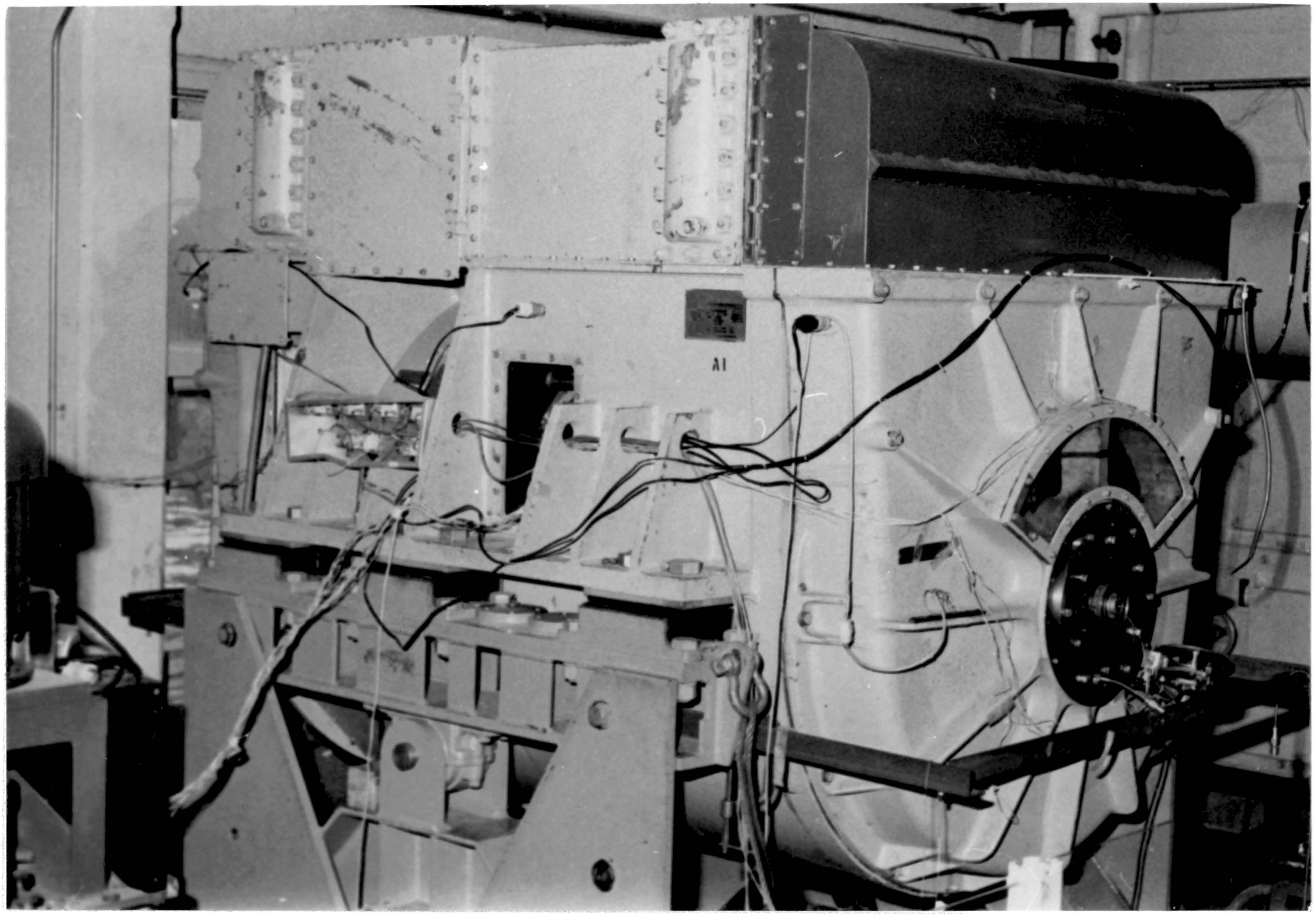

Figure 5. Ship Service Motor-Generator

both bearing/cartridge assemblies are shown in Figures 6 and 7.

The bearings which support the rotor-shaft arrangement were manufactured by NTN Bearing Corporation of America and are designed specifically for noise-critical applications. The bearing type used in the SSMG sets are 6320 series, ABEC 7, open-face deep groove radial ball bearings. Each bearing contains eight balls which are held relative to one another by a pressed steel cage. The bearing outside diameter is 215 mm (8.465 in.), the inside diameter is 100 mm (3.937 in.), and each is made of 52100 hardened steel which has a hardness of 62 R_c.[23] Both bearings are mounted on the unit's rotor-shaft assembly with an interference fit and held against shoulders machined on the shaft by a lockwasher and a locknut. The bearing outer races are housed in cartridge inserts that bolt to the unit's main frame. Both cartridges are made from AISI 1020 steel and have a hardness of approximately 80-90 R_B.[23] A clearance fit exists between the bearing and cartridge.

The test specimens used in the Mark III device match the corresponding SSMG components in geometry, materials, and hardness but of course are much smaller in size. The diameter of a test bearing outer race is 1.588 cm (0.625 in.) and the diameter of the inner race is 0.635 cm (0.250 in.). All tests samples have strict tolerance limits which were rigidly adhered to; a summary of bearing/cartridge tolerances and material characteristics is given for both the SSMG unit and Mark III in Table 2.

Motion Analysis

Figure 8 is a schematic representation of the motion produced in Mark III. Figure 9 is an exaggeration of the motion. The relationship

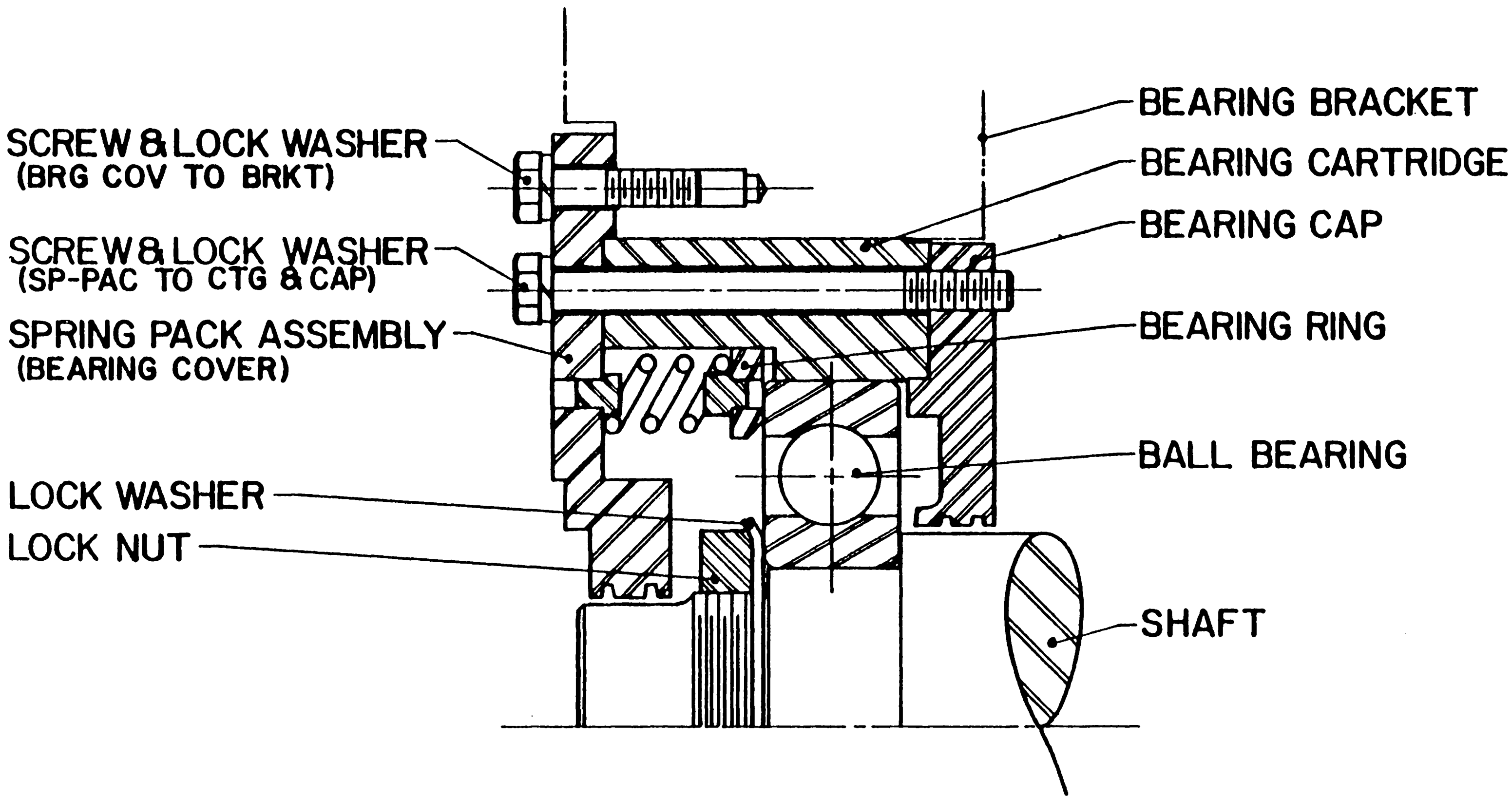

Figure 6.(34) Cross Section of SSMG Bearing Assembly - AC End

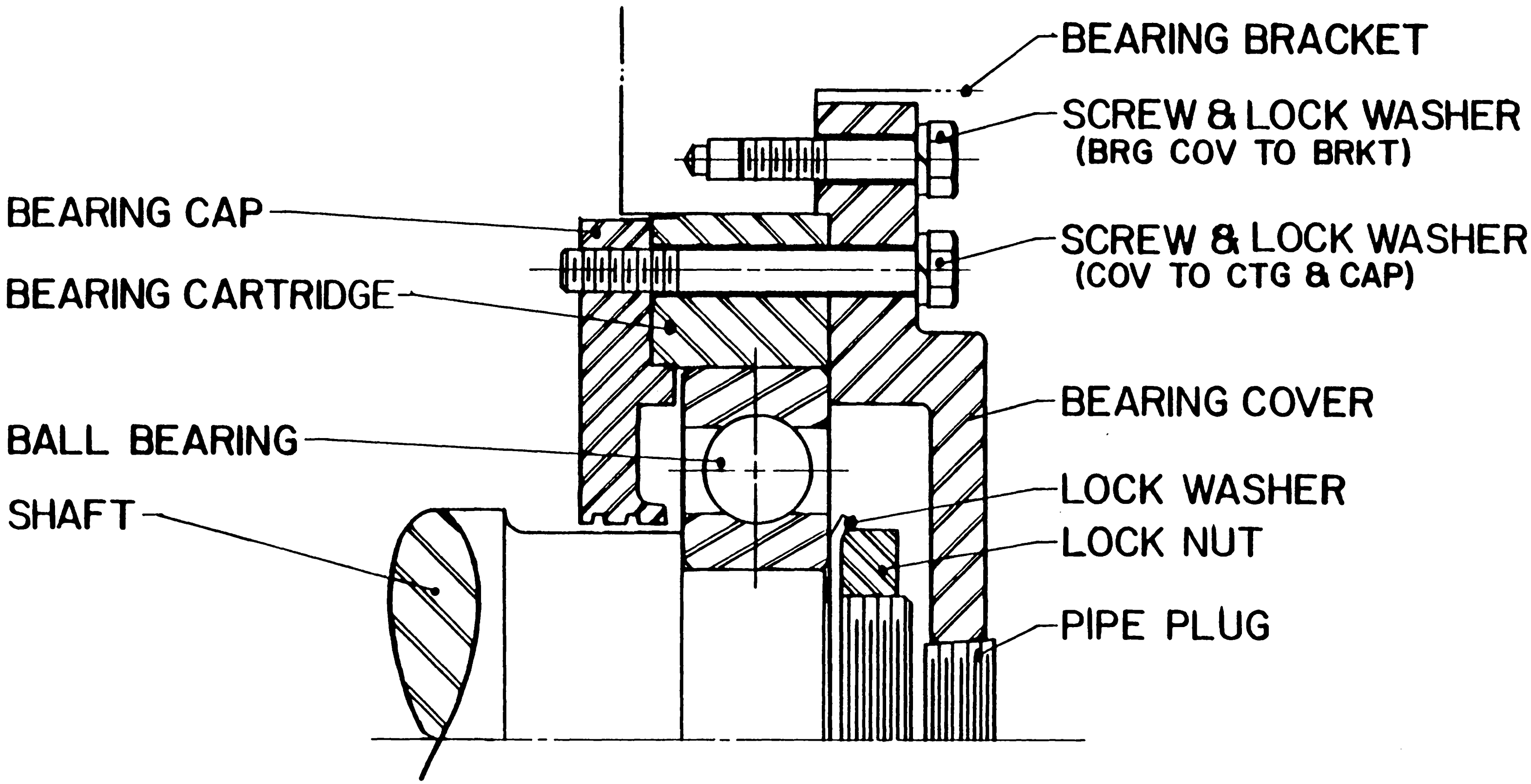

Figure 7.[34] Cross Section of SSMG Bearing Assembly - DC End

TABLE 2

BEARING and CARTRIDGE SIZES, MATERIAL, and TOLERANCES

SSMG UNIT:

1.	Bearing bore[35]	99.9924 - 100.0127 mm (3.9367 - 3.9375 in.)
2.	Bearing outside diameter[35]	214.9873 - 215.0025 mm (8.4641 - 8.4647 in.)
3.	Bearing width[35]	38.00 mm (1.4961 in.)
4.	Bearing material[35]	52100 hardened steel ($\approx$ 62 R_c)
5.	Bearing surface finish	0.30 μm CLA (11.81 μin. CLA)
6.	Cartridge bore[36]	215.0339 - 215.0466 mm (8.4659 - 8.4664 in.)
7.	Cartridge outside diameter[36]	304.775 - 304.800 mm (11.999 - 12.000 in.)
8.	Cartridge material[23]	SAE 1020 steel ($\approx$ 10 R_c)
9.	Cartridge surface finish	0.27 μm CLA (10.63 μin. CLA)

TABLE 2 (continued)

MARK III:

1.	Bearing bore[35]	6.3398 - 6.3525 mm (0.2496 - 0.2501 in.)*
2.	Bearing outside diameter[35]	15.8648 - 15.8775 mm (0.6246 - 0.6251 in.)
3.	Bearing width[35].	4.978 mm (0.196 in.)
4.	Bearing material[35]	52100 hardened steel (≈ 62 R_c)
5.	Bearing surface finish	0.17 μm CLA (6.69 μin. CLA)
6.	Cartridge bore	15.9029 - 15.9131 mm (0.6261 - 0.6265 in.)**
7.	Cartridge outside diameter	25.40 mm (1.00 in.)
8.	Cartridge material	SAE 1020 steel (≈ 10 R_c)
9.	Cartridge surface finish	0.35 μm CLA (13.78 μin. CLA)

*Bearing Source: NTN Bearing Corporation of America (Bearing No. R4).

**Cartridge Source: Precision Hone, 58 Boonton Avenue, Butler, New Jersey, 07405.

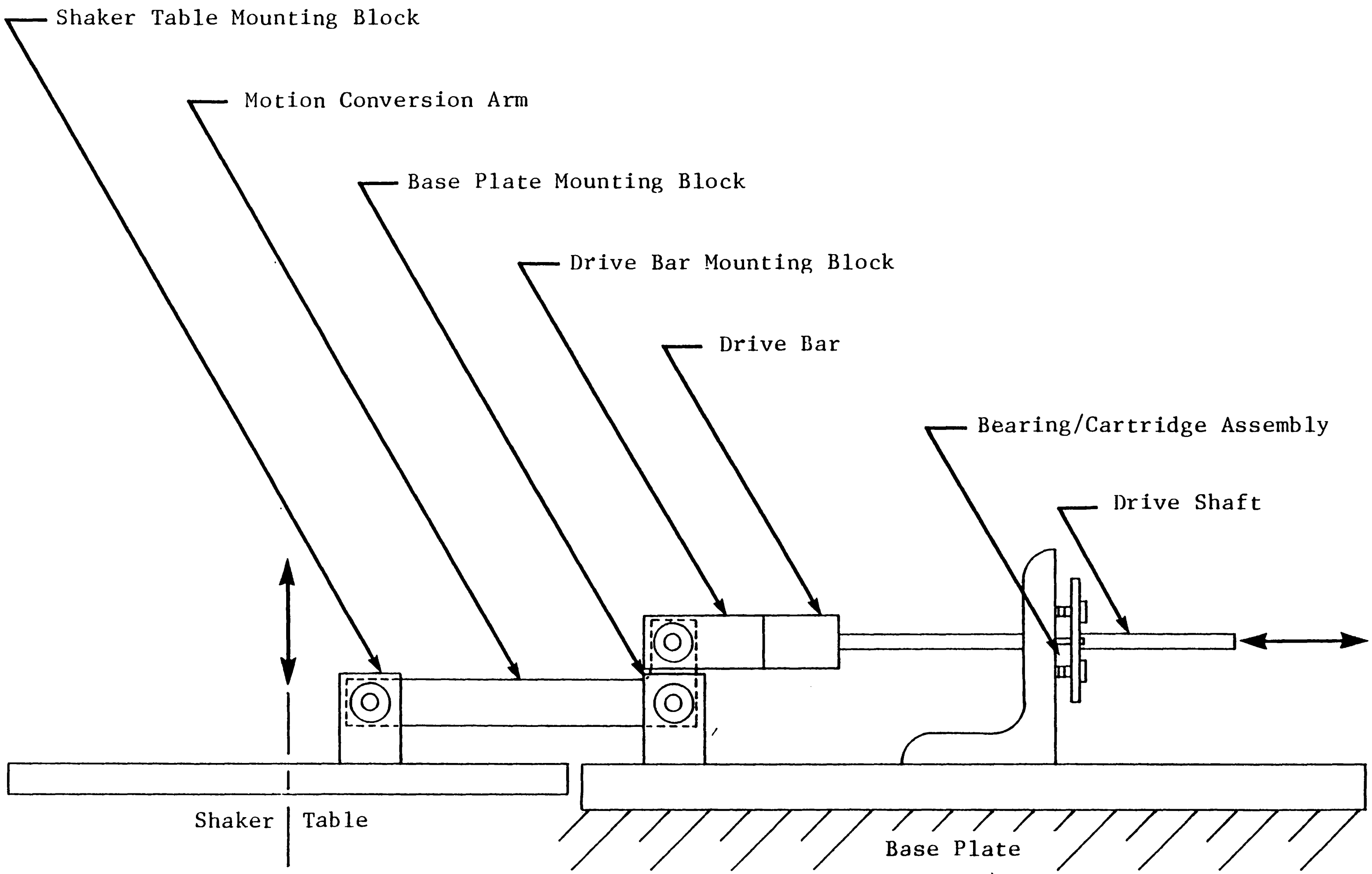

Figure 8. Schematic Representation of Motion in Mark III

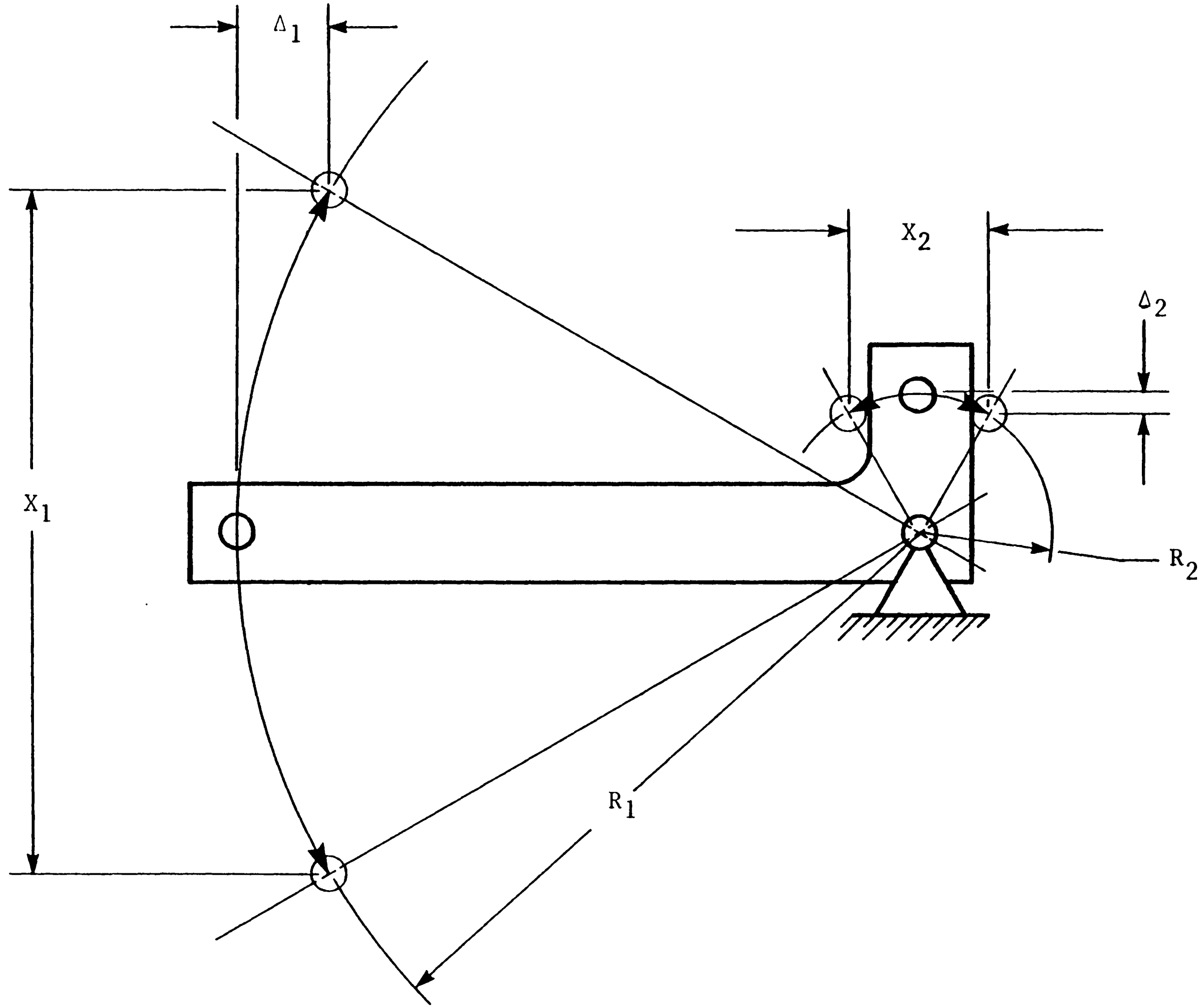

Figure 9. Exaggeration of Motion in Mark III

between the input motion, the output motion, and the dimensions of the motion conversion arms is given below:

$$\frac{X_1}{R_1} = \frac{X_2}{R_2}$$

where X_1 = displacement of shaker table

X_2 = displacement of drive shafts

The relationship between the same parameters and the arc deflections Δ_1 and Δ_2 is given below. The derivation of these relationships can be found in Appendix D.

$$\Delta_1 = R_1 \left\{ 1-\cos\left[\sin^{-1}\left(\frac{X_1}{2R_1}\right)\right]\right\}$$

$$\Delta_2 = R_2 \left\{ 1-\cos\left[\sin^{-1}\left(\frac{X_2}{2R_2}\right)\right]\right\}$$

The displacement of the shaker table is reduced by a factor of five since R_1 and R_2 are equal to 127 mm (5 in.) and 25.4 mm (1 in.) respectively. (It should be noted that amplitude of motion implies zero-to-peak motion as compared to displacement which refers to peak-to-peak motion.)

As Figure 9 reveals, points at which the motion conversion arms connect to other parts of the apparatus move through an arc. As a result, motion imparted to the bearings by the arms is not strictly linear. Theoretically speaking, the axis of the bearing would only be parallel to the axis of the cartridge at maximum displacement. Ordinarily then this might represent a serious limitation of the apparatus in performing fretting corrosion studies. Calculation of Δ_2 and the angle of the bearing axis with respect to the cartridge axis at maximum operating conditions shows that the deviation from linear motion is insignificant.

$$\Delta_1 = 0.0254 \text{ mm } (0.0010 \text{ in.})$$

$$\Delta_2 = 0.0051 \text{ mm } (0.0002 \text{ in.})$$

$$\alpha = 0.0014^{\circ}$$

An angle of tilt equal to 0.0014° means that one side of the bearing is 0.12 μm (4.9×10^{-6} in.) higher than the other. Talysurf traces taken in the axial direction of the bearing and cartridge yield CLA roughness measurements of 0.17 μm and 0.35 μm (6.69×10^{-6} in. and 13.78×10^{-6} in.) for the bearing and cartridge, respectively. (These values are an average of four readings taken at 90° intervals around the circumference of a bearing outer race and a cartridge bore: the bearing/cartridge set from which these readings were taken was randomly chosen from the undamaged supply used in this study.) Taking into account the magnitude of the CLA measurements and the fact that Mark III was run at approximately 30% maximum amplitude for this study, the deviation from linear motion is found to be negligibly small.

Fatigue Testing Machine

The machine that is the source of the relative motion between the bearings and cartridges is a vibration fatigue testing machine which consists essentially of four components: a vertical motion shaker table, a variable speed drive motor, a motor speed control, and a frequency readout gage. The specific name of the vibration machine is The All American Vibration Fatigue Testing Machine, model number 10-VA-T: it was built by the All American Tool and Manufacturing Company of Skokie, Illinois. Rotary motion supplied by the variable speed drive motor turns an eccentric in the shaker table mechanism which displaces the shaker table vertically. All four components are mounted on a cast iron plate which is rigidly attached to a concrete foundation. The foundation is isolated from the floor by four vibration isolation mounts.

Drive Linkage

The drive linkage which converts vertical motion produced by the vibration machine to horizontal motion was designed and built by the author of this thesis and consists essentially of six components:

1. Shaker Table Mounting Blocks
2. Base Plate Mounting Blocks
3. Drive Bar Mounting Blocks
4. Motion Conversion Arms
5. Drive Bar
6. Drive Shafts

All parts used in the drive linkage are made from SAE 1020 cold rolled steel and are shown in Figure 10. A brief discussion of each component and the design criteria used to determine physical dimensions of components will now follow.

Shaker Table Mounting Blocks: The purpose of this component is to connect the motion conversion arms to the shaker table. Each block is 3.81 cm wide by 2.54 cm thick by 3.81 cm tall (1.5 in. by 1.0 in. by 1.5 in.) and is fastened to the shaker table by a 1/4 inch-#20 thread high-strength machine screw. The blocks are machined so that the motion conversion arms connect to them by a shaft that fits into bearings

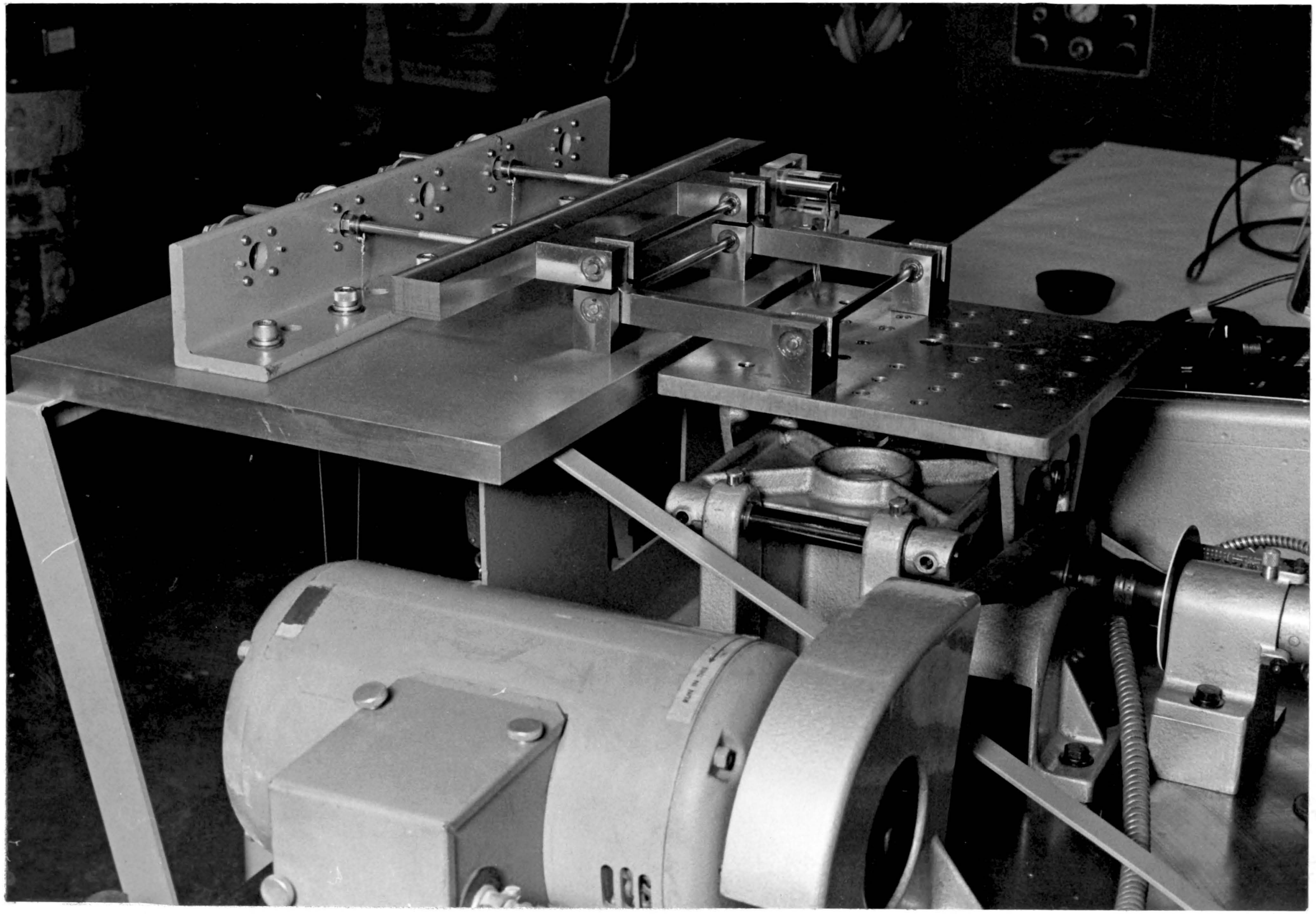

Figure 10. Mark III Drive Linkage

housed by the blocks; each block has two bearings.

<u>Base Plate Mounting Blocks</u>: The base plate mounting blocks connect the motion conversion arms to the base plate. Physical size, machining, and mounting method for these blocks is identical to that for the shaker table mounting blocks.

<u>Drive Bar Mounting Blocks</u>: The purpose of the drive bar mounting blocks is to connect the motion conversion arms to the drive bar. Like other connections made between mounting blocks and the motion conversion arms, a shaft is slid through holes machined in the arms and into bearings held by the blocks. The shaft is then locked into place by set screws in the arms. Each block is 3.81 cm wide by 2.22 cm thick by 5.08 cm long (1.5 in. by 0.9 in. by 2.0 in.) and is machined for two bearings. Connection between the drive bar and the blocks is made by four 1/4 inch-#20 thread high strength machine screws (two screws per block) fitting into counterbores drilled in the drive bar and threading into the base of each block.

<u>Motion Conversion Arms</u>: The strength criteria used to determine section dimensions for the motion conversion arms is based on an assumed coefficient of friction of 1.5 between each bearing and cartridge for simultaneous operation of all five bearing/cartridge sets at maximum loading conditions. Under these circumstances, a section thickness (arm width) of 1.27 cm (0.50 in.) and a section height (arm thickness) of 1.91 cm (0.75 in.) allow a maximum motion loss of 11.37 μm (0.00045 in.) to occur for the total displacement. Though the friction coefficient between a bearing and a cartridge may reach values as high as 1.0[10], a coefficient of 1.5 represents conservative design. It should be noted

though that only two of the five available testing positions on Mark III were used simultaneously in this study. As a result, the motion conversion arms are overly designed but loss of motion due to bending of the arms is minimized.

Drive Bar: The physical dimensions of the drive bar are: 2.22 cm wide by 3.18 cm thick by 43.18 cm long (0.88 in. by 1.25 in. by 17.00 in.). Fastening to the drive bar are five drive shafts; the central shaft is located at the bar's midpoint and the other shafts are placed on either side at a 9.21 cm (3.62 in.) center distance. Using a friction coefficient of 1.5 and maximum loading conditions, the largest calculated deflection that will occur in the bar is 3.18 μm (1.25×10^{-4} in.). This deflection occurs at either end of the bar which simulates loading of a cantilever beam.

Drive Shafts: The main purpose of the drive shafts is to transmit motion from the drive bar to the bearings; a secondary purpose is to provide a means for applying load to the bearings. The drive shafts are made from 1/4 inch-#20 threaded steel rod and have a length of 20.32 cm (8 in.). Each shaft is threaded into the drive bar and locked in place by tightening a nut on the shaft up against the drive bar.

Test Specimen Mounting

Mounting the test specimens in Mark III consists of three steps: first, the bearings are mounted on the drive shafts; next, the cartridges are slid onto the bearings and clamped in place; finally, the loads are suspended from the drive shafts. This brief explanation gives a general outline of the steps involved but a more detailed discussion will be given below since the complete procedure is necessarily more complicated for purposes of reproducibility.

Figure 11 is a photograph of a specimen mounting position on Mark III prior to specimen installation; the drive shaft is shown extending through the cartridge seat. All specimens used in this study are permanently marked so that not only is the test position (one of the five available mounting locations) on Mark III known but the bearing/cartridge rotational alignment and face direction are known also. The nuts and washers shown on the drive shaft form half of the bearing clamping assembly. After a bearing is slid on the drive shaft and up against the first set of nuts and washers, a second set is threaded onto the drive shaft to clamp the bearing in place. The washers which make contact with a bearing have diameters that are slightly smaller than that of a bearing outer race and are covered on one side by paper to avoid metal-to-metal contact with the bearing. The outer washers serve as a back-up and the outer nuts provide positive lock so that vibration will not loosen the assembly during a test. The inner nuts are tightened against the bearing to a maximum of 0.56 Nm (5 in.-lbf) and the outer nuts are snugged against the inner nuts.

A cartridge is now slid onto the installed bearing and up against its seat. Again, paper washers are placed between the cartridge and its clamping surfaces to avoid metallic contact. The diameter of each cartridge seat is larger than the outside diameter of a cartridge to allow for any lateral misalignment that may exist between a drive shaft and the geometric center of a cartridge seat. Once the cartridge is in place, its clamping plate is slid up against it. Four bolts are then installed and alternatly tightened against the plate; the cartridge is

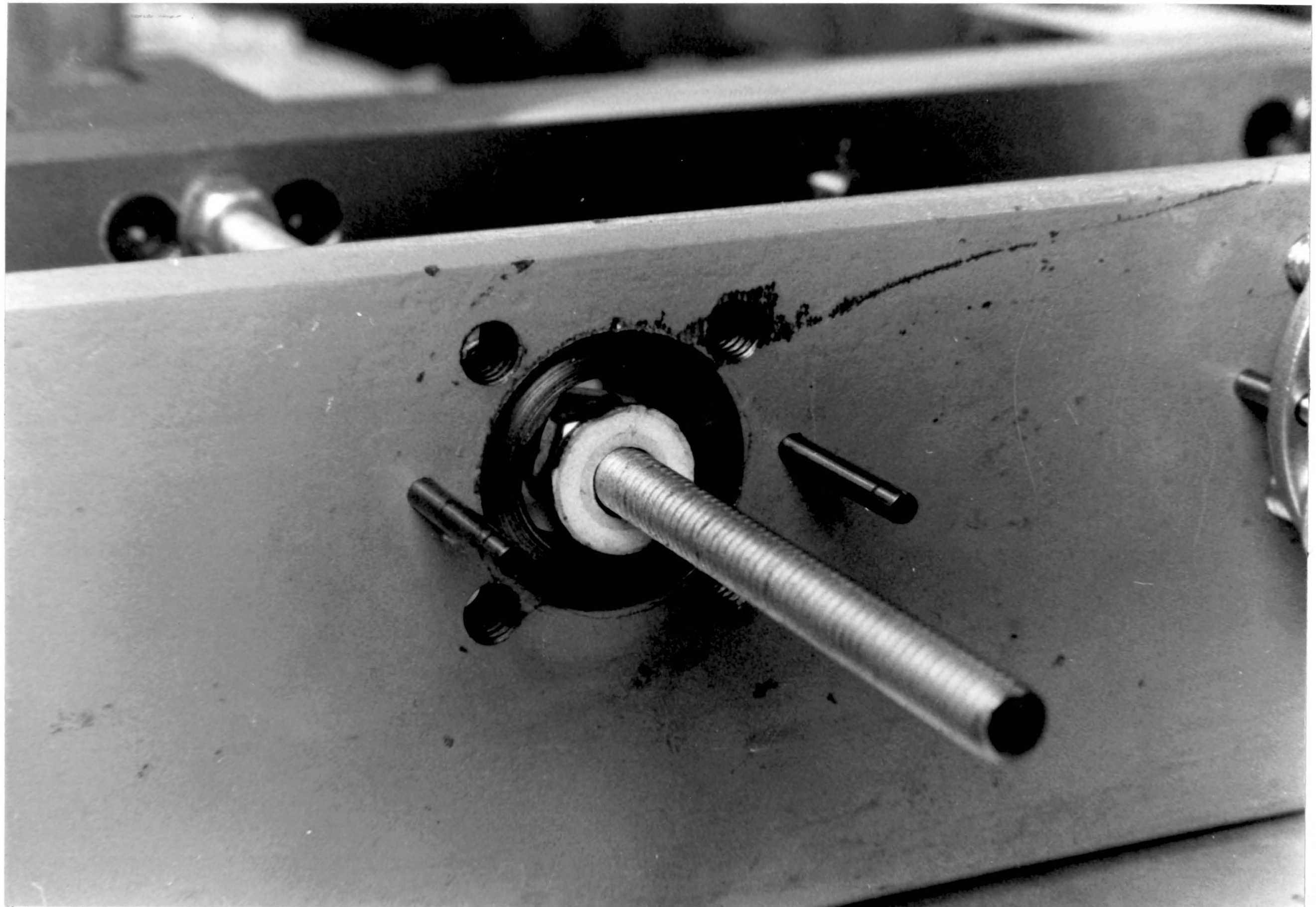

Figure 11. Sample Mounting Position Prior to Installation of Test Sample

now clamped in place by the plate. Finally, the load is suspended from the drive shaft and the bearing/cartridge assembly is ready for testing. Figures 12 through 15 give a complete photographic record of the installation procedure.

Displacement Measurement

Relative motion between a bearing and cartridge is obtained by offsetting an eccentric in the shaker table mechanism. Measurement of this motion is accomplished by a Linear Variable Differential Transformer (LVDT) which connects to the drive bar of the drive linkage. The desired displacement (twice the amplitude) is set in the shaker table mechanism and is subsequently measured by the LVDT under loaded conditions. The same procedure is followed if further adjustment of the eccentric offset is necessary.

Cycle Counter

In a fretting corrosion study of this type, it is essential to know the total relative sliding distance produced between the bearing and cartridge. In Mark III, this was accomplished by electronic means. A circular disk with a small hole near its outer circumference was mounted on the shaker table mechanism drive shaft; a single revolution of the shaft corresponds to one cycle of motion between a bearing and cartridge. Straddling the disk is a photoemitting diode and a collector. When the hole in the disk passes between the diode and the collector, an electrical impulse is sent to a separate timer-counter instrument. The switching speed of the source-sensor assembly is five microseconds which corresponds to a maximum operational frequency of 200 kHz. A Schmidt trigger was

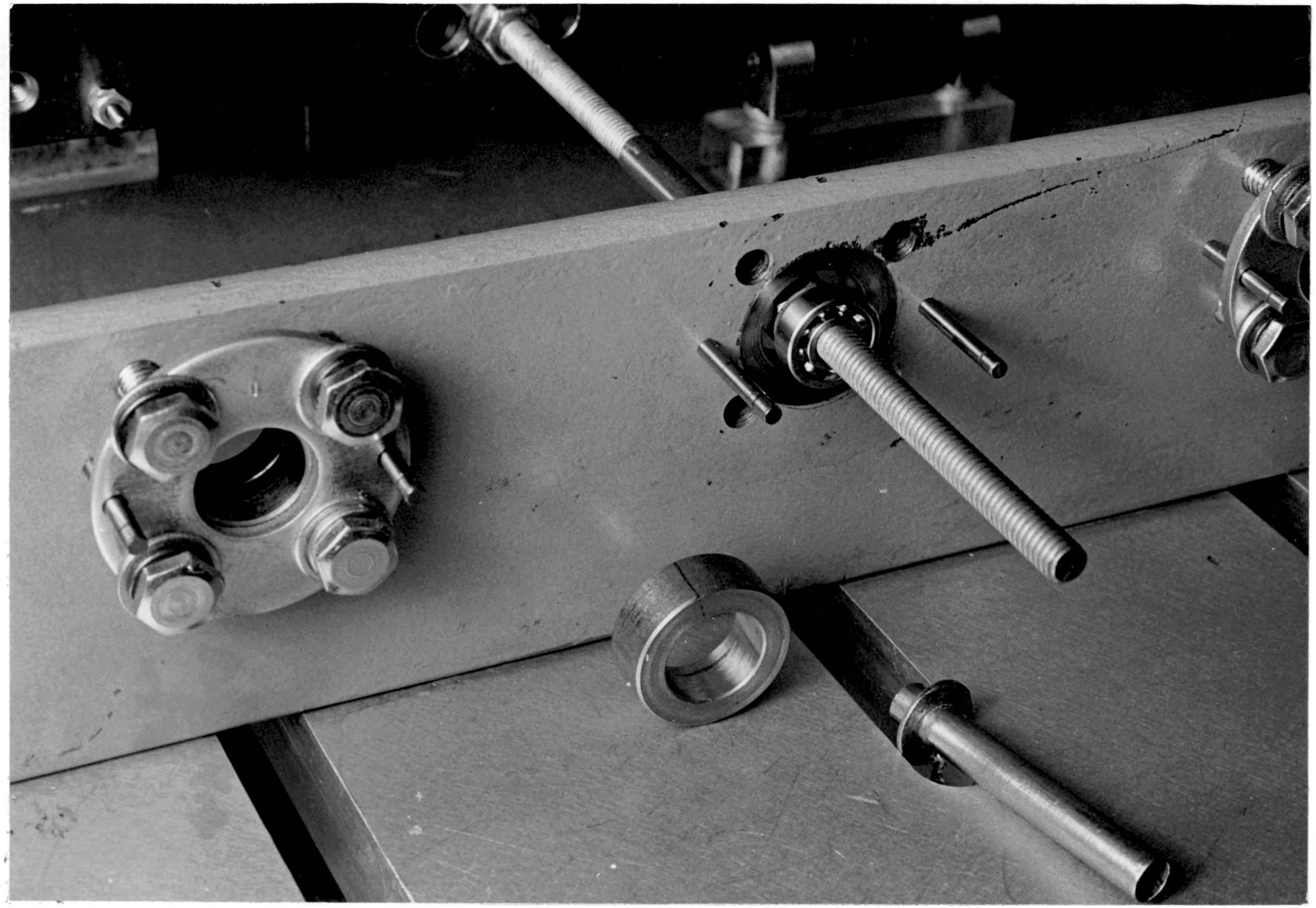

Figure 12. Sample Mounting Position - Bearing Initially Located

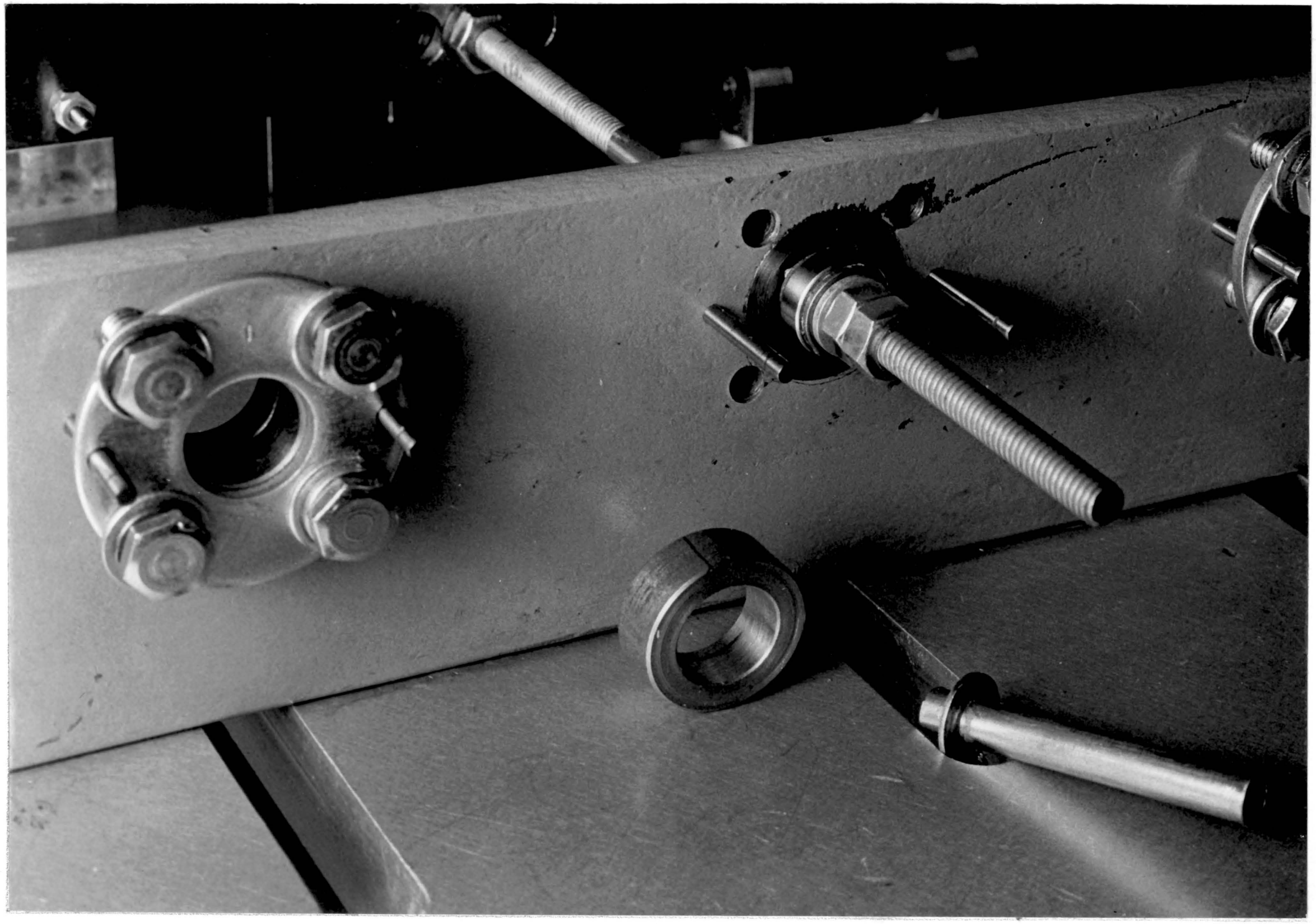

Figure 13. Sample Mounting Position - Bearing Locked in Place

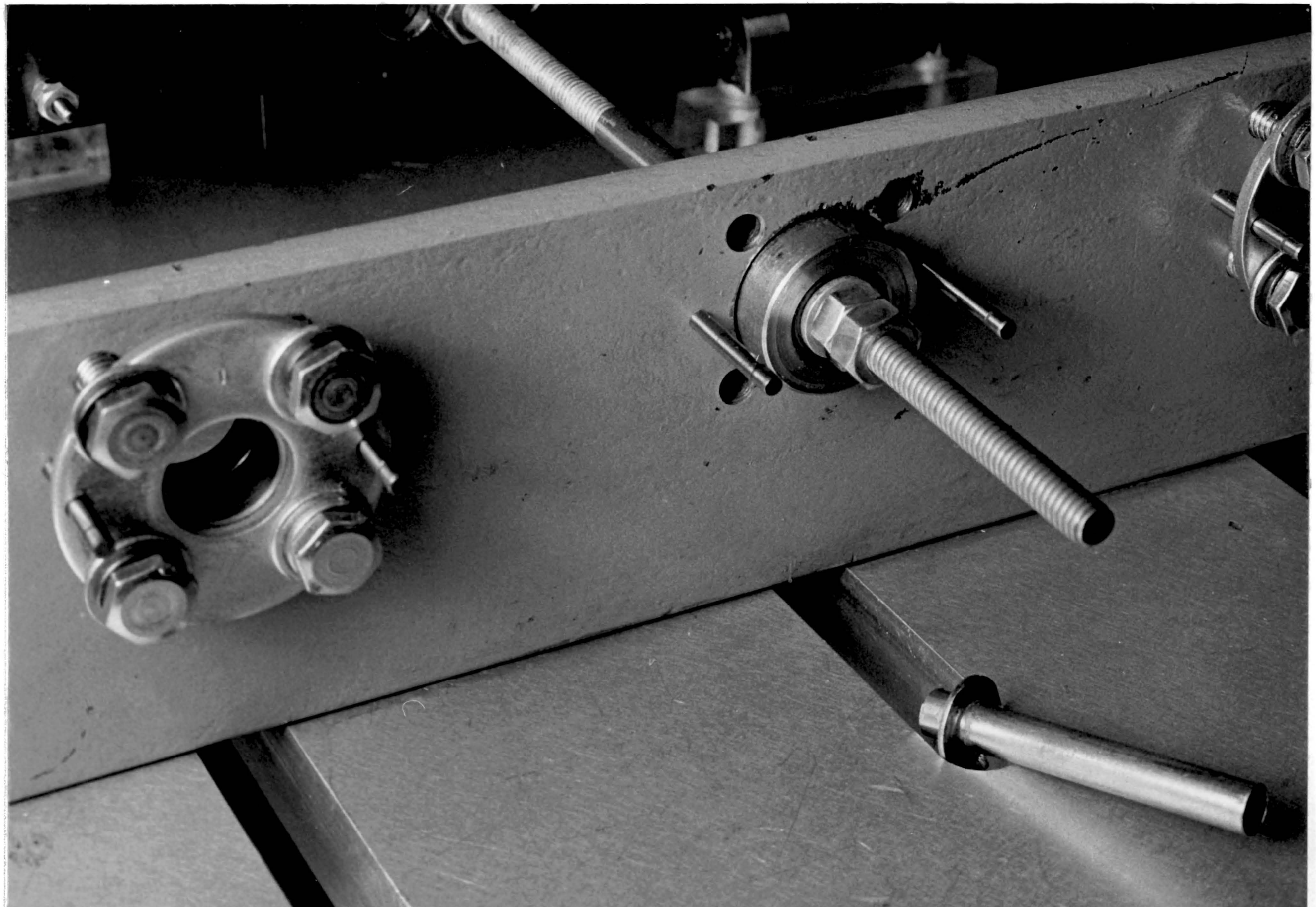

Figure 14. Sample Mounting Position - Cartridge Initially Located

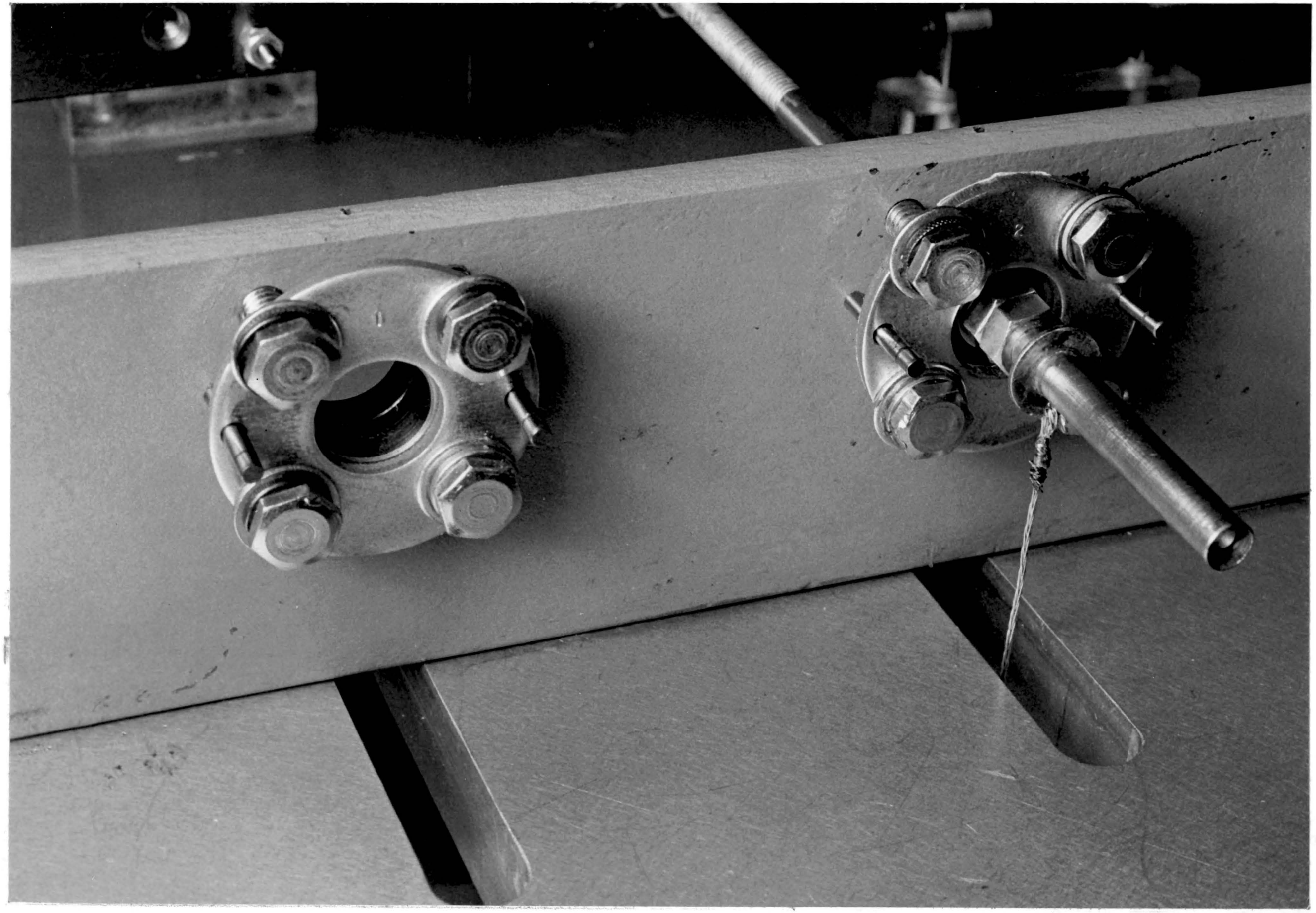

Figure 15. Sample Mounting Position - Bearing/Cartridge Installation Complete

used in the source-sensor circuit to insure that the impulse voltage sent by the collector was either above or below the trigger voltage of the timer-counter. Without the Schmidt trigger the number of cycles recorded by the timer-counter could possibly jump tenfold in a single instance. A photograph of the cycle counter assembly is shown in Figure 16.

The relationship between amplitude, total cycles, and the amount of relative motion produced between the bearing and cartridge is given below.

$$X = 4AN$$

where N = number of cycles

A = amplitude of motion

X = total amount of relative motion

Load Application

Load is applied to each bearing/cartridge assembly by means of a load-pulley-cylinder arrangement. A container carrying lead shot is suspended from a pulley which hangs directly below the bearing's geometric center. A single cable threads through the pulley and attaches to cylinders located on either side of the bearing. Cylinders were used instead of attaching the cable directly to the drive shaft so as to distribute the load more evenly along the shaft. The horizontal component of cable tension, which results from a slight angle made by the cable in traveling from a cylinder to one side of a pulley, keeps the cylinders in contact with the bearing locking nuts during operation. Figure 17 is a photograph of the arrangement.

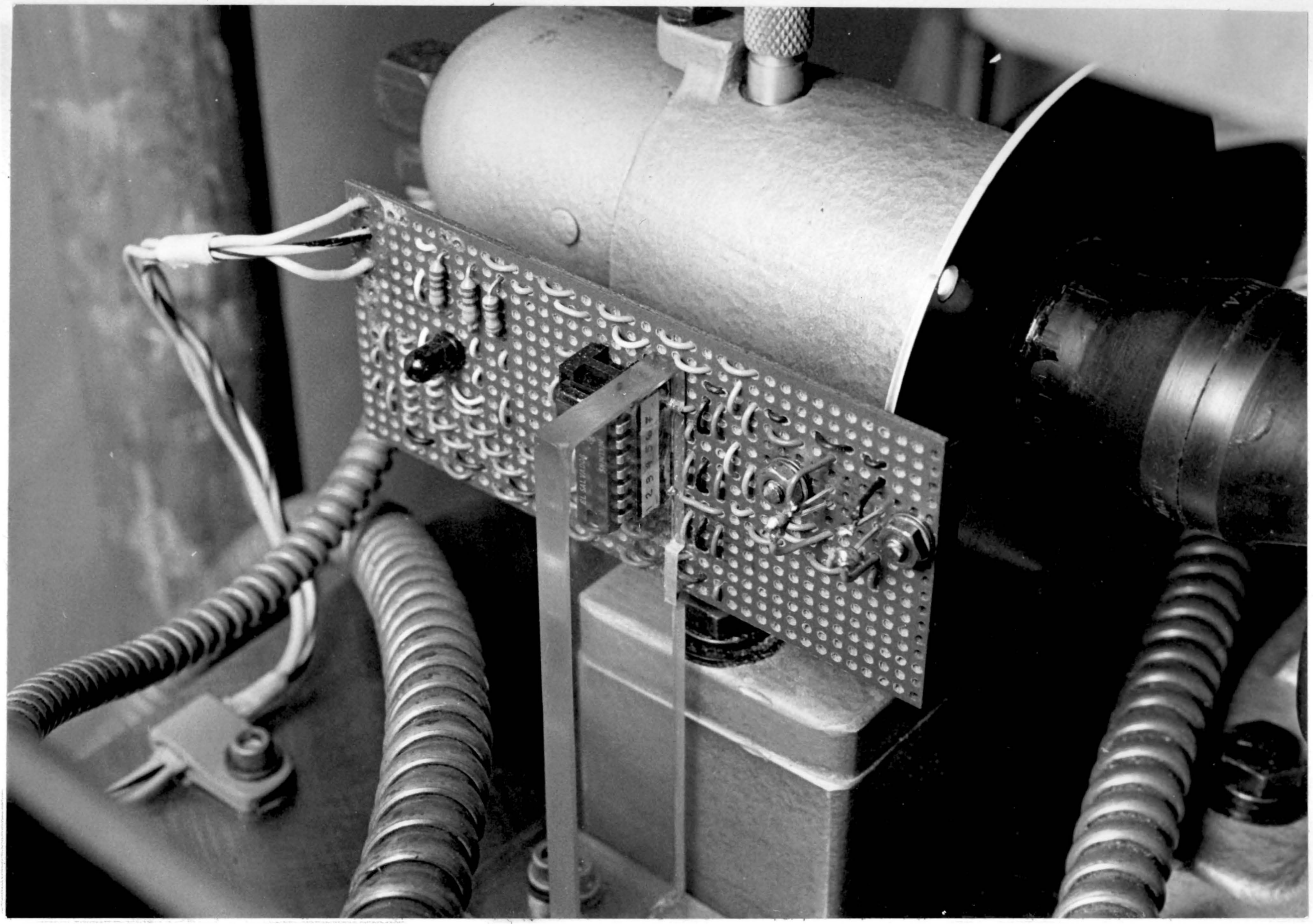

Figure 16. Cycle Counter Assembly

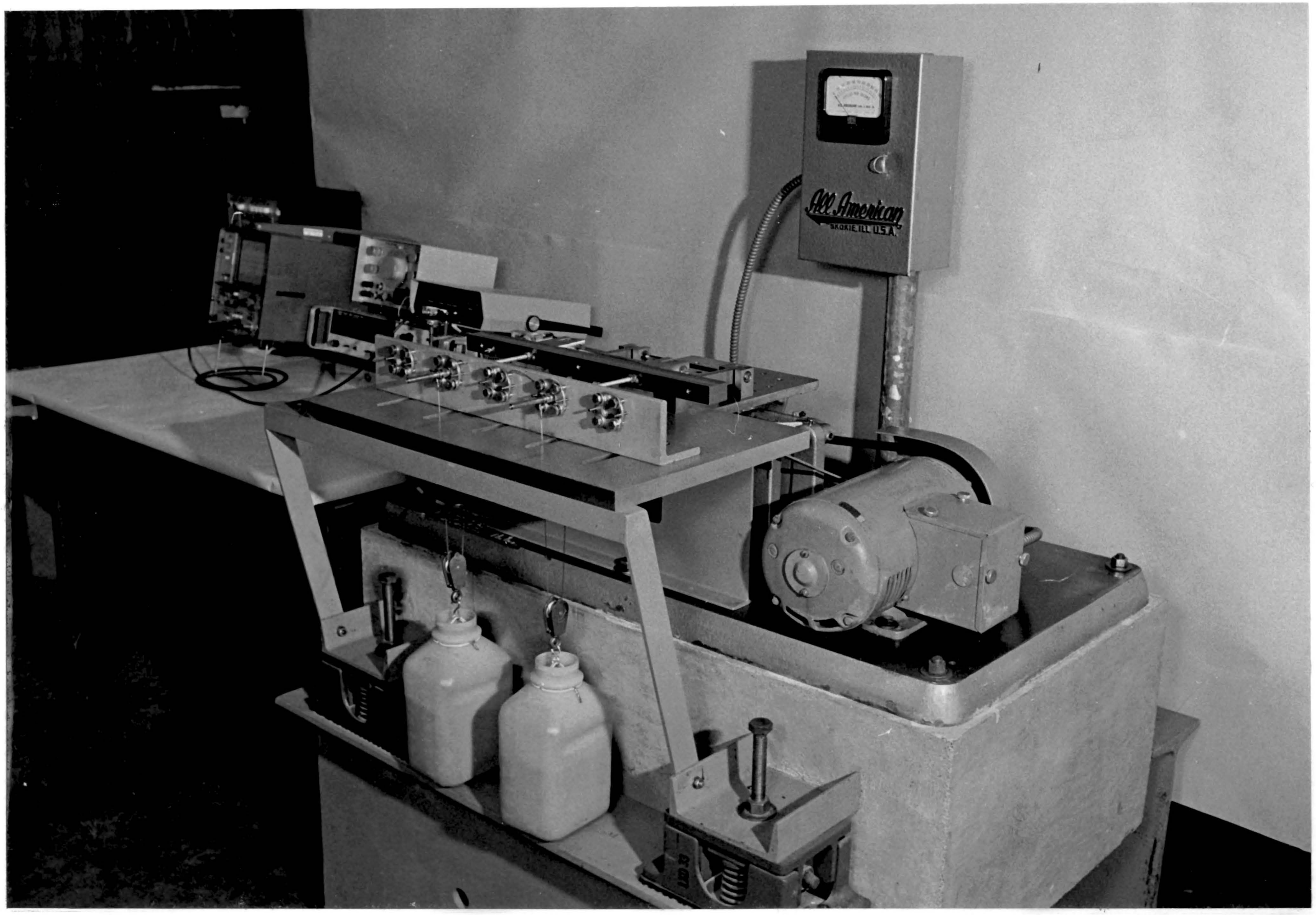

Figure 17. Bearing/Cartridge Loading Arrangement

Preliminary Experiments

Four experiments were run in which only one of three variables was allowed to change in each experiment. The purpose of allowing only one independent variable in each experiment to change was two-fold: first, a better idea of how that variable influences weight loss of a bearing/cartridge assembly could be obtained; secondly, an easier comparison can be made between theoretical and experimental results. The variables examined included cycle duration (distance traveled by the bearing relative to the cartridge), load, and amplitude. The amount of weight lost by the test specimens over the period of an experiment was used as a means of determining the extent of fretting corrosion that occurred at the interface. The experiments are listed below and are discussed in further detail.

1. Weight Loss versus Cycle Duration (dry contact)
2. Weight Loss versus Cycle Duration (lubricated contact)
3. Weight Loss versus Amplitude
4. Weight Loss versus Load

Weight Loss versus Cycle Duration (dry contact): In this experiment, the load was set at 80 N (17.99 lbf), frequency at 30 Hz, and amplitude of relative motion at 100 μm (0.0039 in.). Five separate runs were made using two bearing/cartridge sets for each run. The total distance traveled by the axially oscillating bearing relative to the stationary cartridge for the five runs was 40 m (131.23 ft.), 80 m (262.46 ft.), 120 m (393.70 ft.), 160 m (524.93 ft.), and 200 m (656.16 ft.). Contact between the bearing and cartridge was dry (clean and unlubricated).

Weight Loss versus Cycle Duration (lubricated contact): This experiment is identical to that described above except that the interface between the bearing and cartridge was lubricated by a high performance ball/roller bearing grease (Mobil, DOD-G-24508A). 0.0005 cc (2.79 x 10^{-4} in.^{3}) of this lubricant was applied to each bearing/cartridge set by wiping a thin film of it on the bearing outer race and cartridge bore.

Weight Loss versus Amplitude: Five separate runs, each of a different amplitude, were made in this experiment. The load and frequency were kept at the values set in previous experiments and the total distance traveled by the bearings for each run was 40 m (131.23 ft.). The amplitudes for each of the five runs were 400 μm (0.0157 in.), 200 μm (0.0079 in.), 100 μm (0.0039 in.), 50 μm (0.0020 in.), and 25 μm (0.0010 in.) respectively. Contact between the bearing and cartridge was dry.

Weight Loss versus Load: Again, five separate runs were made--each of a different load. The amplitude was set at 100 μm (0.0039 in.), the frequency at 30 Hz, and the distance traveled by the bearing relative to the cartridge at 120 m (393.70 ft.). The five loads that were investigated were: 160 N (35.98 lbf), 128 N (28.78 lbf), 96 N (21.59 lbf), 64 N (14.39 lbf), and 32 N (7.20 lbf). Contact between the bearing and cartridge was dry.

Statistical Design

A four-factor, two-level designed experiment was carried out to investigate the influence of four parameters, and any interactions thereof, on the extent of fretting corrosion that occurred at the interface of a bearing/cartridge set. The parameters used in this analysis were load, frequency, amplitude, and presence of a grease at the interface. Each parameter has two levels of magnitude which, in an analysis of variance procedure, necessitates sixteen separate runs--four factors at two levels each. In each run, two sets of bearings and cartridges were used to obtain an experimental error. The specific number used to quantify the extent of fretting corrosion at the interface is the total weight lost by each bearing/cartridge set for a run. The total number of cycles for each run is such that the total relative motion produced between a bearing and cartridge is the same for each run. The degree of separation between the two levels for each factor is given below and is followed by a listing of the sixteen runs.

In an analysis of variance procedure, averages are used to estimate two variances which are compared by a two variance F-test. The variation between weight loss measurements obtained for each run is presumably caused by experimental error. The variation between runs of the average weight loss found for each run is presumably caused by both experimental error and any inherent differences between the runs. If the variation among the runs is significantly larger than the variation within the runs, then we can reject the null hypothesis which says each run has the same mean weight loss, i.e., no matter what combination of parameters is used, the average weight loss found for each run will not significantly differ between runs. There are three important advantages of using an analysis of variance procedure, namely:

a. The results of the statistical analysis will indicate which main effects are significant; information concerning the confidence level of each main effect is also given.

b. The results of the analysis will indicate which interactions are significant. Again, confidence levels for each interaction are given.

c. The residual variance (error variance) determined in the analysis will give us a good estimate of the error involved in the weight loss measurements.

TABLE 3

LEVELS USED IN STATISTICALLY-DESIGNED EXPERIMENT

Factor	Level 1	Level 2	Ratio
LOAD	15 N	90 N	6
FREQUENCY	15 Hz	45 Hz	3
AMPLITUDE	50 μm	150 μm	3
GREASE	NO	YES	

TABLE 4

TEST RUNS USED IN STATISTICAL DESIGN

Run Number	Frequency	Grease	Load	Amplitude
1	F_1	No	W_1	A_1
2	F_1	No	W_1	A_2
3	F_1	No	W_2	A_1
4	F_1	No	W_2	A_2
5	F_1	Yes	W_1	A_1
6	F_1	Yes	W_1	A_2
7	F_1	Yes	W_2	A_1
8	F_1	Yes	W_2	A_2
9	F_2	No	W_1	A_1
10	F_2	No	W_1	A_2
11	F_2	No	W_2	A_1
12	F_2	No	W_2	A_2
13	F_2	Yes	W_1	A_1
14	F_2	Yes	W_1	A_2
15	F_2	Yes	W_2	A_1
16	F_2	Yes	W_2	A_2

F_1 = 15 Hz , F_2 = 45 Hz

W_1 = 15 N (3.37 lb.) , W_2 = 90 N (20.24 lb.)

A_1 = 50 μm (0.0020 in.) , A_2 = 150 μm (0.0060 in.)

Test Procedure

The procedures used in this study consist basically of six steps:

1. Test sample cleaning
2. Sample weighing
3. Installation of samples in the apparatus
4. Running the test
5. Test sample cleaning
6. Sample weighing

Initially, each bearing/cartridge set is immersed in a flask of hexane which is placed in an ultrasonic washer. After being washed for approximately ten minutes, the set is removed and placed in the first of four successive flasks of boiling solvent. The first two flasks contain 200 ml of hexane while the remaining two contain 200 ml of methanol. The bearing/cartridge set is then removed from the last flask and allowed to air dry. Each bearing/cartridge set is rinsed with clean solvent (of the same type from which it was removed) immediately after it is taken from a flask. The solvent in each flask is changed after ten washings.

Next, the bearings and cartridges are individually weighed on a chemical balance and the weight is recorded; the balance is accurate to 0.0001 g. The test samples are now installed in Mark III and are ready to run. Before starting a test, the date, time, and percent relative humidity are recorded. The test is now started and allowed to run the requisite number of cycles.

After a test has been completed, the samples are removed and cleaned using the same procedure previously outlined. Samples are then weighed and the weight is recorded. Weight loss for a bearing/cartridge set is determined by addition of the individual losses of a bearing and cartridge. The weight lost by either a bearing or a cartridge is found by subtracting the final weight from the initial weight. After the second weighing, each set is sealed in a marked container and stored for possible future analysis. In conducting the tests, all samples are handled with plastic gloves so that no contact between skin and metal occurs.

RESULTS

General Observations

Generally speaking, the overall performance of Mark III during the course of experimentation was excellent. The device produced fretting corrosion at a bearing/cartridge interface in as little as two cycles and ran successfully for a number of tests which lasted over eleven hours each. The only problem that developed in the apparatus which was not discovered in the shakedown tests was a slight elastic deflection of the drive shafts. The problem was noticed during the preliminary experiments when oscillation of the bearing was viewed through a magnifying glass with the aid of a strobe light. At low amplitude (12.5 μm, 4.92×10^{-4} in.), medium load (90 N, 20.24 lbf) operation, the bottom of the bearing did not appear to have any motion but the top portion did. A force analysis of the bearing showed that its "rocking" motion was a result of a force couple applied to the bearing which produced a bending moment on the drive shaft. The force couple is a consequence of the bearing drive system since the drive shafts impart force to the bearing at its center. The friction force developed between the bearing and cartridge is applied to the bottom portion of the bearing since contact occurs there as a result of the clearance fit that exists between them. The resulting moment arm between the driving force and the friction force is equal to the radius of the bearing outer race (7.9375 mm, 0.3125 in.).

In order to minimize the error in knowing the amplitude present between the bearing and cartridge, a number of tests were run at various amplitudes to determine the point at which relative motion between the bottom of the bearing and the cartridge began. The two loads that were applied to the bearing/cartridge assembly during the tests were the loads to be used in the statistically designed experiment. To determine whether or not relative motion between a bearing and cartridge existed, each set was run at a certain amplitude for 200,000 cycles. During this time, oscillation of the bearing relative to the stationary cartridge was viewed through a magnifying glass with the aid of a strobe light. After a test, the bearing/cartridge set was disassembled and inspected for fretting corrosion. If a set was suspected of having little or no relative motion and later found to have no fretting damage, the amplitude was increased and the test was rerun. The amplitude at which fretting first occurred was then used to correct for the desired amplitude. At the heavier load W_2 (90 N, 20.24 lbf), a correction of 20 μm (0.0008 in.) was necessary but at the lighter load W_1 (15 N, 3.37 lbf), no correction was necessary. Therefore, if a 150 μm amplitude is required and the load is W_2, the amplitude set at the LVDT is 170 μm. If the load is W_1 and the desired amplitude is 150 μm, the LVDT is set at 150 μm.

Experimental Studies

Shakedown Tests

Before running any of the preliminary experiments or the statistically designed experiment, many shakedown tests were run on Mark III. The purpose of the tests was to see whether or not any design modification was needed and to uncover any peculiarities that might have existed in the apparatus. A significant problem was discovered in the first runs made on the apparatus. Cartridges of a smaller bore (15.8775 - 15.8877 mm vs 15.9029 - 15.9131 mm, 0.6251 - 0.6255 in. vs 0.6261 - 0.6265 in.) and same surface finish were originally used in the tests. Early in the runs, at approximately 200 cycles, a high-pitched "hammering" type noise was observed to originate from the bearing/cartridge assemblies. Shortly thereafter, 300 to 700 cycles, the noise ceased and the bearings appeared to be locked up. After removing the assemblies from the machine, a brass rod and hammer were used to dislodge the bearings from the cartridges. Visual examination of the contacting surfaces revealed tiny points around the entire circumference of the interface where welding had occurred. Indeed, welding had occurred since the paths that were gouged into the cartridge bore by the welds upon disassembly were plainly visible. Surrounding the immediate area of each weld was a dark brown debris and at a further distance from the weld, a light brown to reddish colored debris was present. To mitigate the locking problem, cartridges of a larger bore were used in the tests that followed (see sizes above). It was found that fretting corrosion was generally confined to the lower 40% of the bearing outer race and cartridge bore; this is somewhat similar to that observed in the SSMG bearing/cartridge sets. No further problem of bearings becoming locked in the cartridges appeared. No other problems with the device were found.

Weight Loss Method of Fretting Corrosion Quantification

If the bearing/cartridge set is viewed in a material balance sense, two extremes exist with respect to the use of weight loss measurements as a method of quantifying the extent of fretting corrosion at a bearing/cartridge interface. At one extreme, if all the oxides that were formed during the fretting process were removed, weight loss measurements might approximate the actual extent of fretting corrosion to a very high degree. But a knowledge of the exact amount of oxide formed in the fretting process could be obtained only by knowing what portion of the weight loss is oxide and what portion, if any, is metallic debris. On the other hand, if all the debris that was produced during a test run could be kept from escaping, the combination of oxygen and iron, which form the oxides that are characteristic of fretting corrosion, would yield a negative weight loss, or in other words, a weight gain. Whether or not one method is better than the other is not in question since both methods involve a change in weight. Instead, the validity of weight measurements as a method of quantifying the extent of fretting corrosion at the interface should be questioned. The following observations are offered in support of weight loss measurements as a method of quantifying the extent of fretting corrosion that occurs at a bearing/cartridge interface:

1. In most all studies conducted on Mark III, copious amounts of fretting corrosion debris were produced at the bearing/cartridge interface. The debris piled up on either side of the bearing/

cartridge contact zone and eventually fell from the cartridge on to the base plate and floor. Later, when the bearing/cartridge set was cleaned in the ultrasonic washer, very little debris could be found in the flask in which the bearing and cartridge were placed. An estimate of the ratio of the amount of loose debris to the amount of debris found in the flask after washing a set would be about 99 to 1. Therefore, very little debris was found to adhere to the damaged surfaces.

2. In all test runs made in this study, only three showed a gain in weight; and these gains were very slight (0.3, 0.1, and 0.2 mg). Again, very little debris adhered to the damaged surfaces compared to the amount removed by relative motion.
3. In all tests, metallic wear debris was not seen.
4. Five damaged bearing/cartridge sets and one undamaged set were immersed in a 10% (by weight) ammonium citrate solution. The ammonium citrate solution was used to remove oxides from the damaged sets. The undamaged (control) set, which was immersed in the solution, was used to determine the extent of clean, unoxidized metal that was attacked by the solution. Negligible additional weight loss was found for the damaged sets and it is concluded that very little debris remains in contact with the damaged surfaces.

Therefore, in light of these observations, it is concluded that weight loss measurement is an appropriate and relatively accurate means of quantifying the extent of fretting corrosion damage that occurs at the interface of a bearing/cartridge set.

Preliminary Experiments

Weight Loss versus Cycle Duration (dry contact): Figure 18* shows the effect of cycle duration (time) on weight loss of the bearings for dry contact between the bearings and cartridges. The average weight loss of the bearings increases to 0.65 mg at 1×10^5 cycles and remains relatively constant up to 4×10^5 cycles. At 5×10^5 cycles a slight increase is noticed. Figure 19 shows the effect of cycle duration on weight loss of the cartridges. The wear rate appears to be linear up to approximately 3×10^5 cycles where it then begins to taper off and eventually drop. Weight loss of the cartridges is seen to be much greater than that of the bearings. The combined weight loss of the bearings and cartridges is shown in Figure 20. The wear rate decreases at an increasing rate and eventually approaches a steady-state condition at around 5×10^5 cycles.

Weight Loss versus Cycle Duration (lubricated contact): The extent of fretting corrosion of lubricated bearings is shown in Figure 21. Again, the same general trend for weight loss of dry bearings is seen for lubricated bearings except for two major differences: first, the weight loss at any instant for lubricated contact is lower than the weight loss for dry contact up to about 4×10^5 cycles; secondly, at around 5×10^5 cycles a large increase in the wear rate for lubricated bearings occurs.

---

*Each point on all plots is the average weight loss value determined from the losses found for two bearing/cartridge sets used per test run.

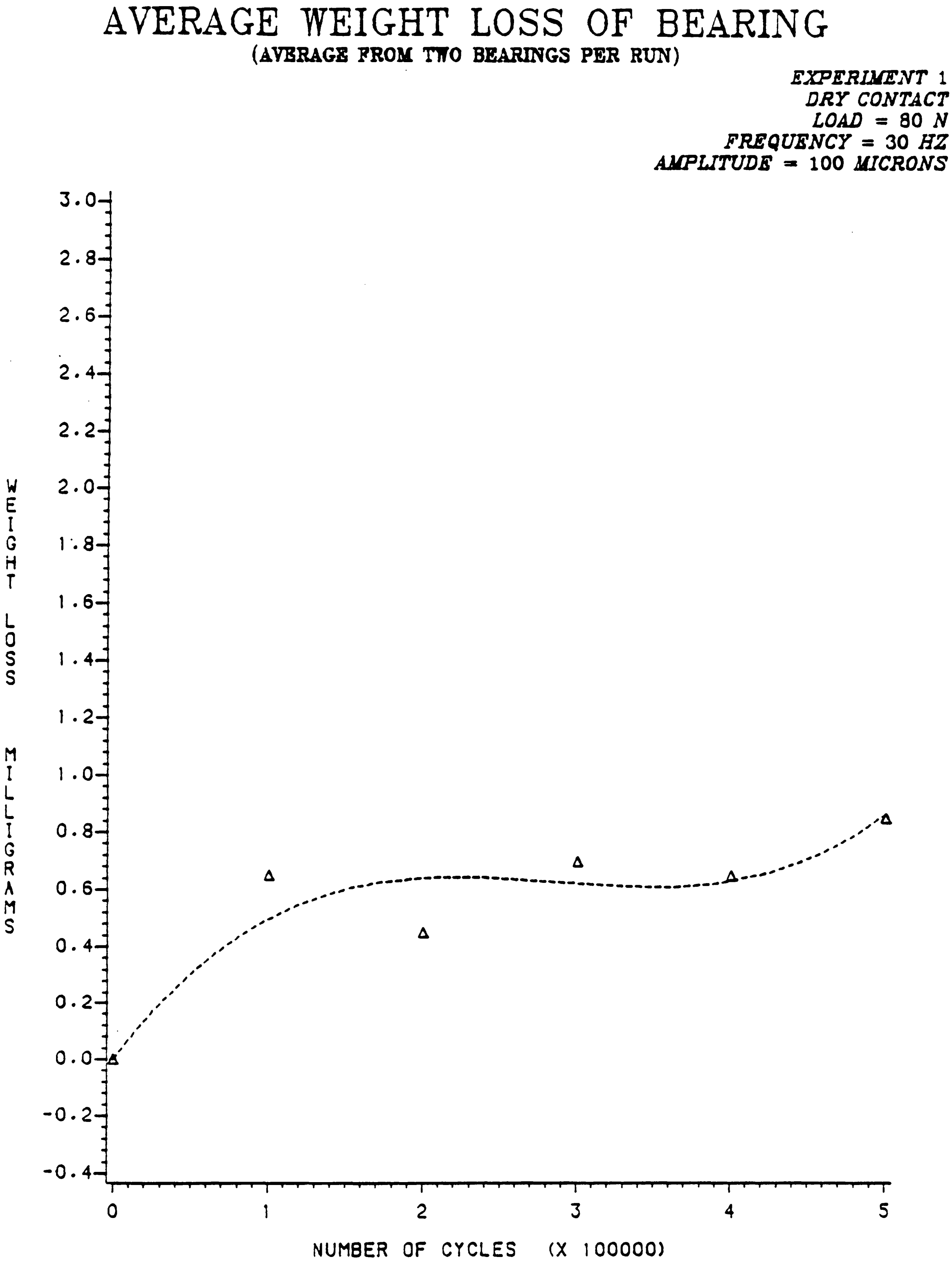

Figure 18. Experimental Weight Loss of Bearing vs Number of Cycles

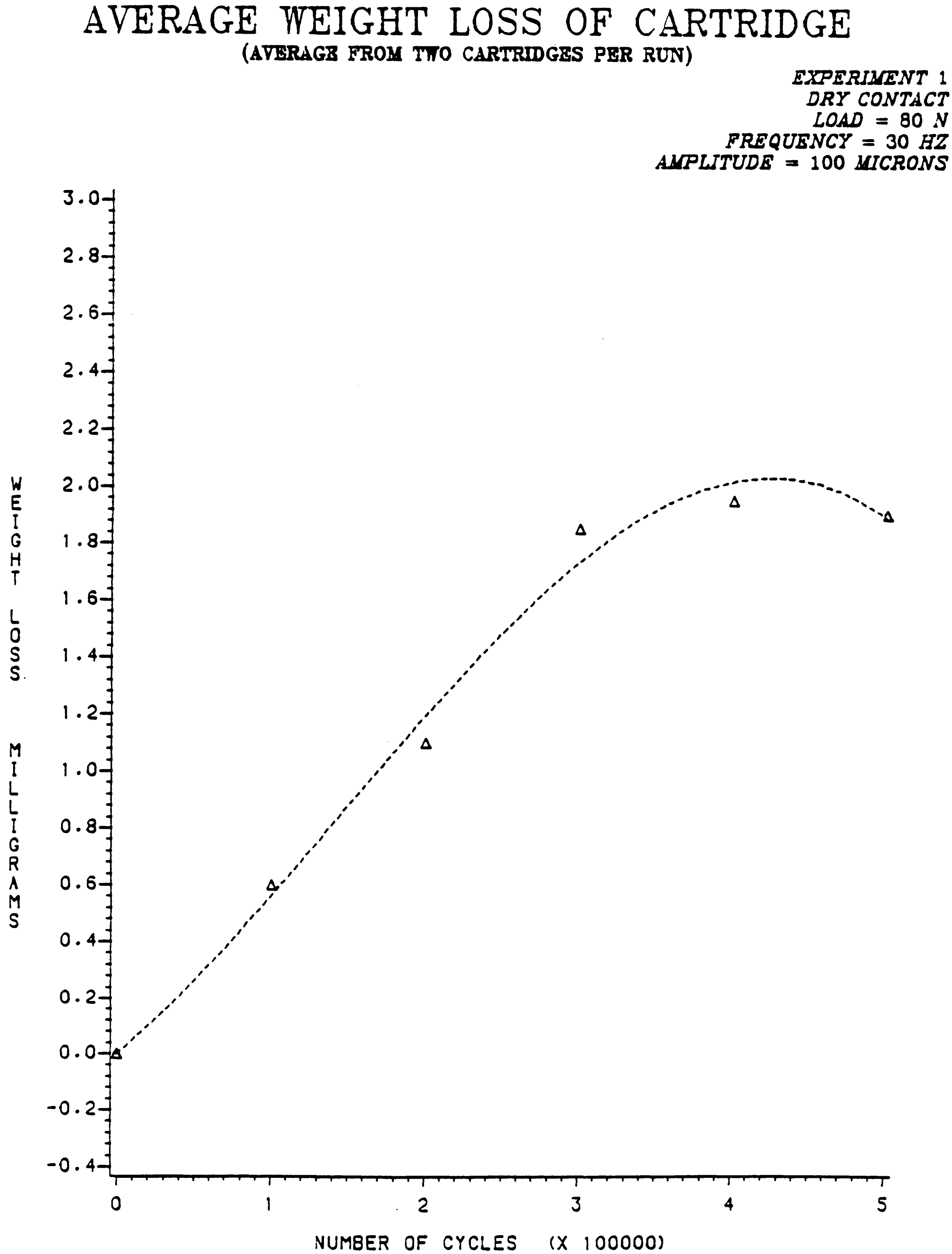

Figure 19. Experimental Weight Loss of Cartridge vs Number of Cycles

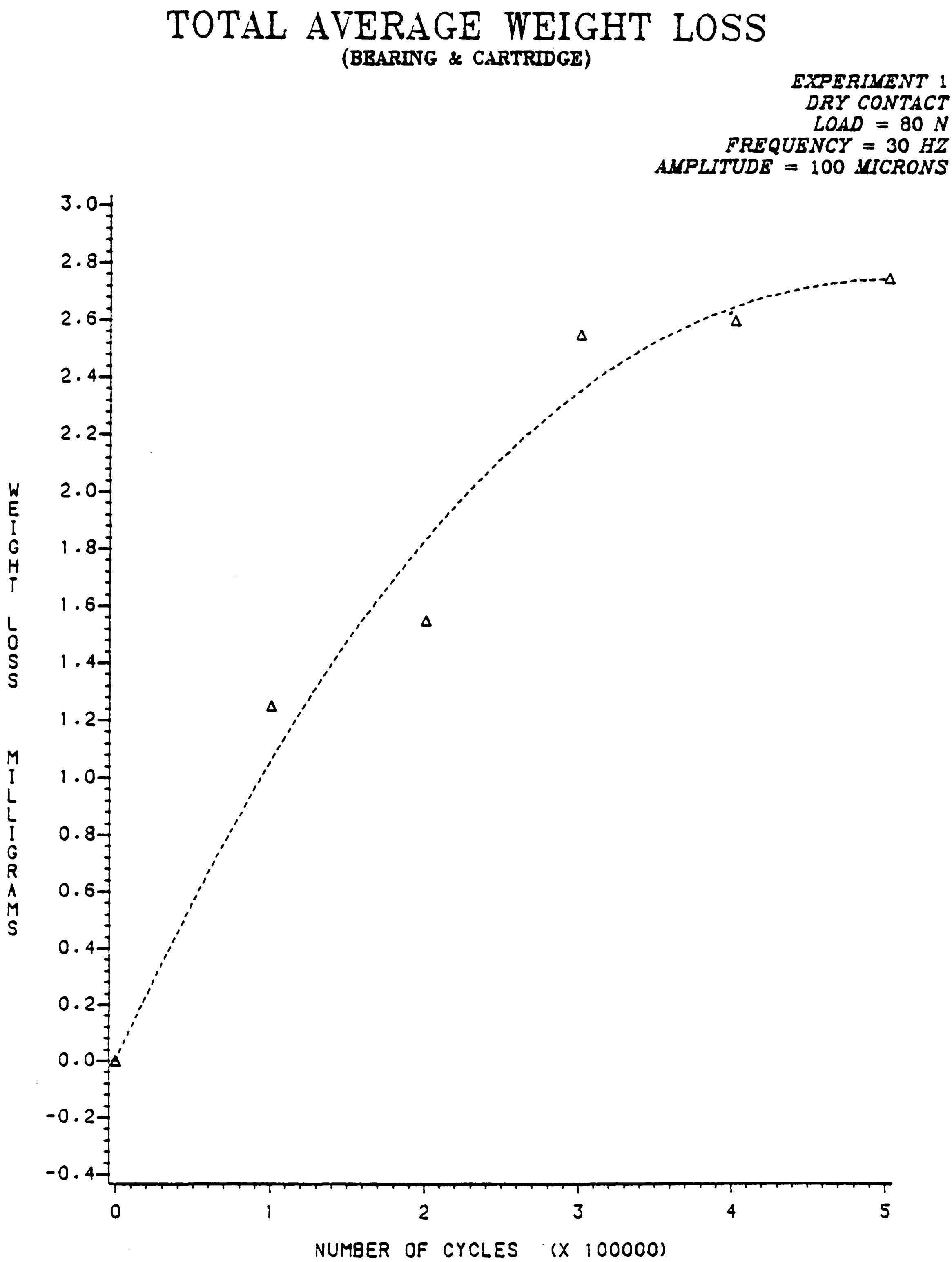

Figure 20. Experimental Weight Loss of Bearing & Cartridge vs Number of Cycles

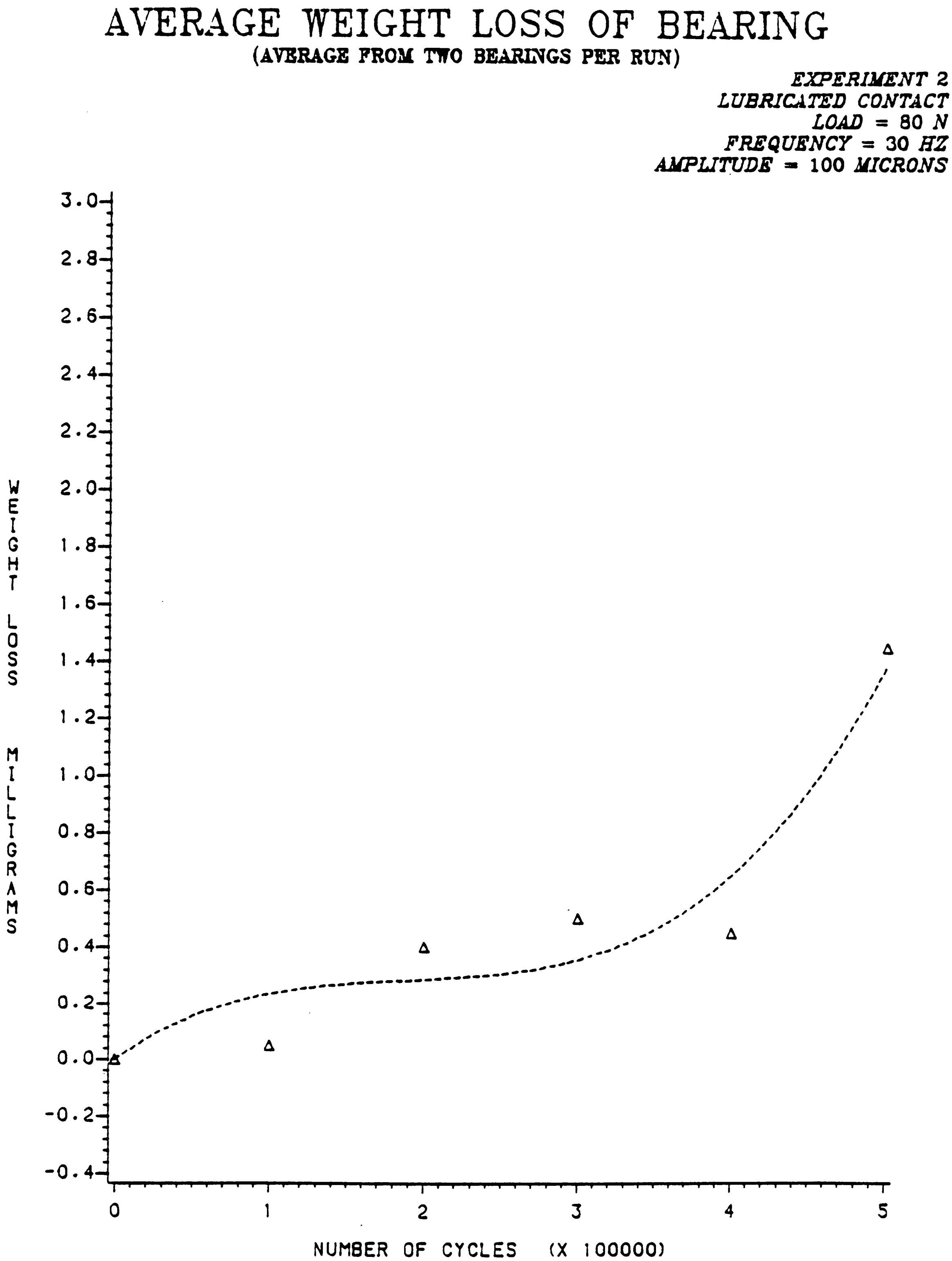

Figure 21. Experimental Weight Loss of Bearing vs Number of Cycles

In Figure 22, the weight loss of the cartridges becomes negative at 1×10^5 cycles. From 1×10^5 to 4×10^5 cycles, fretting of the cartridge appears to increase linearly with respect to time but at 5×10^5 cycles a steady-state condition is reached in which wear appears to be constant and independent of time. Figure 23 gives an overall picture of fretting corrosion for lubricated contact between the bearings and cartridges. The extent of fretting corrosion for lubricated conditions is much lower than it is for dry conditions initially, but then increases at an increasing rate compared to an increase at a decreasing rate for dry contact.

Weight Loss versus Amplitude: The effect of amplitude on weight loss of a bearing and cartridge (dry contact) is shown in Figures 24, 25, and 26. At an amplitude of 25 μm (9.84×10^{-4} in.) the bearing experiences zero weight loss. At 50 μm (19.68×10^{-4} in.) though, the bearing weight loss jumps to 0.6 mg and remains relatively constant thereafter. Wear of the cartridge increases to a peak weight loss of 1.45 mg at an amplitude of 400 μm. Again, the weight loss experienced by the bearings is not as great as that experienced by the cartridges. The overall effect is shown in Figure 26. It can be seen that the wear rate for a bearing/cartridge set increases with amplitude but reaches a peak at around 200 μm where it then remains relatively constant with respect to time.

Weight Loss versus Load: Figures 27, 28, and 29 display the effect of load on fretting corrosion of the bearings and cartridges under dry contact conditions. In both cases, i.e., for the bearings and cartridges, the wear rate is approximately linear with respect to load although load has a much greater affect on fretting corrosion of the cartridges than it does on fretting of the bearings.

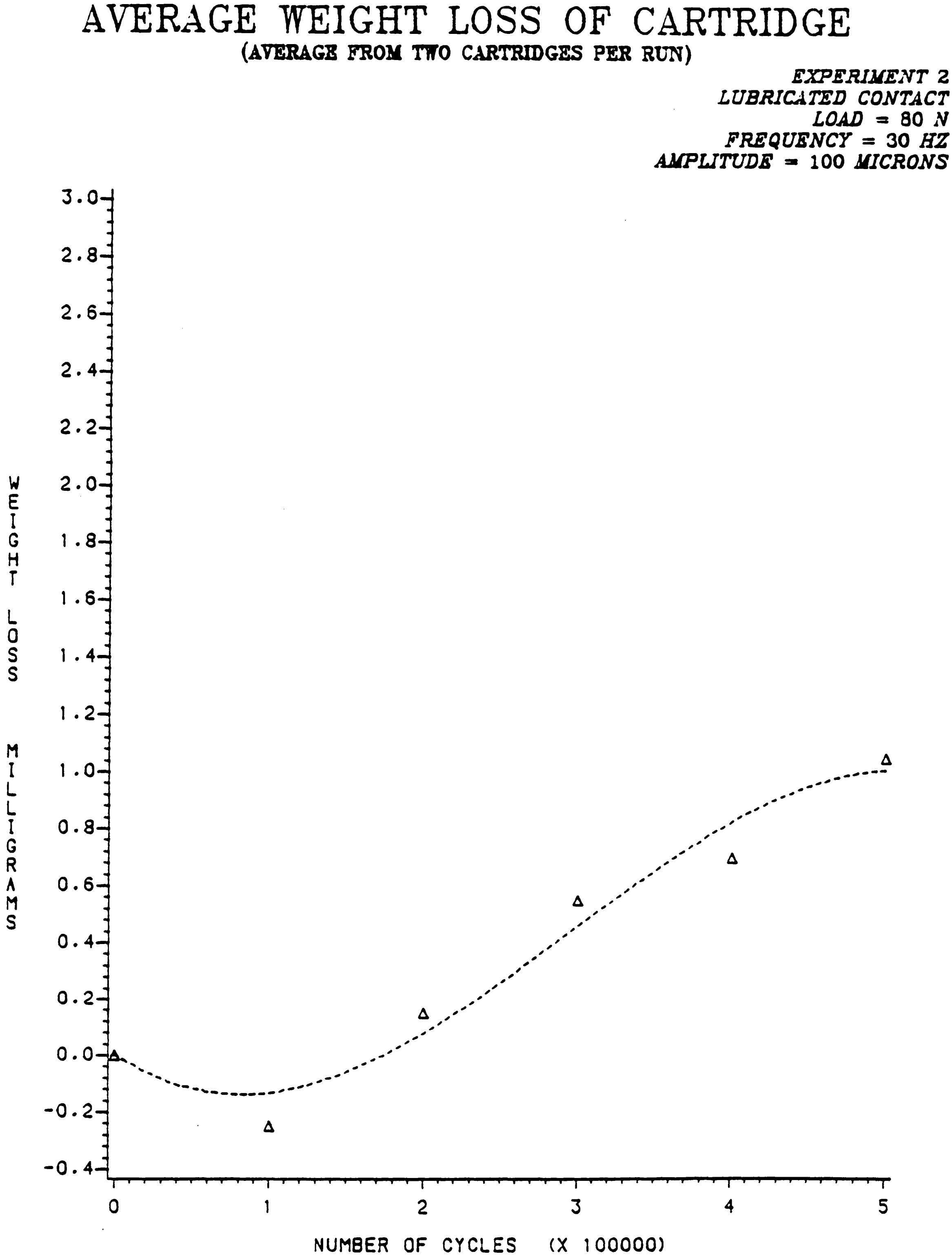

Figure 22. Experimental Weight Loss of Cartridge vs Number of Cycles

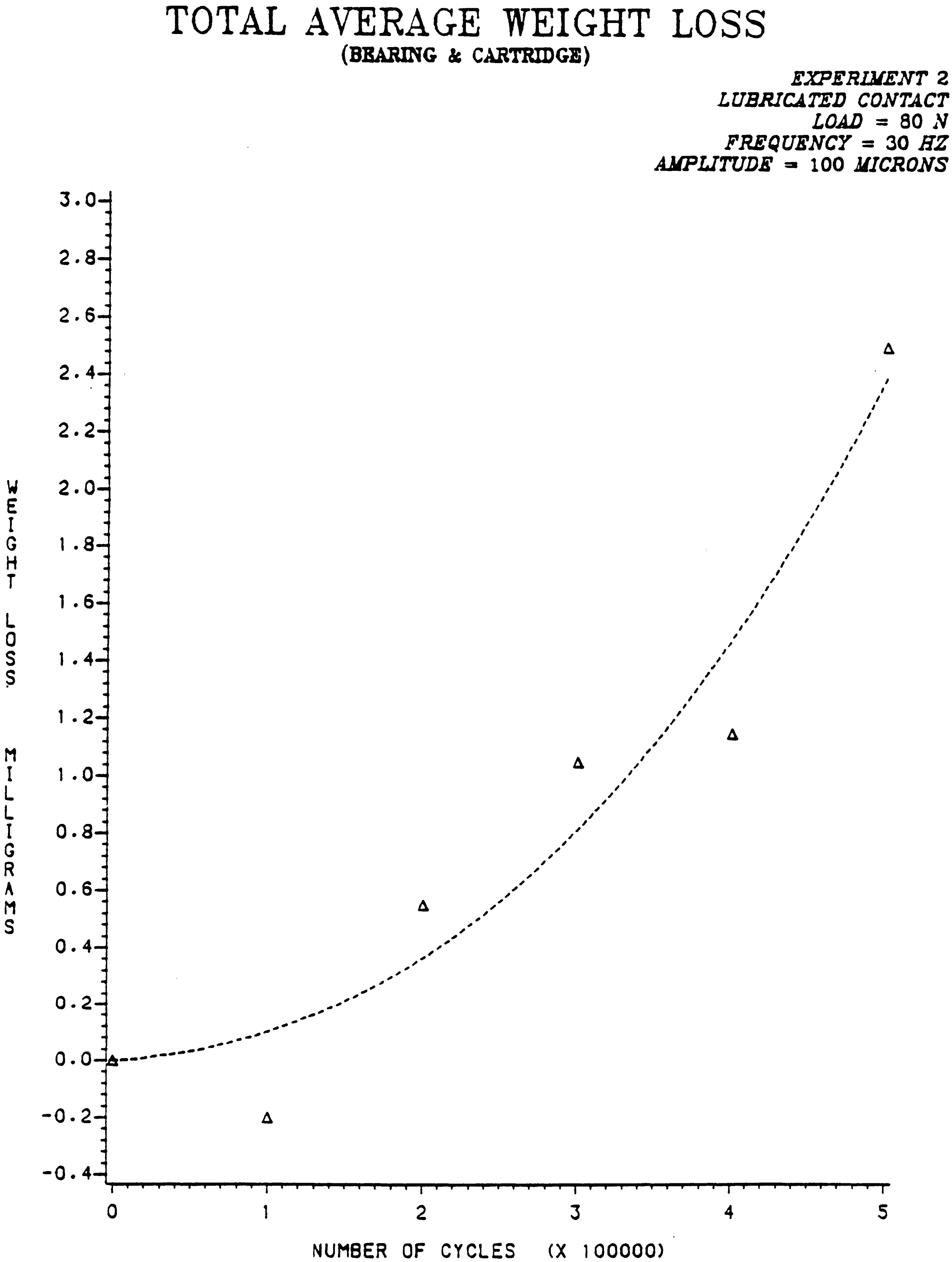

Figure 23. Experimental Weight Loss of Bearing & Cartridge vs Number of Cycles

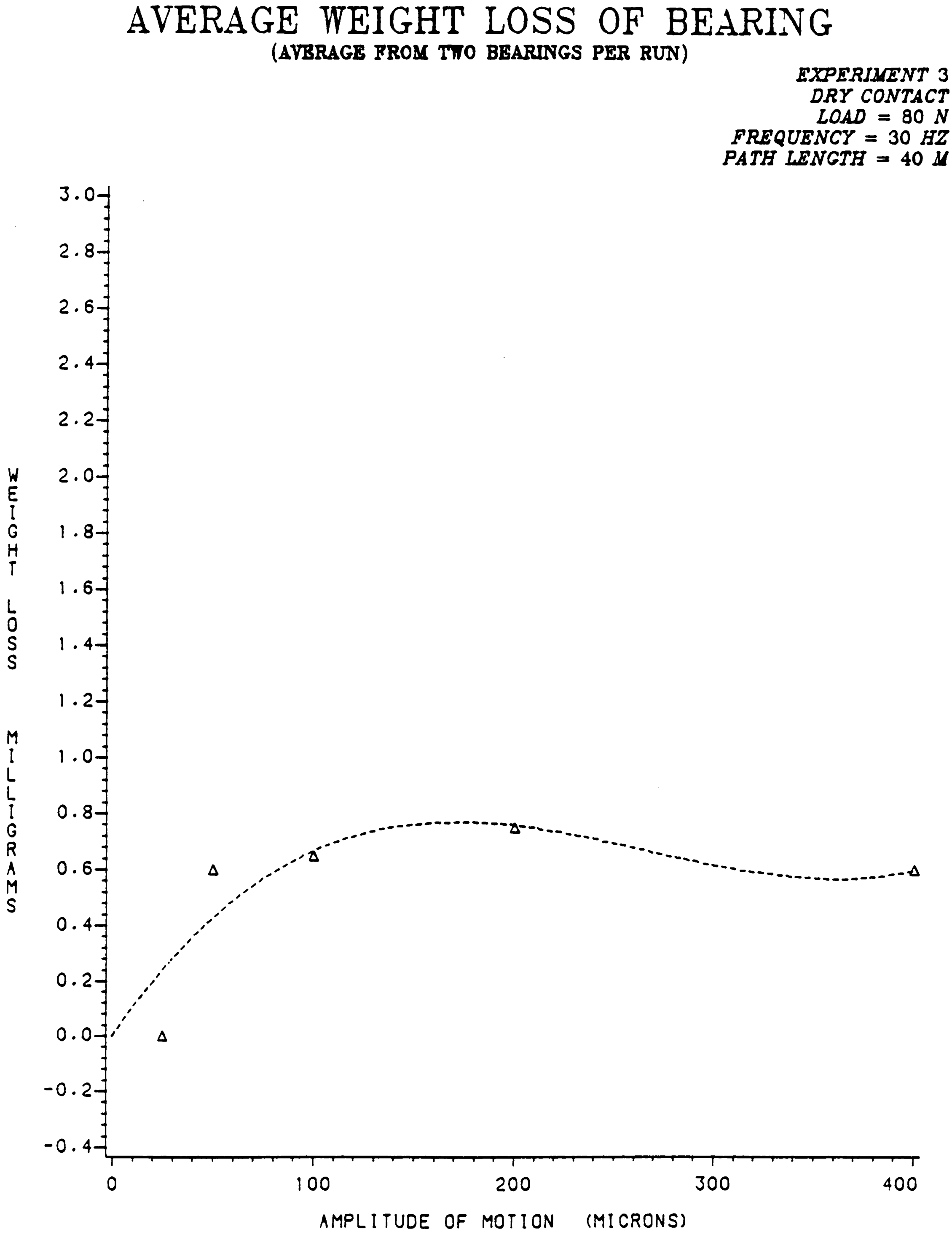

Figure 24. Experimental Weight Loss of Bearing vs Amplitude of Motion

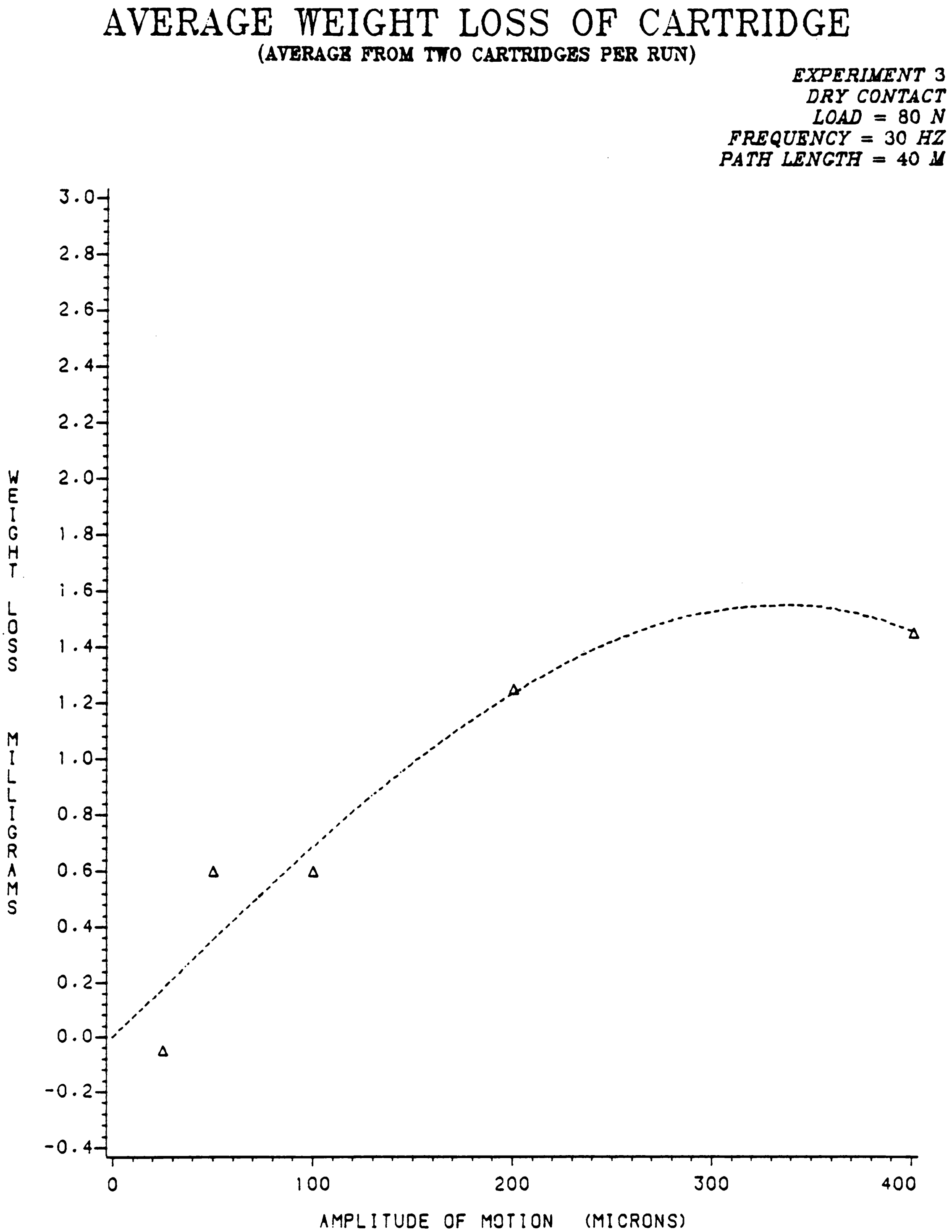

Figure 25. Experimental Weight Loss of Cartridge vs Amplitude of Motion

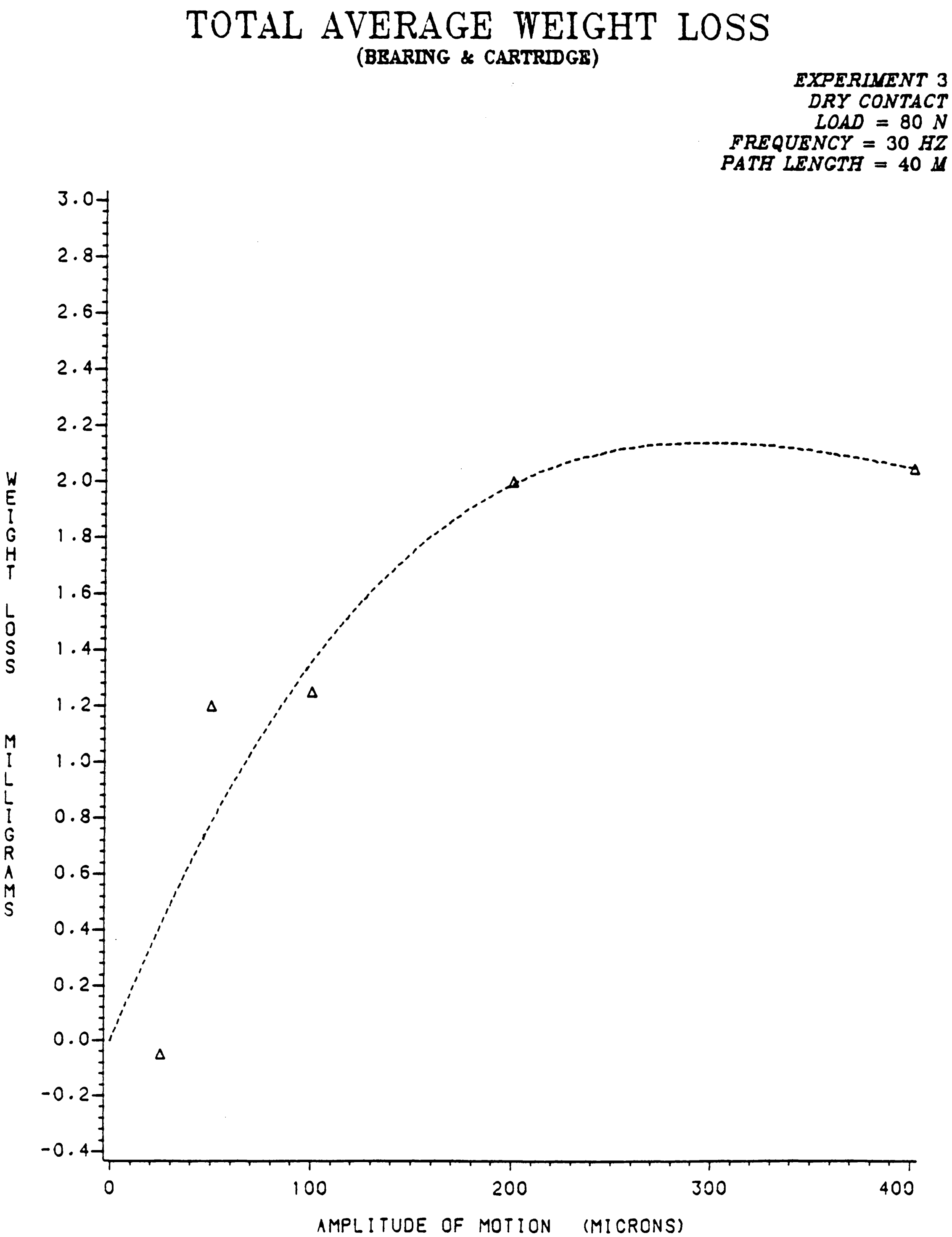

Figure 26. Experimental Weight Loss of Bearing & Cartridge vs Amplitude of Motion

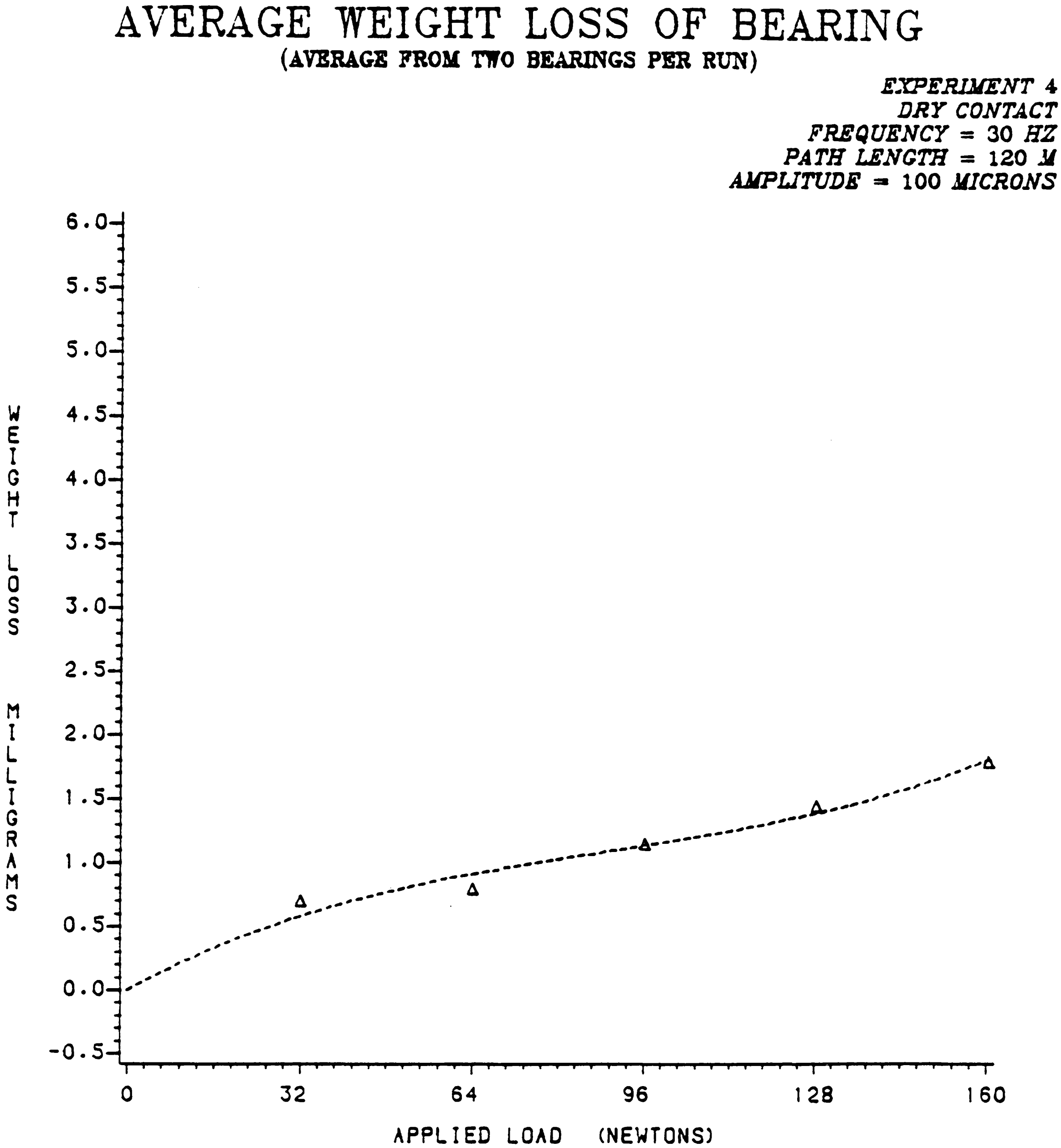

Figure 27. Experimental Weight Loss of Bearing vs Applied Load

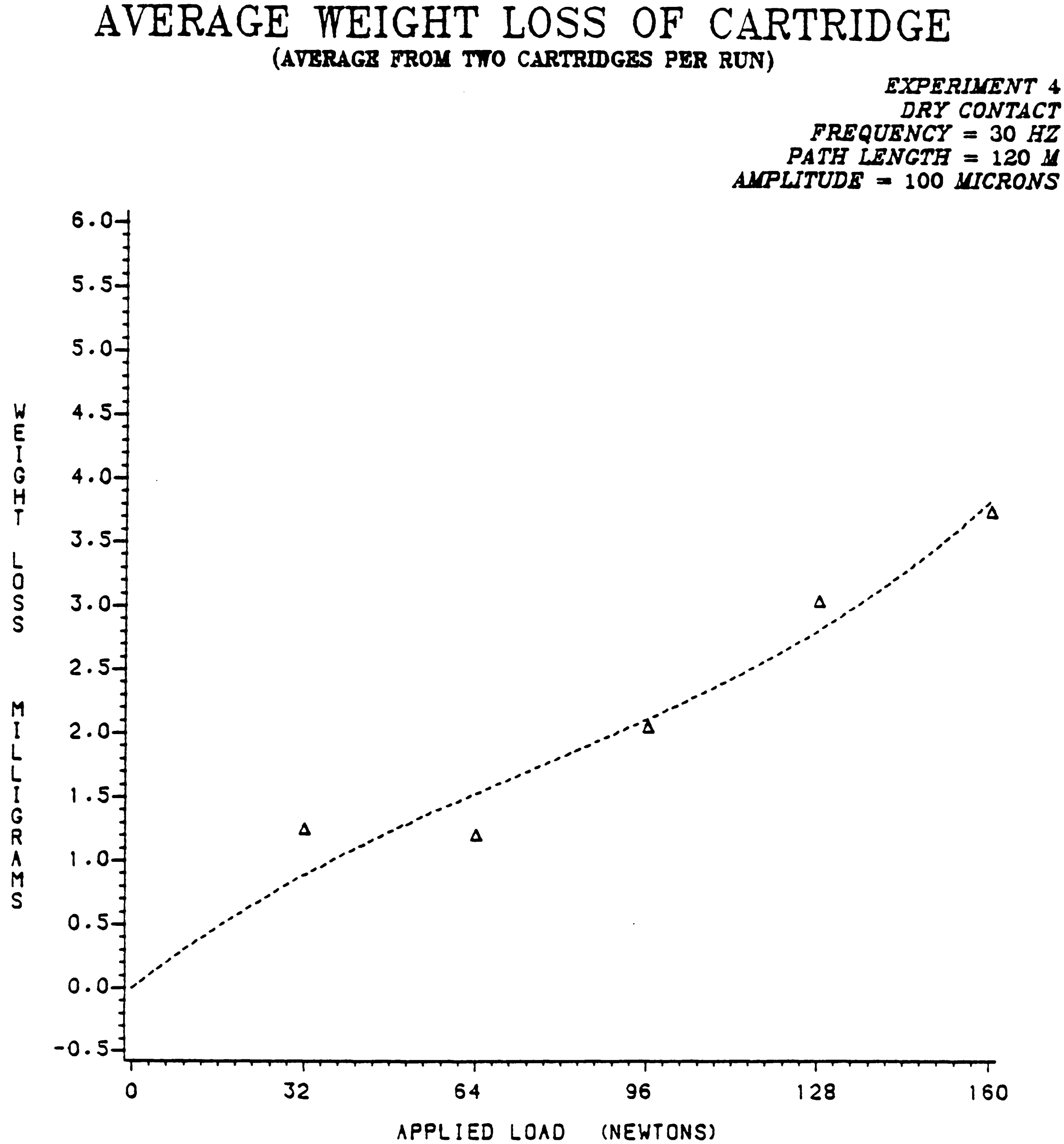

Figure 28. Experimental Weight Loss of Cartridge vs Applied Load

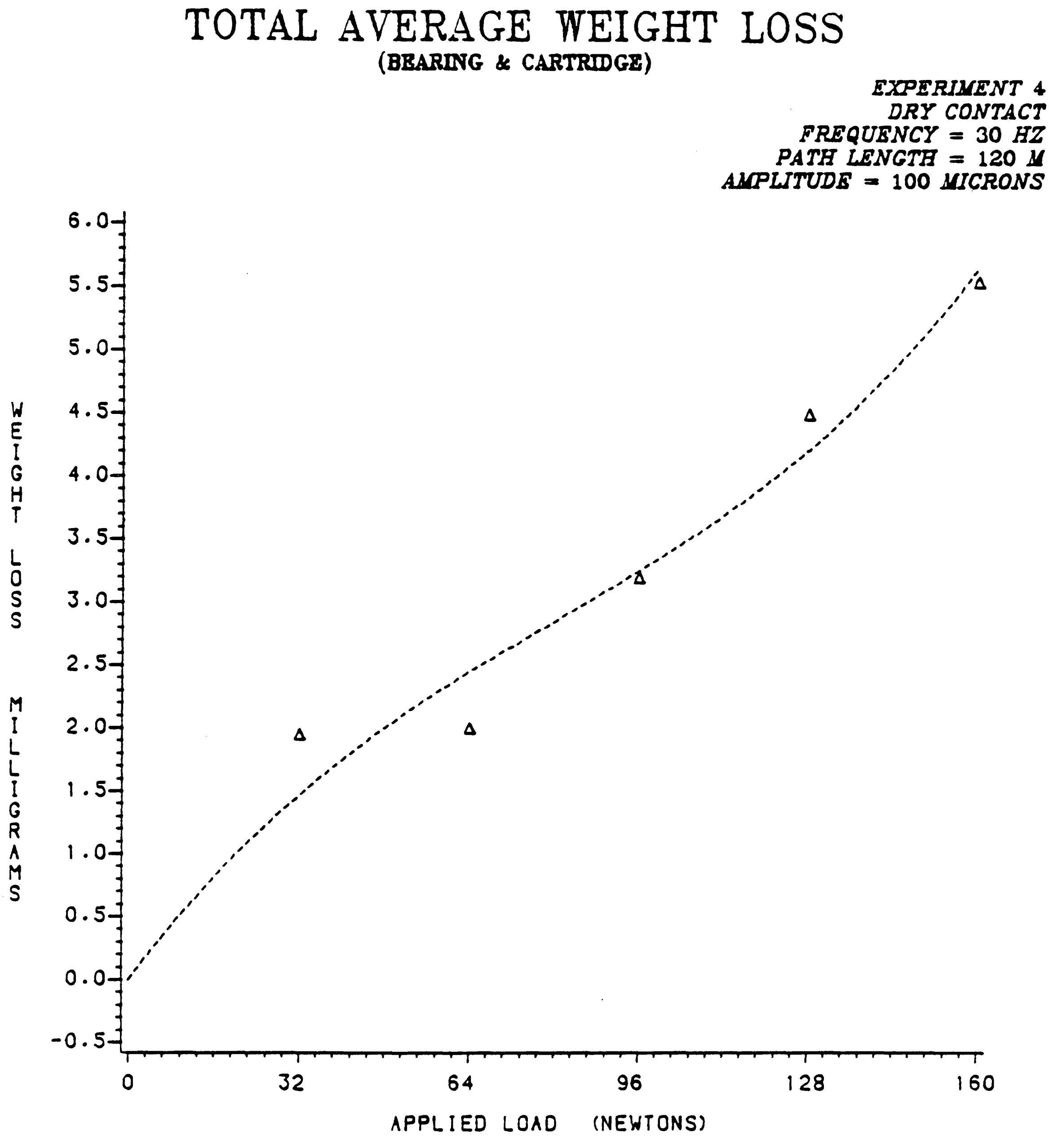

Figure 29. Experimental Weight Loss of Bearing & Cartridge vs Applied Load

Statistically Designed Experiment

General Results: The results of the four factor-two level statistically designed experiment are included in Appendix C. The overall results are graphically illustrated in Figures 30, 31, and 32. The height of the bars in the figures represents the degree of significance for which each parameter, and combinations thereof, affects the extent of fretting corrosion at a bearing/cartridge interface. The reference line shown in each chart indicates the 95% confidence limit.

The overall conclusions that can be drawn at the 95% confidence level are shown in Table 5. The asterisk indicates that:

1. When a single parameter is involved, that parameter does affect the extent of fretting corrosion at the bearing/cartridge interface.
2. When a combination of parameters is involved, an interaction between the parameters exists which affects the extent of fretting corrosion at the bearing/cartridge interface.

Bearing/Cartridge Analysis: As was mentioned earlier, the asterisk shown in Table 5 indicates that an effect is present, but its relative magnitude and how the effect may influence fretting corrosion at the bearing/cartridge interface is not shown. The purpose of this section is to examine the main effects and first order interactions for fretting corrosion of a bearing/cartridge set in more detail. The second and third order interactions are much more difficult to interpret and will not be included in this study.

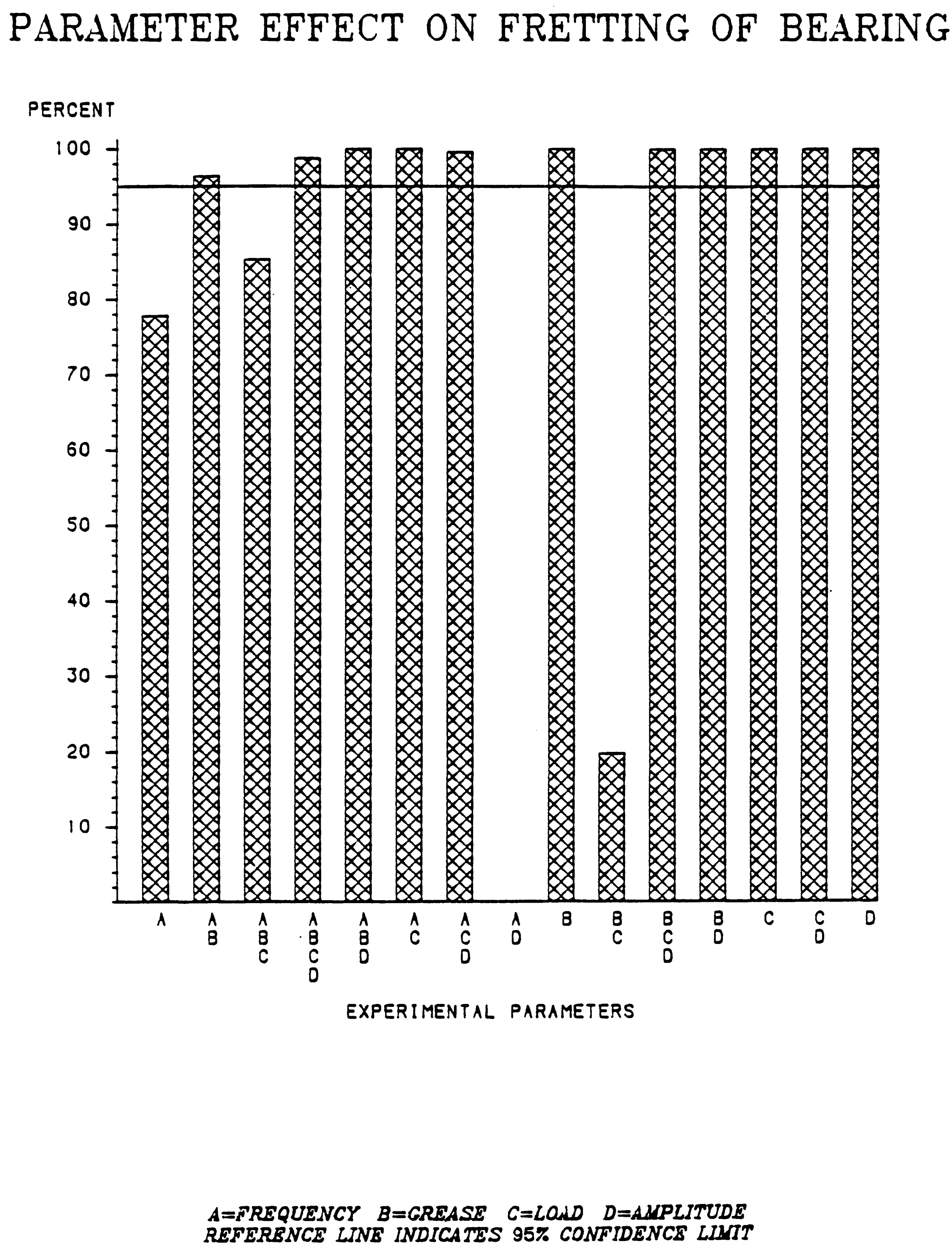

Figure 30. Statistical Significance of Experimental Parameters on Fretting of Bearing

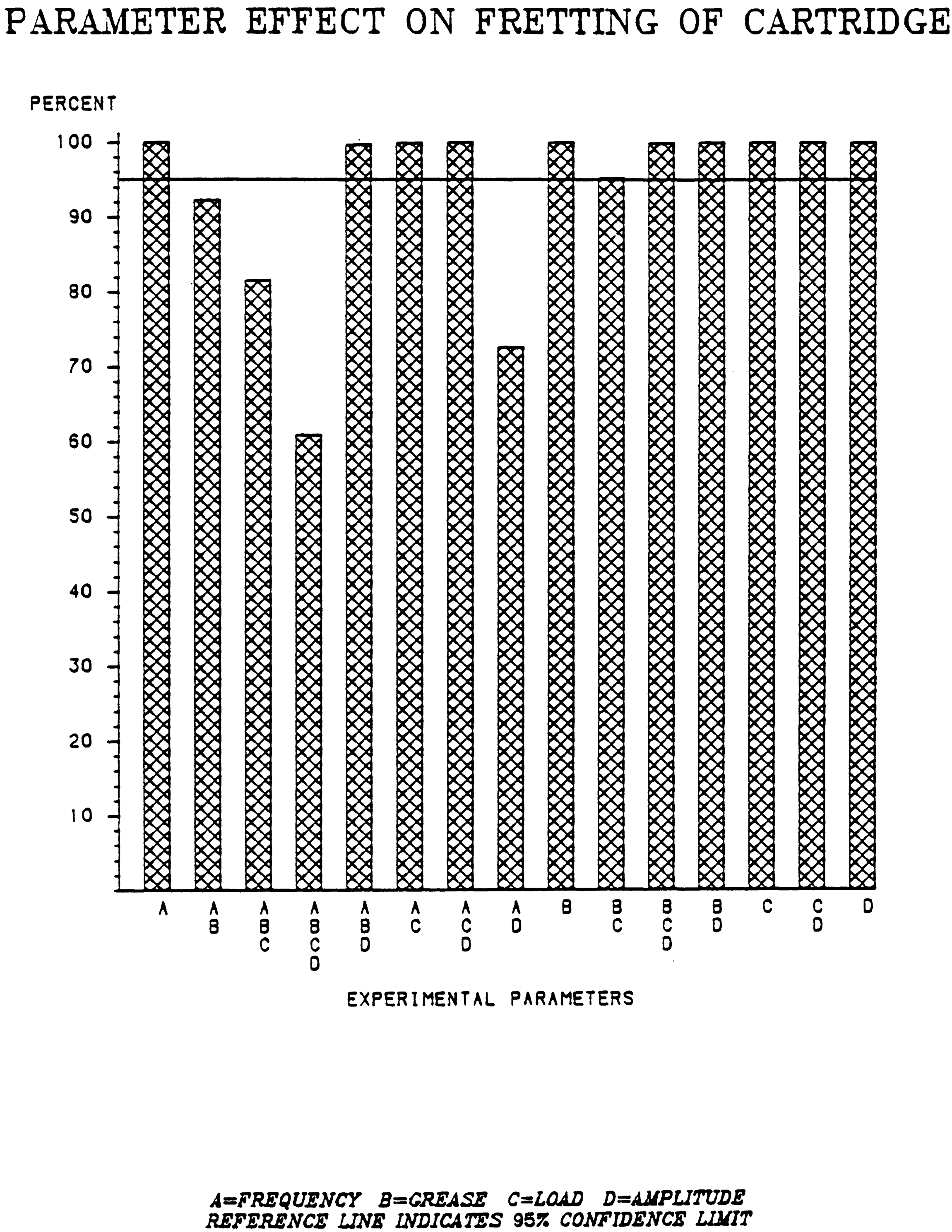

Figure 31. Statistical Significance of Experimental Parameters on Fretting of Cartridge

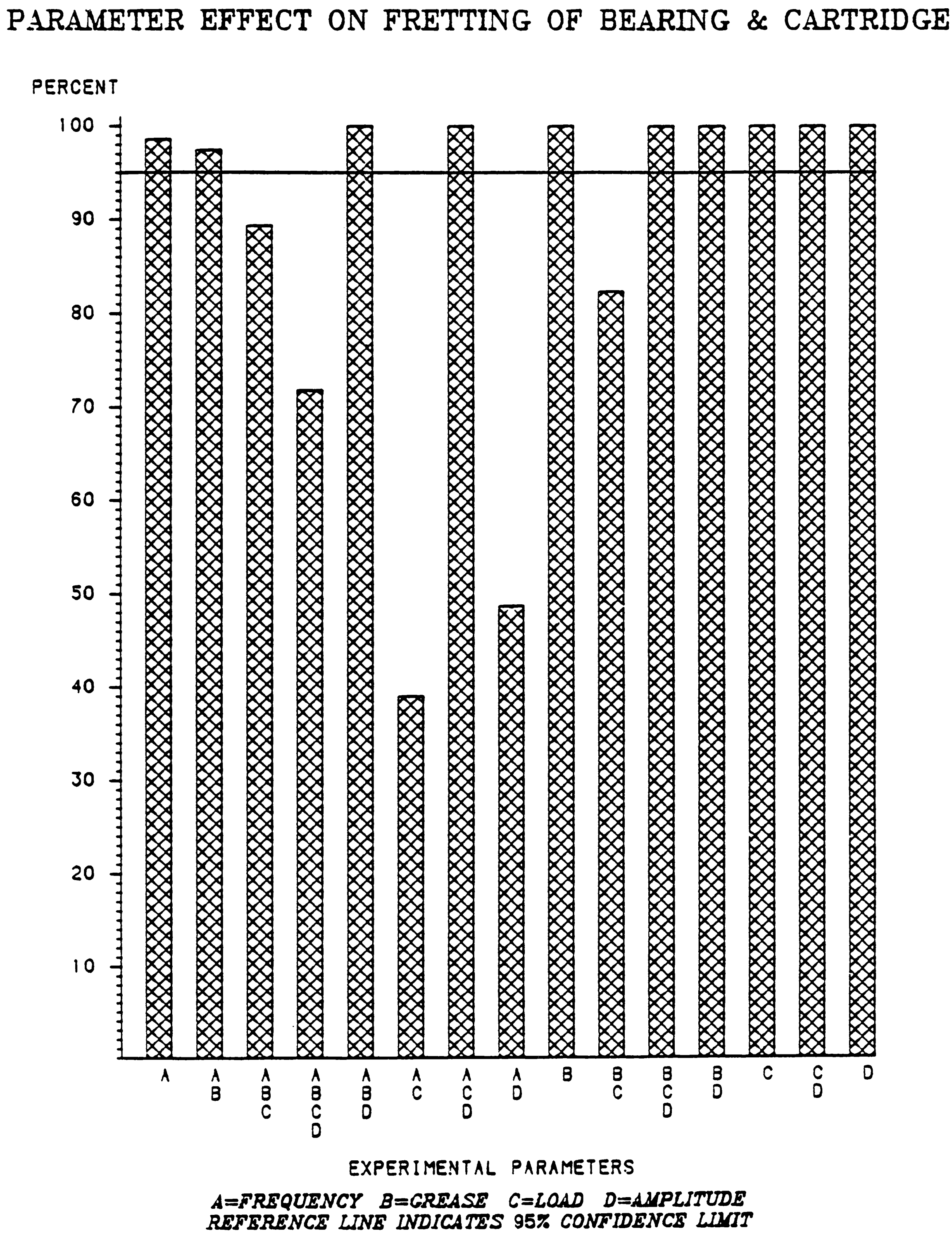

Figure 32. Statistical Significance of Experimental Parameters on Fretting of Bearing & Cartridge

TABLE 5

COMPARISON OF SIGNIFICANT EFFECTS

ABOVE 95% CONFIDENCE LEVEL

Parameter (s)	Bearing	Cartridge	Bearing & Cartridge
Frequency		*	*
Grease	*	*	*
Load	*	*	*
Amplitude	*	*	*
Frequency, Grease	*		*
Frequency, Load	*	*	
Frequency, Amplitude			
Grease, Load		*	
Grease, Amplitude	*	*	*
Load, Amplitude	*	*	*
Frequency, Grease, Load			
Frequency, Grease, Amplitude	*	*	*
Frequency, Load Amplitude	*	*	*
Grease, Load, Amplitude	*	*	*
Frequency, Grease, Load, Amplitude	*		

A summary of the results of the statistical analysis of the bearing/cartridge set is shown in Table 6. The relative magnitude of the variance ratios gives an indication of the degree to which an effect is present. Amplitude is seen to be the most significant main effect and is followed by load, grease, and frequency in order of significance. The most significant first order interaction is that of load and amplitude. Figures 33, 34, 35, and 36 display the mean weight loss values determined for both levels of each significant main effect (95% confidence limit). The conclusions that can be drawn at the 95% confidence level are as follows:

1. An increase in amplitude results in an increase in fretting corrosion at the bearing/cartridge interface (0.38 → 2.00 mg).
2. An increase in load results in an increase in fretting corrosion at the bearing/cartridge interface (0.45 → 1.92 mg).
3. The use of a grease at the interface reduced the average weight loss (1.61 → 0.76 mg).
4. An increase in frequency results in an increase in fretting corrosion at the bearing/cartridge interface (1.07 → 1.30 mg).
5. An interaction exists between frequency and presence of a grease. When no grease is present at the interface, an increase in frequency results in a large increase in fretting corrosion. When grease is present, only a small increase is noticed (see Table 7).
6. An interaction exists between grease and amplitude. At both amplitudes, the application of a grease reduces fretting corrosion (see Table 8).

TABLE 6

RESULTS OF STATISTICAL ANALYSIS

OF BEARING/CARTRIDGE SET

Source of Variance	Sum of Squares	Degrees of Freedom	Variance	Variance Ratio
A	0.43	1	0.43	7.56
B	5.70	1	5.70	100.69
C	17.26	1	17.26	305.11
D	20.96	1	20.96	370.61
AxB	0.34	1	0.34	6.02
AxC	0.02	1	0.02	0.27
AxD	0.03	1	0.03	0.45
BxC	0.11	1	0.11	1.99
BxD	2.82	1	2.82	49.86
CxD	19.07	1	19.07	337.07
AxBxC	0.17	1	0.17	2.92
AxBxD	1.76	1	1.76	31.08
AxCxD	1.67	1	1.67	29.44
BxCxD	3.32	1	3.32	58.61
AxBxCxD	0.07	1	0.07	1.24
Residual	0.91	16	0.06	
Total	74.60	31		

A = Frequency B = Grease

C = Load D = Amplitude

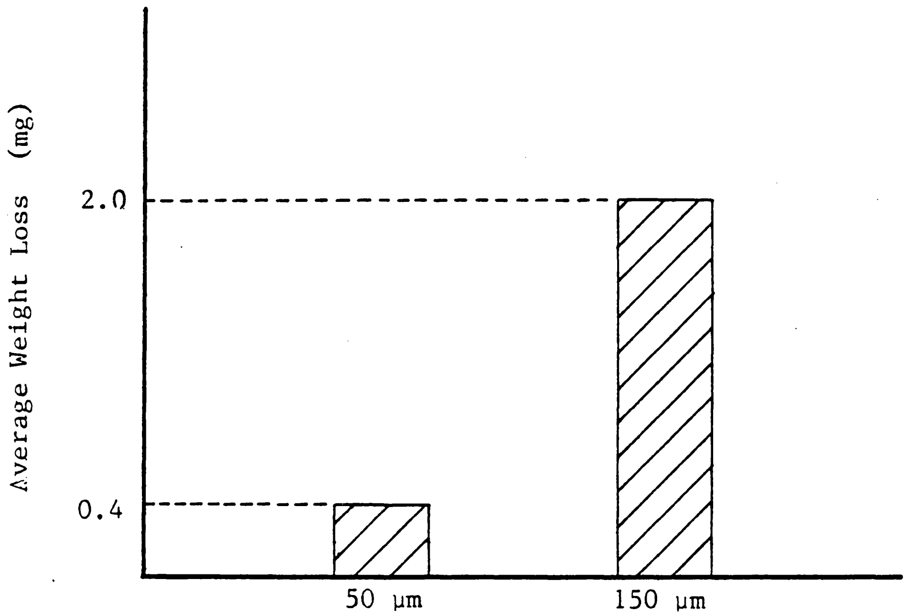

Figure 33. Comparison of Mean Weight Loss Values Found for Amplitude - Experiment #5

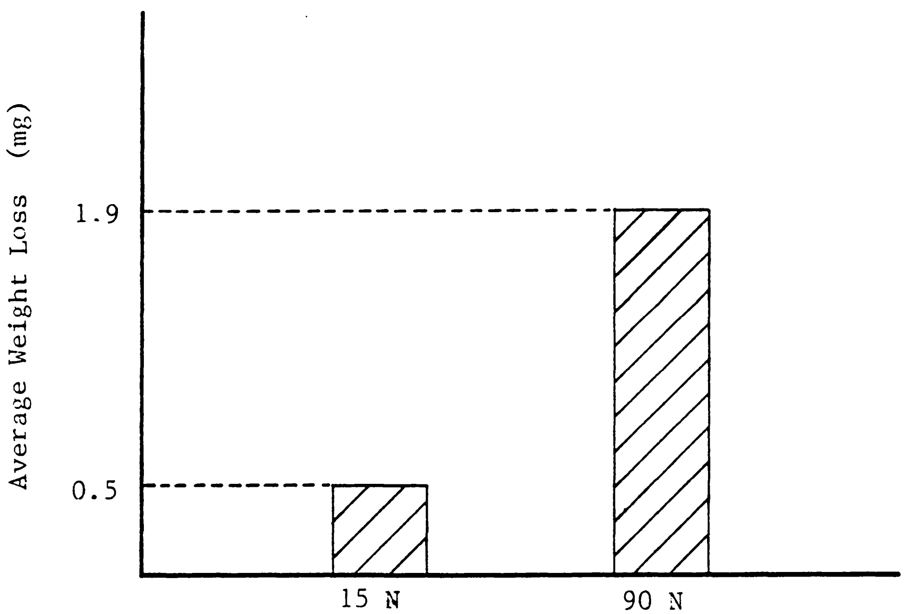

Figure 34. Comparison of Mean Weight Loss Values Found for Load - Experiment #5

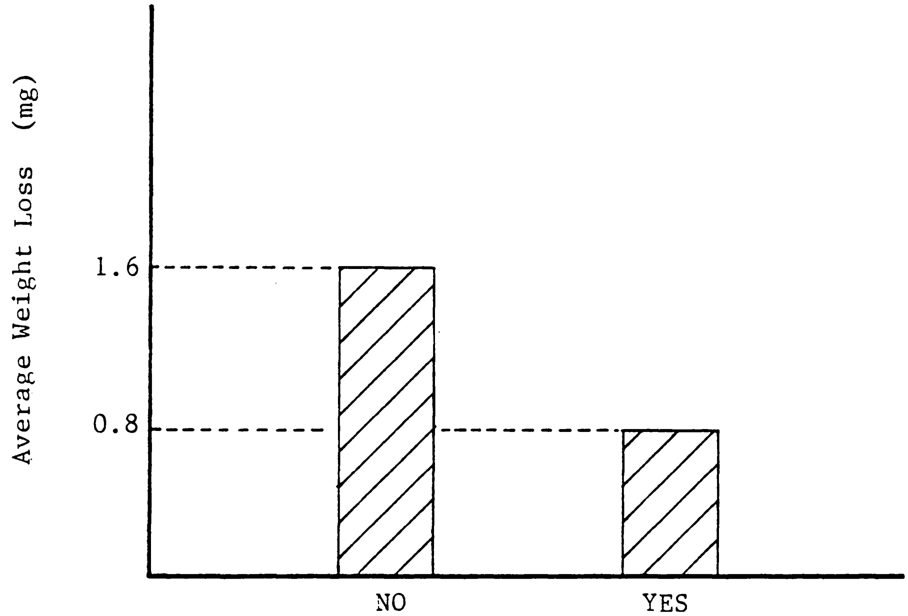

Figure 35. Comparison of Mean Weight Loss Values Found for Grease - Experiment #5

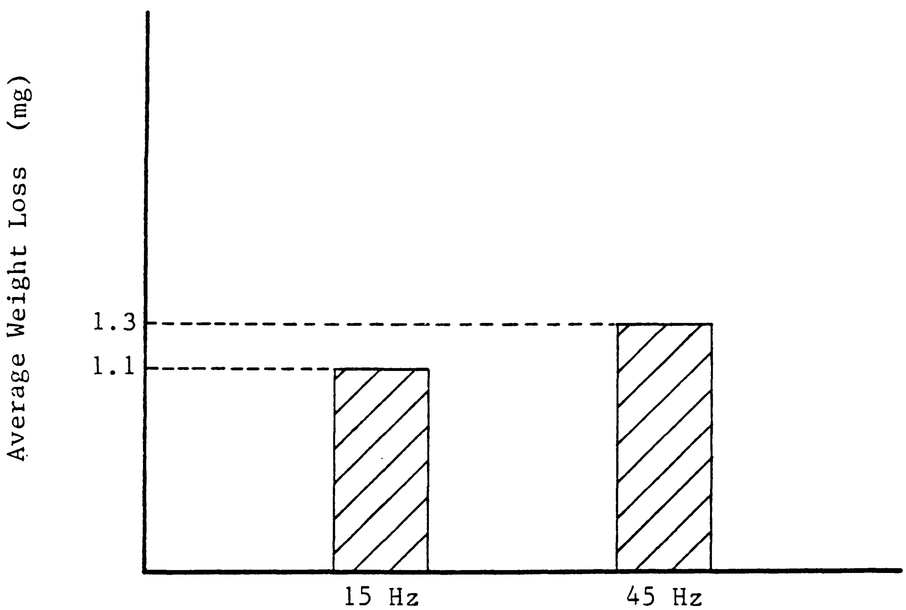

Figure 36. Comparison of Mean Weight Loss Values Found for Frequency - Experiment #5

TABLE 7

FREQUENCY/GREASE INTERACTION: BEARING/CARTRIDGE WEIGHT LOSS

	Average Weight Loss (mg)	
Frequency → / Grease ↓	Low (15 Hz)	High (45 Hz)
NO	1.39	1.83
YES	0.75	0.78

TABLE 8

GREASE/AMPLITUDE INTERACTION: BEARING/CARTRIDGE WEIGHT LOSS

	Average Weight Loss (mg)	
Grease →	NO	YES
Amplitude ↓		
Low (50 μm)	0.50	0.25
High (150 μm)	2.71	1.28

7. An interaction exists between load and amplitude. At low amplitude, an increase in the load results in a decrease in fretting corrosion. At high amplitude, an increase in load results in an increase in fretting corrosion at the interface (see Table 9).

TABLE 9

LOAD/AMPLITUDE INTERACTION: BEARING/CARTRIDGE WEIGHT LOSS

Load → / Amplitude ↓	Average Weight Loss (mg)	
	Low (15 N)	High (90 N)
Low (50 μm)	0.41	0.34
High (150 μm)	0.49	3.50

DISCUSSION

General Comments

The purpose of this research project is to determine the important parameters influencing fretting corrosion at the interface of a bearing outer race and a cartridge bore. The particular system that was modeled (SSMG unit) is one in which fretting corrosion is a serious problem. The basic approach used in the overall research project[37] consists of the following:

1. To learn as much as possible about the nature of fretting corrosion that occurs at the interface of the SSMG bearing/cartridge assembly.
2. To use the information found above in the development of smaller-scale laboratory tests.
3. To use the laboratory tests to determine the significance of various factors (and their interactions) on fretting corrosion.

In general, the information acquired from the SSMG unit shows that relative motion between the bearing and cartridge is very complex.[34] Indeed, the frequency of relative motion between the bearing and cartridge ranges from values as low as 15 Hz to values high as 10 kHz. In addition, relative motion between the bearing and cartridge exists in three directions: axial, tangential, and radial.

In the first two attempts of modeling the SSMG unit (Mark I and Mark II), fretting corrosion between the bearing outer race and cartridge bore was obtained but only after prolonged operation (50 to 1000 hours). The two units that were built essentially modeled the entire SSMG unit, i.e., each model consisted of a rotor mass mounted on a horizontal shaft which was supported at either end by a ball bearing. And, as in the full-scale SSMG unit, the bearing outer races fit into cartridges. In contrast, the bearing/cartridge assemblies mounted in Mark III do not support a rotor mass and can only accommodate axial relative motion between a bearing and cartridge. Although this is a significant departure from the motion found to exist in the SSMG unit, Mark III is capable of obtaining extensive fretting corrosion damage at a bearing/cartridge interface in as little as twenty minutes. In addition, Mark III has the flexibility of examining five bearing/cartridge assemblies at once and will allow variation of magnitude of parameters such as load, frequency, and amplitude. Following now is a discussion of the results obtained using Mark III.

Discussion of Preliminary Experiments

Wear of Cartridge versus Wear of Bearing

From the results of the four preliminary experiments, the cartridge is seen to be more susceptible to fretting wear than the bearing. In experiment 1, for example, the weight loss of the bearings reaches a relatively constant value early in the experiment whereas weight loss of the cartridges continues to increase and reaches a peak value which is approximately three times larger than the average weight loss value of the bearings. The same general trend is seen in experiments 3 and 4, i.e., wear of the cartridge is much greater than wear of the bearings. A possible explanation for this effect is that the fretting wear mechanism which exists for contact between the bearings and cartridges includes abrasive wear, the bearing being less susceptible to abrasive wear than the cartridge. This idea becomes more apparent after examining Table 10 which displays the relative hardness values of the bearing, cartridge, and various iron oxides. The bearing is seen to be 1.7 to 1.9 times harder than the cartridge and 1.1 to 1.4 times harder than the oxides. On the other hand, the oxides are 1.2 to 1.7 times harder than the cartridge. Clearly then, abrasion of the cartridge bore by both the bearing and oxide is possible but abrasion of the bearing outer race is less likely to occur, or, if it does occur, it is less likely to be as severe.

Dry Contact versus Lubricated Contact

Generally speaking, the use of a grease at the bearing/cartridge interface reduced the extent of fretting corrosion to both the bearing and the cartridge initially but had an adverse effect on the bearing after prolonged (500,000 cycles) operation (see Figures 18, 19, 21 and 22). It was suspected when the 500k cycle run was made that bad data or an error in the system had occurred. For that reason all parameter magnitudes were rechecked and the 500k cycle test was rerun. The same result was found to occur again. The reason for this occurrence is not understood. If the grease used to lubricate the interface retained fretting debris, then wear of the cartridge would be expected to increase a substantial amount at 500k cycles. This did not occur. In fact, the average weight loss of dry cartridges at 500k cycles is 1.8 times greater than the weight loss of lubricated cartridges at 500k cycles. Conversely, the average weight loss of dry bearings at 500k cycles is 0.6 times that

TABLE 10

RELATIVE HARDNESS VALUES OF BEARING, CARTRIDGE, and OXIDES

Component	Hardness	Relative Hardness[28]	Reference
BEARING	62 Rockwell C	7.2 MOHS	29
CARTRIDGE	80 - 90 Rockwell B	3.9 - 4.2 MOHS	30
IRON OXIDES:			
Hematite (αFe_2O_3)		5.5 - 6.5 MOHS	31, 32, 33
Magnetite (Fe_3O_4)		5.5 - 6.5 MOHS	33
Josite (FeO)		5.0 MOHS	33

of lubricated bearings for the same number of cycles. The only explanation offered to account for this strange effect is that grease is retained on the surface of the cartridge bore and continues to protect it whereas the grease does not remain on the surface of the bearing outer race and as such does not protect it. The rationale behind this idea is that the rougher surface finish of the cartridge bore (0.35 μm CLA, see Table 2) will retain grease better than the smoother surface of the bearing outer race (0.17 μm CLA, see Table 2). This is consistent with the results of many investigators.[15,20,21]

A discussion of the effect of load and amplitude on the extent of fretting corrosion at the bearing/cartridge interface is given in the following section.

Discussion of Statistically Designed Experiment

Main Effects

The results of the four-factor, two-level analysis of variance experiment show that amplitude, load, presence of a grease at the interface, and frequency all have significant effects (95% confidence level) on fretting corrosion at the bearing/cartridge interface. A brief discussion of how each factor affects fretting corrosion at the interface and why it is thought to do so now follows.

Amplitude was found to have an adverse effect on fretting corrosion at the bearing/cartridge interface; a three-fold increase in amplitude resulted in a five-fold increase in the extent of fretting corrosion. The explanation offered is that the oxide formed during the fretting process is easily removed from the interface. Therefore, an increase in the amplitude would lead to a greater amount of oxide being removed from the interface. At a lower amplitude, the oxide would tend to remain in the contact zone. The idea of the oxide having a low adherence to the damaged surfaces was pointed out earlier in that the ratio of loose debris to adhered debris was found to be very large.

Load was also found to have an adverse effect on fretting corrosion at the interface. A six-fold increase in load was found to increase fretting corrosion by a factor of about four. This is not surprising since increasing load can increase the real area of contact, degree of interaction, and surface temperatures. And load is an important factor influencing damage in all tribological processes--particularly in dry contact situations.[24]

The use of the (Mobil) grease even in small measured quantities reduced the fretting corrosion weight loss by a factor of about two. This general effect is not startling as others have obtained similar results.[15,20,21] Two possible reasons are offered to account for this reduction. First, the use of the grease at the interface would reduce contact and adhesion between the bearing outer race and cartridge bore. This would then reduce surface damage and, ultimately, the production of fretting debris. Secondly, since fretting corrosion involves oxidation, the grease used at the interface prevented oxygen from getting to the surfaces of the interface, thus minimizing iron oxide formation.

The effect of frequency on fretting corrosion at the interface is unexpected. An increase in frequency has generally been found to result in a decrease in fretting corrosion.[3,9,21] Although the difference between the average weight loss values found for the two frequencies is relatively small, the fact still remains that an increase in frequency resulted in an increase in the extent of fretting corrosion at the interface (see Figure 36). One possible explanation for this is that an increase in frequency results in an increase in the velocity of sliding that occurs between the bearing and cartridge. This could result in an increase in the surface temperature of the contact zone which would lead to a greater oxidation rate[18] and, eventually, to a greater production of fretting debris at the interface. Removal of the debris would then result in a greater weight loss.

Interactions

Three first-order interactions were significant, namely load/amplitude, grease/amplitude, and frequency/grease. The load/amplitude interaction is the most striking. At low amplitude (50 μm), the influence of load is small and the weight loss values are small. But at the higher amplitude (150 μm), the increase in load results in a suprisingly large (over seven-fold) increase in fretting corrosion. Ordinarily, one might suspect that when the heavier load was applied (in the case of low amplitude) a significant portion of the motion imparted to the bearings would be taken up by elastic deflection in the apparatus. Indeed, this problem was not at all uncommon where low amplitude, high loads were involved in a fretting corrosion study.[9,15,17,20,21] But, as explained earlier, the loss of motion due to elastic deflection was corrected by increasing the amplitude set at the LVDT by 20 μm . (This was necessary only in test runs that involved the 90 N, W_2, load.) A possible explanation for this striking effect is that at the higher amplitude (150 μm), a greater amount of energy is transferred to the contacting surfaces than is transferred at the lower amplitude (50 μm) for the same increase in load. The increase in energy then leads to much more severe fretting corrosion conditions and, ultimately, a greater weight loss.

The interactions involving the presence of the grease are difficult to visualize and perhaps even more difficult to explain. These effects should be examined carefully.

Comparison of Archard Wear Theory with Experimental Results

In a paper published in 1973, Stowers and Rabinowicz found that the material loss produced by fretting wear resembles that produced by unidirectional adhesive wear much more closely than it does that produced by other types of wear and that the amount of wear may be computed by the use of Archard's wear equation. Therefore, in an attempt to compare the experimental weight loss data with theoretical predictions, Archard's wear theory(11,24) was used. The following relationships were used in this analysis:

$$V = \frac{KW}{P_m}(X) \quad . \; . \; . \; . \; 1$$

$$X = 4AN \quad . \; . \; . \; . \; 2$$

$$V = \frac{W_\ell}{\rho} \quad . \; . \; . \; . \; 3$$

where K = fretting wear coefficient

W = load (N)

P_m = hardness of the softer metal, the cartridge in this case (kg/mm^2)

X = total accumulated relative sliding distance (μm)

ρ = density of metal (kN/m^3)

A = amplitude of motion (μm)

N = total number of cycles

W_ℓ = predicted weight loss (mg)

Equation 1 is recognized as Archard's wear equation, equation 2 relates the total relative sliding distance to the amplitude and number of cycles, and equation 3 relates weight loss to volume. Combining equations 1, 2, and 3 yields the following expression which relates weight loss to load, amplitude, and cycle duration:

$$W_\ell = \frac{KW\rho}{P_m}\ (4AN) \qquad \ldots . \ 4$$

Using the constants given below, equation 4 reduces to equations 5 and 6 which can be used to predict weight losses for dry and lubricated conditions respectively:

P_m = 220 kg/mm^2 (11)

ρ = 76.5 kN/m^3 (26)

K = 30 x 10^6 for well-lubricated contact, steel-on-steel system(25)

K = 300 x 10^6 for unlubricated or poorly lubricated contact, steel-on-steel system(25)

DRY CONTACT:

$$W_\ell = 4.3389 \times 10^{-9}\ (WAN) \qquad \ldots . \ 5$$

LUBRICATED CONTACT:

$$W_\ell = 4.3389 \times 10^{-10}\ (WAN) \qquad \ldots . \ 6$$

In Figure 37, the weight loss values found in experiment 1 were plotted along with the values determined using Archard's equation. As can be seen, the weight loss determined by Archard's equation is linear with respect to the number of cycles (time) and has a much greater slope than what was found experimentally. Furthermore, it is seen that the

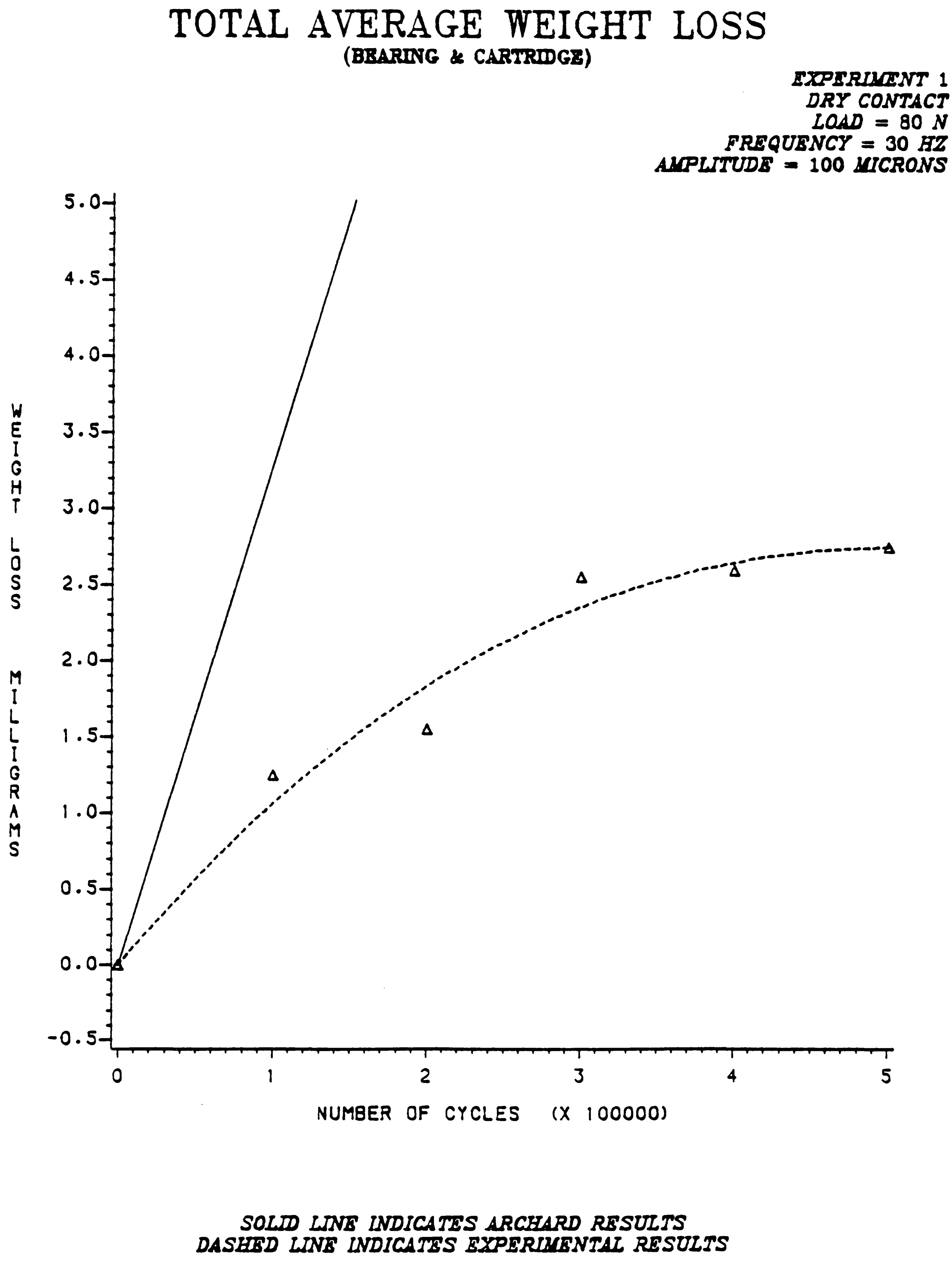

Figure 37. Comparison of Archard Wear Theory with Experimental Results

wear rate found experimentally decreases with respect to time. Although a decrease in the slope of Archard's equation (a lower wear coefficient) would result in closer agreement between experimental and theoretical results, a fundamental difference in the wear rate exists between the two. Two possible explanations to account for this difference are given. First, Archard's wear equation was never designed for a fretting analysis; it does not take into account chemical reaction (e.g., oxidation). Secondly, the wear rate found experimentally appears to have a "wear-in" period. The rate is high initially but then settles down to a steady-state wear rate in which the production of oxides by the fretting corrosion process is roughly equivalent to the rate at which they are removed.

In Figure 38, the weight loss values found for lubricated contact between the bearing and cartridge were plotted along with the values determined using Archard's equation. Agreement between the curves is much closer than what was found for dry contact between the bearing and cartridge but the general trend of the experimental data does not appear to be linear. In contrast to the wear rate found in experiment 1 for dry contact between the bearing and cartridge, the wear rate found for lubricated contact increases with time. Possible explanations for this effect were discussed in a previous section regarding the preliminary experiments.

Shown in Figure 39 is a comparison of the experimental and theoretical results found for the effect of amplitude on weight loss that occurs at the bearing/cartridge interface. Again, major differences exist between the weight loss values found experimentally and those determined using Archard's equation. Archard's equation shows weight loss as being

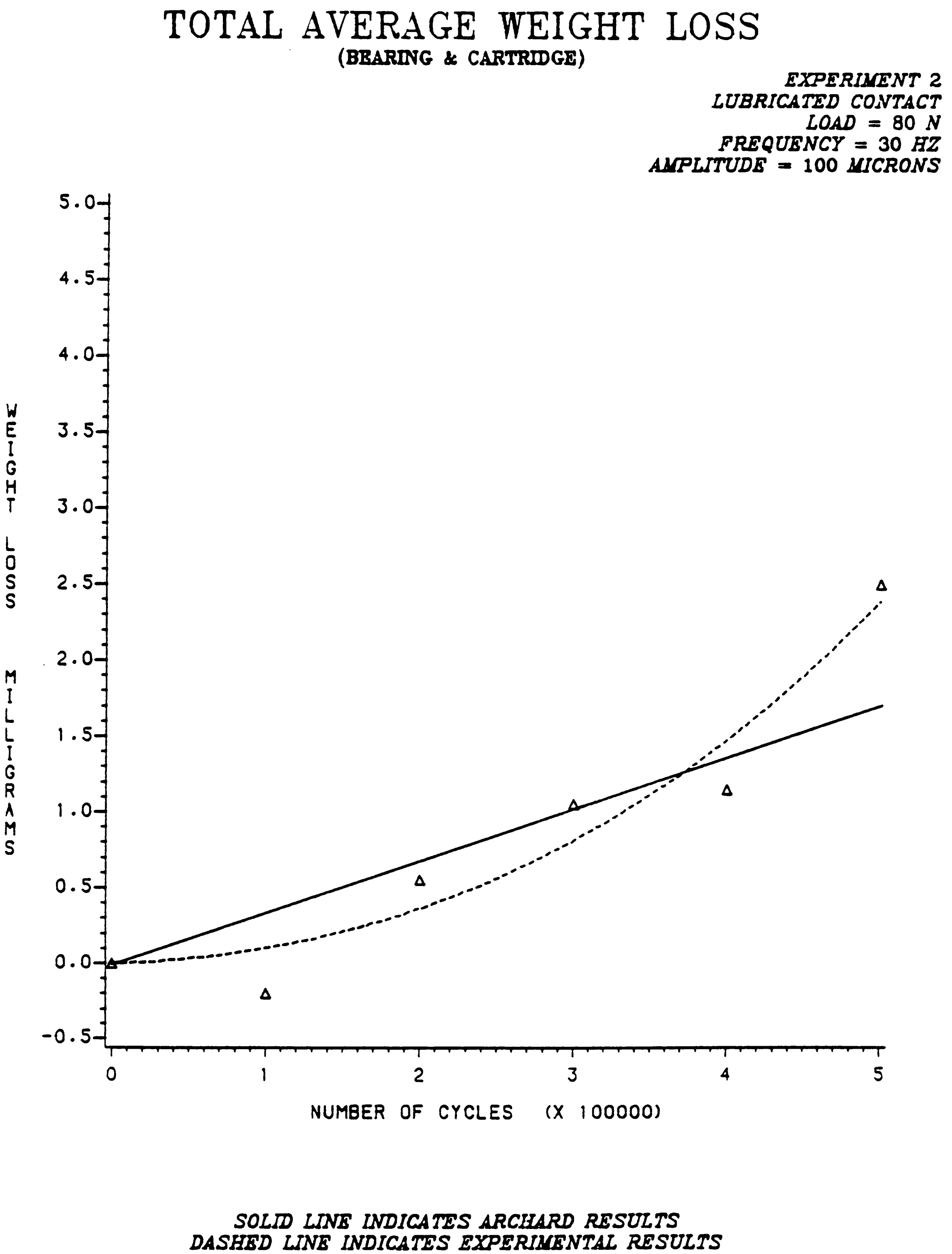

Figure 38. Comparison of Archard Wear Theory with Experimental Results

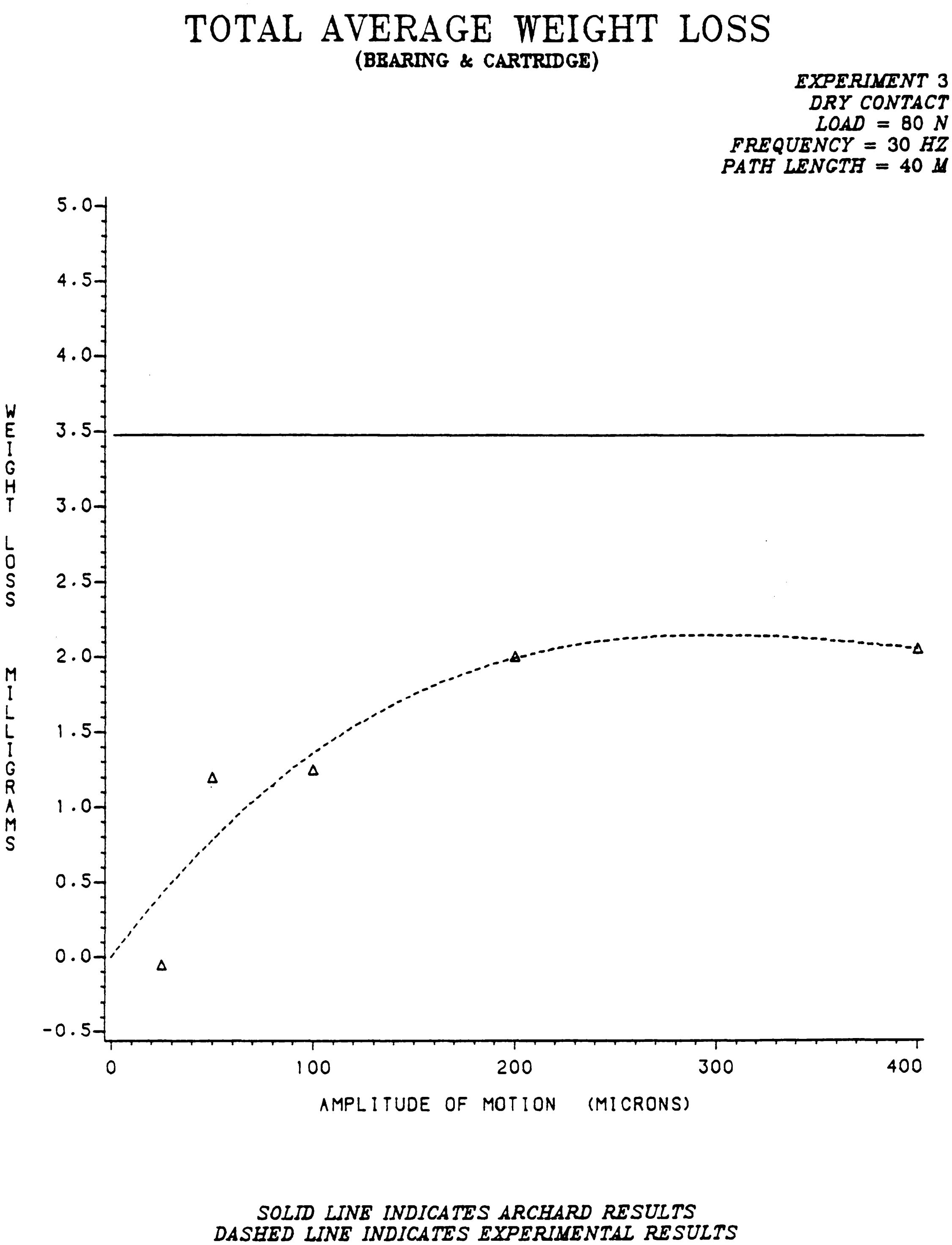

Figure 39. Comparison of Archard Wear Theory with Experimental Results

constant and independent of amplitude whereas the weight loss found experimentally is relatively small for lower amplitudes but then increases and appears to become constant with amplitude. A possible explanation for this effect is that at higher amplitudes, the oscillatory relative motion produced between the bearing and cartridge more closely resembles that found in unidirectional wear. For all amplitudes though, the weight loss found experimentally is much lower than that determined theoretically.

In Figure 40, the experimental weight loss is seen to be approximately linear with respect to load and has a slope of about 0.4. The slope for the theoretical weight loss is approximately 2.0. The difference between the experimental and theoretical results shown here could be attributed to the fretting wear coefficient used in Archard's equation. A smaller wear coefficient would result in a lower slope so that the weight loss determined using Archard's equation would be very similar to that found experimentally.

Although the results suggest that the use of a smaller fretting wear coefficient would tend to reduce the differences found between the experimental and theoretical weight loss, greater fundamental differences exist between the two. Therefore, in concluding this discussion, it is generally felt that Archard's wear equation cannot be used to predict fretting wear rates for a bearing/cartridge geometry.

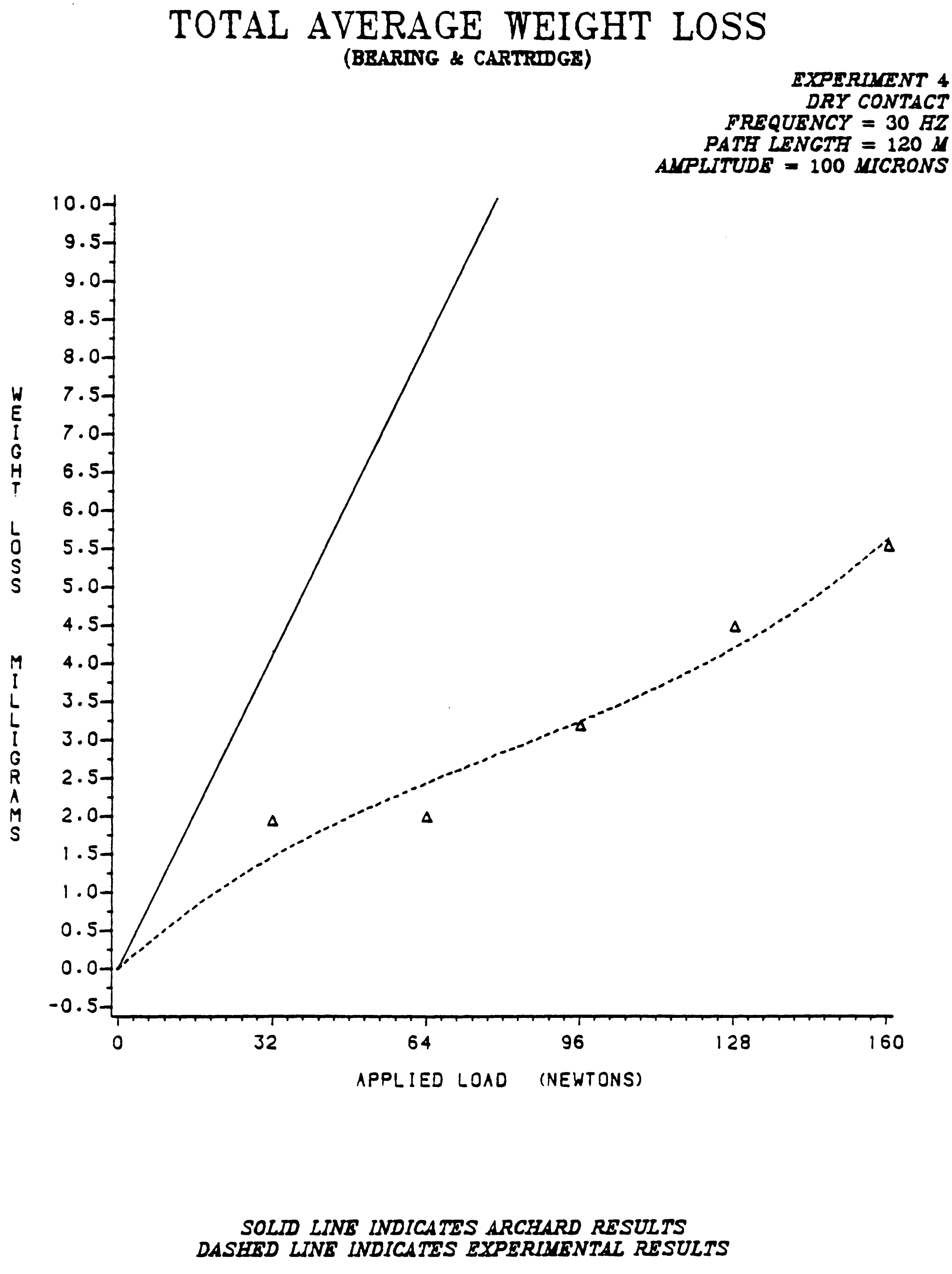

Figure 40. Comparison of Archard Wear Theory with Experimental Results

CONCLUSIONS

In this investigation, an apparatus has been built which is capable of studying fretting corrosion phenomena at a bearing/cartridge interface. The device produces axial relative motion between a bearing and cartridge and will allow a variation in the magnitude of load from zero to 200 N (45 lbf), amplitude of vibration from zero to 500 μm (0.0197 in.), and frequency from 2.5 to 100 Hz. Five sets of bearings and cartridges can be tested simultaneously at the same amplitude and frequency. Using this device with 52100 hardened steel bearings mounted in SAE 1020 steel cartridges, five separate investigations were carried out: the first four examine the influence of cycle duration (time), amplitude, and load on the extent of fretting corrosion at the interface; the fifth determines the significance of load, frequency, amplitude, and presence of a grease on the extent of fretting corrosion at the interface. The amount of weight lost by a bearing/cartridge set in a test run was used as the means of quantifying the extent of fretting corrosion at the interface. The results of this investigation are as follows:

1. The cartridge is more susceptible to fretting corrosion than is the bearing.
2. Fretting corrosion increases with increasing load and amplitude.
3. Fretting corrosion at a bearing/cartridge interface increases with time for both dry and lubricated contact between the bearing and cartridge.
4. Load, frequency, amplitude, and presence of a grease at the interface all have a significant effect (95% confidence level)

on fretting corrosion at the bearing/cartridge interface.

5. Amplitude has the effect of greatest magnitude and is followed by load, grease, and frequency in order of magnitude.
6. An interaction exists (95% confidence level) between the parameters of each set given below which has an effect on fretting corrosion at a bearing/cartridge interface.
    a. Load, Amplitude
    b. Grease, Load, Amplitude
    c. Grease, Amplitude
    d. Frequency, Grease, Amplitude
    e. Frequency, Load, Amplitude
    f. Frequency, Grease
7. The grease used in shipboard service to lubricate SSMG bearing/cartridge assemblies (which is the same grease used in this study) effectively prolongs the initiation of fretting corrosion. But once fretting begins, the grease acts in a manner which appears to increase the severity of fretting corrosion of the bearings but not that of the cartridges.
8. Archard's equation is not an appropriate means of predicting fretting wear between a bearing and cartridge.

RECOMMENDATIONS

The recommendations offered for the continuation of this study are separated into two parts. The first part is concerned with improvements in the apparatus: the second part includes future studies that should be undertaken. Both parts are discussed below.

1. A better means for measuring the amplitude of motion should be examined. An improved method would be to measure the amplitude at the interface. Such a method would eliminate the possibility of elastic deflection as being a source of error.
2. Heavier drive shafts should be installed on the apparatus as a major portion of the motion loss is suspected as originating from deflection of the shafts.
3. A study should be undertaken to investigate the effectiveness of various lubricants. A particularly exciting lubrication concept which would be especially applicable to the situation at hand is Furey's[27] "in situ" polymeric film concept. An investigation of this type is well suited for the apparatus that was designed and built for this project since it is capable of obtaining severe fretting corrosion in a very short amount of time.
4. A study should be undertaken to investigate the influence of material combinations, surface finish, and environmental conditions on the extent of fretting corrosion at the interface. Investigation of factors such as these would be particularly

easy to accomplish due to the design of the apparatus.

5. A study should be undertaken to investigate the effectiveness of other various anti-fretting approaches such as surface films, coatings, and surface treatments (e.g., ion-implantation).

6. The results of this study should be tied in with the results of the surface analytical studies being carried out by the Naval Research Laboratories on damaged Mark III bearings and cartridges. This would provide a better understanding of the fretting corrosion process that occurs at the bearing/cartridge interface.

REFRENCES

1. Furey, M. J., and Mabie, H. H., An Investigation of Fretting Corrosion of Rolling Element Bearings in Power Transmission Systems, Project Report 1 Sept. 1980 - 31 Aug. 1981, VPI & SU, p. 2.

2. Tomlinson, G. A., "The Rusting of Steel Surfaces in Contact," Proceedings of the Royal Society, Ser. A 115, 1927, pp. 472-486.

3. Furey, M. J., and Mabie, H. H., An Investigation of Fretting Corrosion of Rolling Element Bearings in Power Transmission Systems, Research Proposal, VPI & SU, Dec. 1979.

4. Glossary of Terms and Definitions in the Field of Friction, Wear, and Lubrication - Tribology, OECD, 1969, p. 35.

5. Tomlinson, G. A., Thorpe, P. L., and Gough, H. J., "An Investigation of Fretting Corrosion of Closely Fitting Surfaces," Proceedings, Institute of Mechanical Engineers, Vol. 141, No. 3, 1939, pp. 223-249.

6. Godfrey, D., "Investigation of Fretting Corrosion by Microscopic Observation," NACA TN 1009, 1951.

7. Godfrey, D., and Baily, J. M., "Coefficient of Friction and Damage to Contact Area During the Early Stages of Fretting," NACA TN 3011, Part 1, 1953.

8. Feng, I. M., and Rightmire, B. G., "The Mechanism of Fretting," Lubrication Engineering, Vol, 9, No. 3, June 1953, pp. 134-136, 158-161.

9. Uhlig, H. H., et al., "A Fundamental Investigation of Fretting Corrosion," NACA TN 3029, 1953.

10. Halliday, J. S., and Hirst, W., "The Fretting Corrosion of Mild Steel," Proceedings of Royal Society, Ser. A 256, Aug. 1956, pp. 411-425.

11. Stowers, I. F., and Rabinowicz, E., "The Mechanism of Fretting Wear," Journal of Lubrication Technology, Trans. of ASME, Vol. 95, No. 1, Jan. 1973, pp. 65-70.

12. Waterhouse, R. B., "The Effect of Environment in Wear Processes and the Mechanisms of Fretting Wear," Fundamentals of Tribology, edited by N. P. Suh and N. Saka, MIT Press, Cambridge, Mass., 1978, pp. 567-584.

13. Bill, R. C., "The Role of Oxidation in the Fretting Wear Process," Wear of Materials, ASME, New York, N. Y., 1981, pp. 238-250.

14. Almen, J. O., "Fretting Corrosion," Corrosion Handbook, edited by H. H. Uhlig, John Wiley and Sons Inc., New York, N. Y., 1948, pp. 590-597.

15. Campbell, W. E., "Fretting," Boundary Lubrication, An Appraisal of World Literature, ASME, New, York, N. Y., 1969, pp. 119-131.

16. Feng, I. M., and Uhlig, H. H., "Fretting Corrosion of Mild Steel in Air and Nitrogen," Journal of Applied Mechanics, Vol. 21, Dec. 1954, pp. 395-400.

17. Waterhouse, R. B., Fretting Corrosion, Pergamon Press, New York, N. Y., 1972, p. 126.

18. Kayaba, T., and Iwabuchi, A., "The Fretting Wear of 0.45 Percent Carbon Steel and Austenitic Stainless Steel From 20° C up to 650° C in Air," Wear of Materials, ASME, New York, N. Y., 1981, pp. 229-237.

19. Quinn, T. F. J., "Oxidational Wear," Wear, Vol. 18, 1971, pp. 413-419.

20. Barnett, R. S., "Fretting Corrosion," Lubrication Engineering, Vol. 8, No. 4, Aug. 1952, pp. 186-188, 205-206.

21. "Fretting and Fretting Corrosion," Lubrication, Vol. 52, No. 4, Texaco Incorporated, 1966, pp. 49-64.

22. Technical Manual, DC/AC or AC/DC Motor-Generator Set and Associated Control Equipment, Commander, Naval Sea Systems Command, Oct. 1973.

23. Craig, R. J., Anderson, D. R., and Czyryca, E. J., "Examination of Ball Bearings on Ship Service Motor-Generator Sets Aboard SSN 688 Class Submarines," David W. Taylor Naval Ship Research and Development Center Report SME 78-96, Apr. 1979. p. 12, 30.

24. Archard, J. F., "Wear Theory and Mechanisms," Wear Control Handbook, edited by M. B. Peterson and W. O. Winer, ASME, New York, N. Y., 1980, pp. 35-80.

25. Rabinowicz, E., "Wear Coefficients," Wear Control Handbook, edited by M. B. Peterson and W. O. Winer, ASME, New York, N. Y., 1980, pp. 475-506.

26. Shigley, J. E., Mechanical Engineering Design, McGraw-Hill Book Co., New York, N. Y., 1977, p. 636.

27. Furey, M. J., "The Formation of Polymeric Films Directly on Rubbing Surfaces to Reduce Wear," Wear, Vol. 26, 1973, pp. 369-392.

28. Kinney. G. F., Engineering Properties and Applications of Plastics, John Wiley and Sons Inc., New York, N. Y., 1957, p. 102.

29. Craig, op. cit., p. 13.

30 Craig, op. cit., p. 30.

31. Waterhouse, R. B., Fretting Corrosion, Pergamon Press, New York, N. Y., 1972, p. 120.

32. Kayaba, op, cit., p. 234

33. Samsonov, G. V., The Oxide Handbook, IFI/Plenum, New York, N. Y., 1973, p. 255.

34. Elliott, K. B., Mabie, H. H., Furey, M. J., and Mitchell, L. D., "A Vibrational Analysis of a Bearing/Cartridge Interface for a Fretting Corrosion Study," ASME Paper No. 82-Lub-19, 1982.

35. "Ball and Roller Bearings," NTN Bearing Corporation of America, Catalog No. A1000-11, 1979.

36. Bearing Cartridge DC End, Drawing No. 36A162439AB, General Electric Direct Current and Motor-Generator Dept., Erie, Pa.

37. Furey, M. J., and Mabie, H. H., The Prevention of Fretting Corrosion Between the Outer Race and Cartridge of Rolling Element Bearings, Project Report 1 April 1982 - 30 September 1983, VPI & SU.

APPENDIX A

EQUIPMENT LIST

1. Vibration Fatigue Testing Machine

   Manufacturer: All American Tool & Mfg. Co.

   Model No.: 10-VA-T

2. Digital Voltmeter

   Manufacturer: Keithley

   Model No.: 168

   Serial No.: 37276

3. Oscilloscope

   Manufacturer: Tektronix

   Model No.: T922

   Serial No.: T922 B012298

4. Power Supply

   Manufacturer: Hewelett Packard

   Model No.: 721A

   Serial No.: 5H5053

5. Signal Generator

   Manufacturer: Wavtek

   Model No.: 111

   Serial No.: 129754

6. Cycle Counter

   Manufacturer: Hewlett Packard

   Model No.: 5326B

   Serial No.: 1612A03614

7. Linear Voltage Displacement Transformer

    Manufacturer: Schaevitz Engineering

    Model No.: E200

    Serial No.: 5328

8. Potentiometer

    Manufacturer: Allen Bradley

    Model No.: KS-13790-L4

    Serial No.: 113176

9. Chemical Balance

    Manufacturer: Mettler

    Model No.: H5

    Serial No.: 113176

10. Ultrasonic Cleaner

    Manufacturer: Fisher Scientific

    Model No.: B-92

    Serial No.: 0131 (VPI & SU)

APPENDIX B

EXPERIMENTAL DATA

TABLE B-1

DATA FROM EXPERIMENT #1

Number of cycles	Bearing Weight Loss Position #2	Bearing Weight Loss Position #4	Cartridge Weight Loss Position #2	Cartridge Weight Loss Position #4	Average Weight Loss of Bearings	Average Weight Loss of Cartridges	Total** Weight Loss
$1x10^5$	0.7*	0.6	0.6	0.6	0.65	0.60	1.25
$2x10^5$	0.5	0.4	0.8	1.4	0.45	1.10	1.55
$3x10^5$	0.6	0.8	1.6	2.1	0.70	1.85	2.55
$4x10^5$	0.6	0.7	2.0	1.9	0.65	1.95	2.60
$5x10^5$	1.0	0.7	1.7	2.1	0.85	1.90	2.75

Load: 80 N (17.99 lbs.)
Amplitude: 100 μm (0.0039 in.), as set with LVDT (uncorrected for possible elastic losses)
Frequency: 30 Hz
Relative Humidity: Mean = 64.4%, Standard Deviation = 1.5
Dry Contact

* All weight loss values given in milligrams.

** Determined using average weight loss of bearings and cartridges.

TABLE B-2

DATA FROM EXPERIMENT #2

Number of Cycles	Bearing Weight Loss Position #2	Bearing Weight Loss Position #4	Cartridge Weight Loss Position #2	Cartridge Weight Loss Position #4	Average Weight Loss of Bearings	Average Weight Loss of Cartridges	Total** Weight Loss
$1x10^5$	0.0*	0.1	-0.2	-0.3	0.05	-0.25	-0.20
$2x10^5$	0.4	0.4	0.3	0.0	0.40	0.15	0.55
$3x10^5$	0.5	0.5	0.6	0.5	0.50	0.55	1.05
$4x10^5$	0.7	0.2	0.6	0.8	0.45	0.70	1.15
$5x10^5$	1.1	1.8	1.0	1.1	1.45	1.05	1.50

Load: 80 N (17.99 lbs.)
Amplitude: 100 μm (0.0039 in.), as set with LVDT (uncorrected for possible elastic losses)
Frequency: 30 Hz
Relative Humidity: Mean = 74.4%, Standard Deviation = 1.5
Lubricated Contact

* All weight loss values given in milligrams.

** Determined using average weight loss of bearings and cartridges.

TABLE B-3

DATA FROM EXPERIMENT #3

Amplitude	Bearing Weight Loss Position #2	Bearing Weight Loss Position #4	Cartridge Weight Loss Position #2	Cartridge Weight Loss Position #4	Average Weight Loss of Bearings	Average Weight Loss of Cartridges	Total** Weight Loss
25 μm*** (0.0010 in.)	0.0*	0.0	-0.1	0.0	0.00	-0.05	-0.05
50 μm (0.0020 in.)	0.6	0.6	0.7	0.5	0.60	0.60	1.20
100 μm (0.0039 in.)	0.7	0.6	0.6	0.6	0.65	0.60	1.25
200 μm (0.0079 in.)	0.7	0.8	1.3	1.2	0.75	1.25	2.00
400 μm (0.0157 in.)	0.5	0.7	1.7	1.2	0.60	1.45	2.05

Load: 80 N (17.99 lbs.)
Frequency: 30 Hz
Path Length: 40 m (131.23 ft.)
Relative Humidity: Mean = 68.8%, Standard Deviation = 3.2
Dry Contact

* All weight loss values given in milligrams.

** Determined using average weight loss of bearings and cartridges.

*** Amplitudes given in this table represent actual LVDT settings (uncorrected for elastic losses)

TABLE B-4

DATA FROM EXPERIMENT #4

Load	Bearing Weight Loss Position #2	Bearing Weight Loss Position #4	Cartridge Weight Loss Position #2	Cartridge Weight Loss Position #4	Average Weight Loss of Bearings	Average Weight Loss of Cartridges	Total** Weight Loss
32 N (7.20 lbs.)	0.7*	0.7	1.2	1.3	0.70	1.25	1.95
64 N (14.39 lbs.)	0.7	0.9	1.2	1.2	0.80	1.20	2.00
96 N (21.59 lbs.)	1.1	1.2	1.9	2.2	1.15	2.05	3.20
128 N (28.78 lbs.)	1.4	1.5	3.1	3.0	1.45	3.05	4.50
160 N (35.98 lbs.)	1.9	1.7	3.6	3.9	1.80	3.75	5.55

Amplitude: 100 μm (0.0039 in.), as set with LVDT (uncorrected for elastic losses)
Frequency: 30 Hz
Path Length: 120 m (393.70 ft.)
Relative Humidity: Mean = 68.6%, Standard Deviation = 5.1
Dry Contact

* All weight loss values given in milligrams.

** Determined using average weight loss of bearings and cartridges.

TABLE B-5

DATA FROM EXPERIMENT #5

Test Run Number	Bearing Weight Loss Position #2	Bearing Weight Loss Position #4	Cartridge Weight Loss Position #2	Cartridge Weight Loss Position #4	Bearing & Cartridge Weight Loss Position #2	Bearing & Cartridge Weight Loss Position #4
1	0.1*	0.0	0.0	0.1	0.1	0.1
2	0.1	0.3	0.6	0.8	0.7	1.1
3	0.0	0.0	0.0	0.1	0.0	0.1
4	2.2	1.5	2.7	2.6	4.9	4.1
5	0.0	0.0	0.0	0.1	0.0	0.1
6	0.0	0.0	0.3	0.1	0.3	0.1
7	0.9	1.0	0.0	0.0	0.9	1.0
8	0.2	0.4	1.2	1.8	1.4	2.2
9	0.7	0.8	0.7	0.8	1.4	1.6
10	0.3	0.2	0.6	0.4	0.9	0.6

TABLE B-5 (Continued)

Test Run Number	Bearing Weight Loss Position #2	Bearing Weight Loss Position #4	Cartridge Weight Loss Position #2	Cartridge Weight Loss Position #4	Bearing & Cartridge Weight Loss Position #2	Bearing & Cartridge Weight Loss Position #4
11	0.0	0.0	0.3	0.4	0.3	0.4
12	1.3	1.3	3.4	3.4	4.7	4.7
13	0.0	0.0	0.0	0.0	0.0	0.0
14	0.0	0.0	0.1	0.1	0.1	0.1
15	0.0	0.0	0.0	0.0	0.0	0.0
16	0.5	0.6	2.3	2.6	2.8	3.2

Relative Humidity: Mean = 64.3%, Standard Deviation = 3.1

* All weight loss values are given in milligrams and have been corrected for elastic losses.

APPENDIX C

STATISTICAL ANALYSIS COMPUTER OUTPUT

TABLE C-1

TEST RUNS USED IN STATISTICAL DESIGN

Run Number	Frequency	Grease	Load	Amplitude
1	F_1	No	W_1	A_1
2	F_1	No	W_1	A_2
3	F_1	No	W_2	A_1
4	F_1	No	W_2	A_2
5	F_1	Yes	W_1	A_1
6	F_1	Yes	W_1	A_2
7	F_1	Yes	W_2	A_1
8	F_1	Yes	W_2	A_2
9	F_2	No	W_1	A_1
10	F_2	No	W_1	A_2
11	F_2	No	W_2	A_1
12	F_2	No	W_2	A_2
13	F_2	Yes	W_1	A_1
14	F_2	Yes	W_1	A_2
15	F_2	Yes	W_2	A_1
16	F_2	Yes	W_2	A_2

F_1 = 15 Hz , F_2 = 45 Hz

W_1 = 15 N (3.37 lb.) , W_2 = 90 N (20.24 lb.)

A_1 = 50 μm (0.0020 in.), A_2 = 150 μm (0.0060 in.)

NOTE:

For all W_2 combinations, amplitude set on LVDT was increased by 20 μm (0.0008 in.) to correct for elastic losses (e.g., for run number 3, LVDT was set at 70 μm; for run number 4, LVDT was set at 170 μm).

EXPERIMENT 5 (BEARING ANALYSIS)

OBS	A	B	C	D	Y
1	F1	N	W1	A1	0.1
2	F1	N	W1	A1	0.0
3	F1	N	W1	A2	0.1
4	F1	N	W1	A2	0.3
5	F1	N	W2	A1	0.0
6	F1	N	W2	A1	0.0
7	F1	N	W2	A2	2.2
8	F1	N	W2	A2	1.5
9	F1	Y	W1	A1	0.0
10	F1	Y	W1	A1	0.0
11	F1	Y	W1	A2	0.0
12	F1	Y	W1	A2	0.0
13	F1	Y	W2	A1	0.9
14	F1	Y	W2	A1	1.0
15	F1	Y	W2	A2	0.2
16	F1	Y	W2	A2	0.4
17	F2	N	W1	A1	0.7
18	F2	N	W1	A1	0.8
19	F2	N	W1	A2	0.3
20	F2	N	W1	A2	0.2

EXPERIMENT 5 (BEARING ANALYSIS)

OBS	A	B	C	D	Y
21	F2	N	W2	A1	0.0
22	F2	N	W2	A1	0.0
23	F2	N	W2	A2	1.3
24	F2	N	W2	A2	1.3
25	F2	Y	W1	A1	0.0
26	F2	Y	W1	A1	0.0
27	F2	Y	W1	A2	0.0
28	F2	Y	W1	A2	0.0
29	F2	Y	W2	A1	0.0
30	F2	Y	W2	A1	0.0
31	F2	Y	W2	A2	0.5
32	F2	Y	W2	A2	0.6

EXPERIMENT 5 (BEARING ANALYSIS)

ANALYSIS OF VARIANCE PROCEDURE

CLASS LEVEL INFORMATION

CLASS	LEVELS	VALUES
A	2	F1 F2
B	2	N Y
C	2	W1 W2
D	2	A1 A2

NUMBER OF OBSERVATIONS IN DATA SET = 32

EXPERIMENT 5 (BEARING ANALYSIS)

ANALYSIS OF VARIANCE PROCEDURE

DEPENDENT VARIABLE: Y

SOURCE	DF	SUM OF SQUARES	MEAN SQUARE
MODEL	15	9.34500000	0.62300000
ERROR	16	0.31000000	0.01937500
CORRECTED TOTAL	31	9.65500000	

MODEL F = 32.15 PR > F = 0.0001

R-SQUARE	C.V.	STD DEV	Y MEAN
0.967892	35.9211	0.13919411	0.38750000

EXPERIMENT 5 (BEARING ANALYSIS)

ANALYSIS OF VARIANCE PROCEDURE

DEPENDENT VARIABLE: Y

SOURCE	DF	ANOVA SS	F VALUE	PR > F
A	1	0.03125000	1.61	0.2222
B	1	0.84500000	43.61	0.0001
C	1	1.71125000	88.32	0.0001
D	1	0.91125000	47.03	0.0001
A*B	1	0.10125000	5.23	0.0362
A*C	1	0.50000000	25.81	0.0001
A*D	1	0.00000000	0.00	1.0000
B*C	1	0.00125000	0.06	0.8027
B*D	1	1.05125000	54.26	0.0001
C*D	1	1.44500000	74.58	0.0001
A*B*C	1	0.04500000	2.32	0.1470
A*B*D	1	0.72000000	37.16	0.0001
A*C*D	1	0.21125000	10.90	0.0045
B*C*D	1	1.62000000	83.61	0.0001
A*B*C*D	1	0.15125000	7.81	0.0130

EXPERIMENT 5 (BEARING ANALYSIS)

ANALYSIS OF VARIANCE PROCEDURE

DUNCAN'S MULTIPLE RANGE TEST FOR VARIABLE: Y
NOTE: THIS TEST CONTROLS ERROR RATES AT DIFFERENT LEVELS
DEPENDING ON THE NUMBER OF MEANS BETWEEN EACH PAIR
BEING COMPARED. ITS OPERATING CHARACTERISTICS SOMEWHAT
RESEMBLE FISHER'S UNPROTECTED LSD TEST.
ALPHA=0.05 DF=16 MSE=0.019375

MEANS WITH THE SAME LETTER ARE NOT SIGNIFICANTLY DIFFERENT.

DUNCAN GROUPING	MEAN	N	A
A	0.41875	16	F1
A			
A	0.35625	16	F2

EXPERIMENT 5 (BEARING ANALYSIS)

ANALYSIS OF VARIANCE PROCEDURE

DUNCAN'S MULTIPLE RANGE TEST FOR VARIABLE: Y
NOTE: THIS TEST CONTROLS ERROR RATES AT DIFFERENT LEVELS

```
      DEPENDING ON THE NUMBER OF MEANS BETWEEN EACH PAIR
      BEING COMPARED. ITS OPERATING CHARACTERISTICS SOMEWHAT
      RESEMBLE FISHER'S UNPROTECTED LSD TEST.
ALPHA=0.05   DF=16   MSE=0.019375

MEANS WITH THE SAME LETTER ARE NOT SIGNIFICANTLY DIFFERENT.

DUNCAN    GROUPING              MEAN        N  B

                A           0.55000      16  N

                B           0.22500      16  Y

EXPERIMENT 5 (BEARING ANALYSIS)

ANALYSIS OF VARIANCE PROCEDURE

DUNCAN'S MULTIPLE RANGE TEST FOR VARIABLE: Y
NOTE: THIS TEST CONTROLS ERROR RATES AT DIFFERENT LEVELS
      DEPENDING ON THE NUMBER OF MEANS BETWEEN EACH PAIR
      BEING COMPARED. ITS OPERATING CHARACTERISTICS SOMEWHAT
      RESEMBLE FISHER'S UNPROTECTED LSD TEST.
ALPHA=0.05   DF=16   MSE=0.019375

MEANS WITH THE SAME LETTER ARE NOT SIGNIFICANTLY DIFFERENT.

DUNCAN    GROUPING              MEAN        N  C

                A           0.61875      16  W2

                B           0.15625      16  W1

EXPERIMENT 5 (BEARING ANALYSIS)

ANALYSIS OF VARIANCE PROCEDURE

DUNCAN'S MULTIPLE RANGE TEST FOR VARIABLE: Y
NOTE: THIS TEST CONTROLS ERROR RATES AT DIFFERENT LEVELS
      DEPENDING ON THE NUMBER OF MEANS BETWEEN EACH PAIR
      BEING COMPARED. ITS OPERATING CHARACTERISTICS SOMEWHAT
      RESEMBLE FISHER'S UNPROTECTED LSD TEST.
ALPHA=0.05   DF=16   MSE=0.019375

MEANS WITH THE SAME LETTER ARE NOT SIGNIFICANTLY DIFFERENT.

DUNCAN    GROUPING              MEAN        N  D

                A           0.55625      16  A2

                B           0.21875      16  A1
```

EXPERIMENT 5 (CARTRIDGE ANALYSIS)

OBS	A	B	C	D	Y
1	F1	N	W1	A1	0.0
2	F1	N	W1	A1	0.1
3	F1	N	W1	A2	0.6
4	F1	N	W1	A2	0.8
5	F1	N	W2	A1	0.0
6	F1	N	W2	A1	0.1
7	F1	N	W2	A2	2.7
8	F1	N	W2	A2	2.6
9	F1	Y	W1	A1	0.0
10	F1	Y	W1	A1	0.1
11	F1	Y	W1	A2	0.3
12	F1	Y	W1	A2	0.1
13	F1	Y	W2	A1	0.0
14	F1	Y	W2	A1	0.0
15	F1	Y	W2	A2	1.2
16	F1	Y	W2	A2	1.8
17	F2	N	W1	A1	0.7
18	F2	N	W1	A1	0.8
19	F2	N	W1	A2	0.6
20	F2	N	W1	A2	0.4

EXPERIMENT 5 (CARTRIDGE ANALYSIS)

OBS	A	B	C	D	Y
21	F2	N	W2	A1	0.3
22	F2	N	W2	A1	0.4
23	F2	N	W2	A2	3.4
24	F2	N	W2	A2	3.4
25	F2	Y	W1	A1	0.0
26	F2	Y	W1	A1	0.0
27	F2	Y	W1	A2	0.1
28	F2	Y	W1	A2	0.1
29	F2	Y	W2	A1	0.0
30	F2	Y	W2	A1	0.0
31	F2	Y	W2	A2	2.3
32	F2	Y	W2	A2	2.6

EXPERIMENT 5 (CARTRIDGE ANALYSIS)

ANALYSIS OF VARIANCE PROCEDURE

CLASS LEVEL INFORMATION

CLASS	LEVELS	VALUES
A	2	F1 F2
B	2	N Y
C	2	W1 W2
D	2	A1 A2

NUMBER OF OBSERVATIONS IN DATA SET = 32

EXPERIMENT 5 (CARTRIDGE ANALYSIS)

ANALYSIS OF VARIANCE PROCEDURE

DEPENDENT VARIABLE: Y

SOURCE	DF	SUM OF SQUARES	MEAN SQUARE
MODEL	15	36.31468750	2.42097917
ERROR	16	0.31500000	0.01968750
CORRECTED TOTAL	31	36.62968750	

MODEL F = 122.97 PR > F = 0.0001

R-SQUARE	C.V.	STD DEV	Y MEAN
0.991400	17.6078	0.14031215	0.79687500

EXPERIMENT 5 (CARTRIDGE ANALYSIS)

ANALYSIS OF VARIANCE PROCEDURE

DEPENDENT VARIABLE: Y

SOURCE	DF	ANOVA SS	F VALUE	PR > F
A	1	0.69031250	35.06	0.0001
B	1	2.15281250	109.35	0.0001
C	1	8.10031250	411.44	0.0001
D	1	13.13281250	667.06	0.0001
A*B	1	0.07031250	3.57	0.0770
A*C	1	0.34031250	17.29	0.0007
A*D	1	0.02531250	1.29	0.2735
B*C	1	0.09031250	4.59	0.0479
B*D	1	0.42781250	21.73	0.0003
C*D	1	10.01281250	508.59	0.0001
A*B*C	1	0.03781250	1.92	0.1848
A*B*D	1	0.22781250	11.57	0.0036
A*C*D	1	0.69031250	35.06	0.0001
B*C*D	1	0.30031250	15.25	0.0013
A*B*C*D	1	0.01531250	0.78	0.3909

EXPERIMENT 5 (CARTRIDGE ANALYSIS)

ANALYSIS OF VARIANCE PROCEDURE

DUNCAN'S MULTIPLE RANGE TEST FOR VARIABLE: Y
NOTE: THIS TEST CONTROLS ERROR RATES AT DIFFERENT LEVELS DEPENDING ON THE NUMBER OF MEANS BETWEEN EACH PAIR BEING COMPARED. ITS OPERATING CHARACTERISTICS SOMEWHAT RESEMBLE FISHER'S UNPROTECTED LSD TEST.
ALPHA=0.05 DF=16 MSE=.0196875

MEANS WITH THE SAME LETTER ARE NOT SIGNIFICANTLY DIFFERENT.

DUNCAN GROUPING	MEAN	N	A
A	0.94375	16	F2
B	0.65000	16	F1

EXPERIMENT 5 (CARTRIDGE ANALYSIS)

ANALYSIS OF VARIANCE PROCEDURE

DUNCAN'S MULTIPLE RANGE TEST FOR VARIABLE: Y
NOTE: THIS TEST CONTROLS ERROR RATES AT DIFFERENT LEVELS

```
      DEPENDING ON THE NUMBER OF MEANS BETWEEN EACH PAIR
      BEING COMPARED. ITS OPERATING CHARACTERISTICS SOMEWHAT
      RESEMBLE FISHER'S UNPROTECTED LSD TEST.
ALPHA=0.05  DF=16  MSE=.0196875

MEANS WITH THE SAME LETTER ARE NOT SIGNIFICANTLY DIFFERENT.

DUNCAN   GROUPING              MEAN       N  B

               A             1.0562      16  N

               B             0.5375      16  Y

EXPERIMENT 5 (CARTRIDGE ANALYSIS)

ANALYSIS OF VARIANCE PROCEDURE

DUNCAN'S MULTIPLE RANGE TEST FOR VARIABLE: Y
NOTE: THIS TEST CONTROLS ERROR RATES AT DIFFERENT LEVELS
      DEPENDING ON THE NUMBER OF MEANS BETWEEN EACH PAIR
      BEING COMPARED. ITS OPERATING CHARACTERISTICS SOMEWHAT
      RESEMBLE FISHER'S UNPROTECTED LSD TEST.
ALPHA=0.05  DF=16  MSE=.0196875

MEANS WITH THE SAME LETTER ARE NOT SIGNIFICANTLY DIFFERENT.

DUNCAN   GROUPING              MEAN       N  C

               A             1.3000      16  W2

               B             0.2937      16  W1

EXPERIMENT 5 (CARTRIDGE ANALYSIS)

ANALYSIS OF VARIANCE PROCEDURE

DUNCAN'S MULTIPLE RANGE TEST FOR VARIABLE: Y
NOTE: THIS TEST CONTROLS ERROR RATES AT DIFFERENT LEVELS
      DEPENDING ON THE NUMBER OF MEANS BETWEEN EACH PAIR
      BEING COMPARED. ITS OPERATING CHARACTERISTICS SOMEWHAT
      RESEMBLE FISHER'S UNPROTECTED LSD TEST.
ALPHA=0.05  DF=16  MSE=.0196875

MEANS WITH THE SAME LETTER ARE NOT SIGNIFICANTLY DIFFERENT.

DUNCAN   GROUPING              MEAN       N  D

               A             1.4375      16  A2

               B             0.1562      16  A1
```

EXPERIMENT 5 (BEARING & CARTRIDGE ANALYSIS)

OBS	A	B	C	D	Y
1	F1	N	W1	A1	0.1
2	F1	N	W1	A1	0.1
3	F1	N	W1	A2	0.7
4	F1	N	W1	A2	1.1
5	F1	N	W2	A1	0.0
6	F1	N	W2	A1	0.1
7	F1	N	W2	A2	4.9
8	F1	N	W2	A2	4.1
9	F1	Y	W1	A1	0.0
10	F1	Y	W1	A1	0.1
11	F1	Y	W1	A2	0.3
12	F1	Y	W1	A2	0.1
13	F1	Y	W2	A1	0.9
14	F1	Y	W2	A1	1.0
15	F1	Y	W2	A2	1.4
16	F1	Y	W2	A2	2.2
17	F2	N	W1	A1	1.4
18	F2	N	W1	A1	1.6
19	F2	N	W1	A2	0.9
20	F2	N	W1	A2	0.6

EXPERIMENT 5 (BEARING & CARTRIDGE ANALYSIS)

OBS	A	B	C	D	Y
21	F2	N	W2	A1	0.3
22	F2	N	W2	A1	0.4
23	F2	N	W2	A2	4.7
24	F2	N	W2	A2	4.7
25	F2	Y	W1	A1	0.0
26	F2	Y	W1	A1	0.0
27	F2	Y	W1	A2	0.1
28	F2	Y	W1	A2	0.1
29	F2	Y	W2	A1	0.0
30	F2	Y	W2	A1	0.0
31	F2	Y	W2	A2	2.8
32	F2	Y	W2	A2	3.2

EXPERIMENT 5 (BEARING & CARTRIDGE ANALYSIS)

ANALYSIS OF VARIANCE PROCEDURE

CLASS LEVEL INFORMATION

CLASS	LEVELS	VALUES
A	2	F1 F2
B	2	N Y
C	2	W1 W2
D	2	A1 A2

NUMBER OF OBSERVATIONS IN DATA SET = 32

EXPERIMENT 5 (BEARING & CARTRIDGE ANALYSIS)

ANALYSIS OF VARIANCE PROCEDURE

DEPENDENT VARIABLE: Y

SOURCE	DF	SUM OF SQUARES	MEAN SQUARE
MODEL	15	73.69718750	4.91314583
ERROR	16	0.90500000	0.05656250
CORRECTED TOTAL	31	74.60218750	

MODEL F = 86.86 PR > F = 0.0001

R-SQUARE	C.V.	STD DEV	Y MEAN
0.987869	20.0805	0.23782872	1.18437500

EXPERIMENT 5 (BEARING & CARTRIDGE ANALYSIS)

ANALYSIS OF VARIANCE PROCEDURE

DEPENDENT VARIABLE: Y

SOURCE	DF	ANOVA SS	F VALUE	PR > F
A	1	0.42781250	7.56	0.0142
B	1	5.69531250	100.69	0.0001
C	1	17.25781250	305.11	0.0001
D	1	20.96281250	370.61	0.0001
A*B	1	0.34031250	6.02	0.0260
A*C	1	0.01531250	0.27	0.6100
A*D	1	0.02531250	0.45	0.5131
B*C	1	0.11281250	1.99	0.1770
B*D	1	2.82031250	49.86	0.0001
C*D	1	19.06531250	337.07	0.0001
A*B*C	1	0.16531250	2.92	0.1067
A*B*D	1	1.75781250	31.08	0.0001
A*C*D	1	1.66531250	29.44	0.0001
B*C*D	1	3.31531250	58.61	0.0001
A*B*C*D	1	0.07031250	1.24	0.2813

EXPERIMENT 5 (BEARING & CARTRIDGE ANALYSIS)

ANALYSIS OF VARIANCE PROCEDURE

DUNCAN'S MULTIPLE RANGE TEST FOR VARIABLE: Y
NOTE: THIS TEST CONTROLS ERROR RATES AT DIFFERENT LEVELS DEPENDING ON THE NUMBER OF MEANS BETWEEN EACH PAIR BEING COMPARED. ITS OPERATING CHARACTERISTICS SOMEWHAT RESEMBLE FISHER'S UNPROTECTED LSD TEST.
ALPHA=0.05 DF=16 MSE=.0565625

MEANS WITH THE SAME LETTER ARE NOT SIGNIFICANTLY DIFFERENT.

DUNCAN GROUPING	MEAN	N	A
A	1.3000	16	F2
B	1.0687	16	F1

EXPERIMENT 5 (BEARING & CARTRIDGE ANALYSIS)

ANALYSIS OF VARIANCE PROCEDURE

DUNCAN'S MULTIPLE RANGE TEST FOR VARIABLE: Y
NOTE: THIS TEST CONTROLS ERROR RATES AT DIFFERENT LEVELS

DEPENDING ON THE NUMBER OF MEANS BETWEEN EACH PAIR
BEING COMPARED. ITS OPERATING CHARACTERISTICS SOMEWHAT
RESEMBLE FISHER'S UNPROTECTED LSD TEST.
ALPHA=0.05 DF=16 MSE=.0565625

MEANS WITH THE SAME LETTER ARE NOT SIGNIFICANTLY DIFFERENT.

DUNCAN GROUPING	MEAN	N	B
A	1.6062	16	N
B	0.7625	16	Y

EXPERIMENT 5 (BEARING & CARTRIDGE ANALYSIS)

ANALYSIS OF VARIANCE PROCEDURE

DUNCAN'S MULTIPLE RANGE TEST FOR VARIABLE: Y
NOTE: THIS TEST CONTROLS ERROR RATES AT DIFFERENT LEVELS
DEPENDING ON THE NUMBER OF MEANS BETWEEN EACH PAIR
BEING COMPARED. ITS OPERATING CHARACTERISTICS SOMEWHAT
RESEMBLE FISHER'S UNPROTECTED LSD TEST.
ALPHA=0.05 DF=16 MSE=.0565625

MEANS WITH THE SAME LETTER ARE NOT SIGNIFICANTLY DIFFERENT.

DUNCAN GROUPING	MEAN	N	C
A	1.9187	16	W2
B	0.4500	16	W1

EXPERIMENT 5 (BEARING & CARTRIDGE ANALYSIS)

ANALYSIS OF VARIANCE PROCEDURE

DUNCAN'S MULTIPLE RANGE TEST FOR VARIABLE: Y
NOTE: THIS TEST CONTROLS ERROR RATES AT DIFFERENT LEVELS
DEPENDING ON THE NUMBER OF MEANS BETWEEN EACH PAIR
BEING COMPARED. ITS OPERATING CHARACTERISTICS SOMEWHAT
RESEMBLE FISHER'S UNPROTECTED LSD TEST.
ALPHA=0.05 DF=16 MSE=.0565625

MEANS WITH THE SAME LETTER ARE NOT SIGNIFICANTLY DIFFERENT.

DUNCAN GROUPING	MEAN	N	D
A	1.9937	16	A2
B	0.3750	16	A1

APPENDIX D

MARK III MOTION ANALYSIS

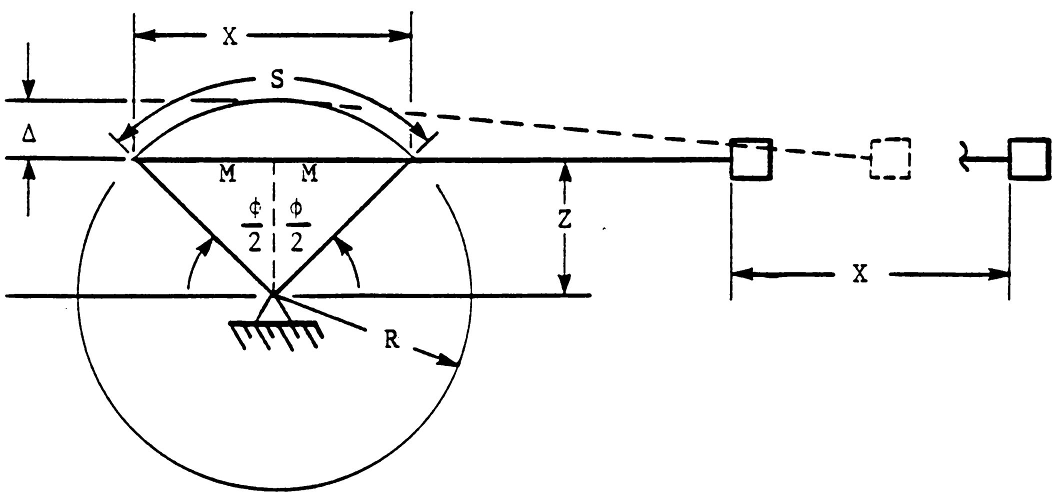

Figure D-1. Mark III Drive Linkage Motion Analysis Schematic

From Fig. D-1,

$$\cos \frac{\phi}{2} = \frac{Z}{R}$$

$$Z = R \cos \frac{\phi}{2} \quad . \; . \; . \; . \; . \; . \; . \; . \; . \; . \; . \; . \; . \quad 1$$

$$\Delta = R - Z \quad . \; . \; . \; . \; . \; . \; . \; . \; . \; . \; . \; . \; . \; . \quad 2$$

From equations #1 and #2:

$$\Delta = R - R \cos \frac{\phi}{2}$$

$$\frac{\phi}{2} = \cos^{-1}\left(\frac{R - \Delta}{R}\right) \quad . \; . \; . \; . \; . \; . \; . \; . \; . \; . \; . \quad 3$$

$$\sin \frac{\phi}{2} = \frac{M}{R}$$

$$\frac{\phi}{2} = \sin^{-1}\left(\frac{M}{R}\right) \quad . \; . \; . \; . \; . \; . \; . \; . \; . \; . \; . \; . \; . \quad 4$$

$$X = 2M \quad . \; . \; . \; . \; . \; . \; . \; . \; . \; . \; . \; . \; . \; . \; . \quad 5$$

Combining equations #4 and #5:

$$\frac{\phi}{2} = \sin^{-1}\left(\frac{X}{2R}\right) \quad . \; . \; . \; . \; . \; . \; . \; . \; . \; . \; . \quad 6$$

Equating equations #3 and #6:

$$\cos^{-1}\left(\frac{R - \Delta}{R}\right) = \sin^{-1}\left(\frac{X}{2R}\right)$$

$$\Delta = R\left\{1 - \cos\left[\sin^{-1}\left(\frac{X}{2R}\right)\right]\right\} \quad . \; . \; . \; . \quad 7$$

Δ = arc deflection produced by movement of motion conversion arms (mm).

X = total displacement, twice the amplitude of motion (mm).

R = length of motion conversion arms from pivot to swing of arc (mm).

APPENDIX E

INSTRUMENTATION CONNECTION SCHEMATIC DIAGRAM

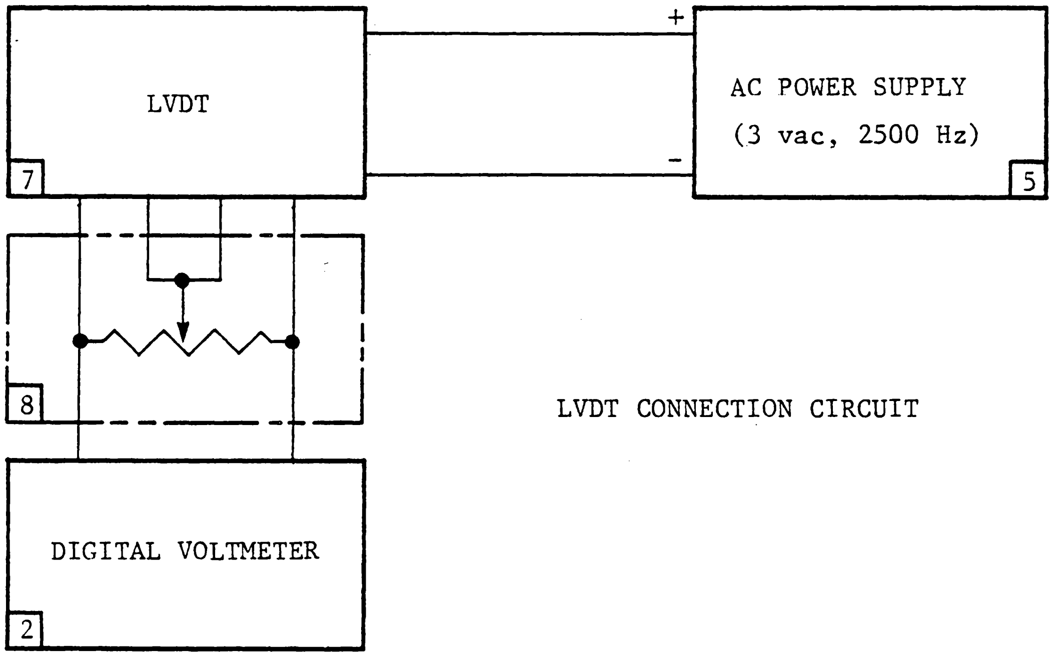

LVDT CONNECTION CIRCUIT

SOURCE-SENSOR
CONNECTION CIRCUIT

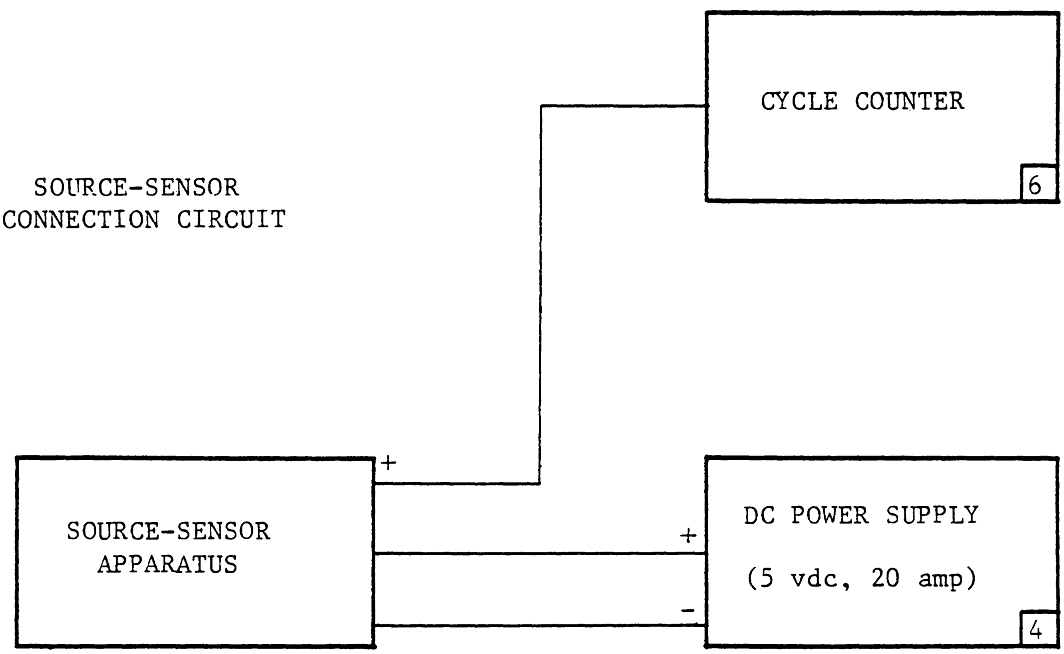

NOTE:
All equipment shown above (as numbered) can be found in Appendix A.

The vita has been removed from the scanned document

AN EXPERIMENTAL STUDY OF FRETTING CORROSION

AT A BEARING/CARTRIDGE INTERFACE

by

Robert Dean Frantz

(ABSTRACT)

A device has been built to study fretting corrosion phenomena at a bearing/cartridge interface. The research is a continuation of a larger study funded by the Naval Research Laboratory. Its main objective is to determine the important parameters influencing fretting and fretting corrosion in rolling element bearings. The new device is capable of varying load from zero to 200 N (45 lbf), amplitude of vibration from zero to 500 um (0.0197 in.), and frequency from 2.5 to 100 Hz for axial relative motion. Five sets of bearings and cartridges can be tested simultaneously at the same amplitude and frequency of vibration. Using this device with 52100 hardened steel bearings mounted in SAE 1020 steel cartridges, five analyses were carried out to investigate how load, frequency, amplitude, and presence of a grease influence the extent of fretting corrosion at the interface.